AN ABSTRACT OF THE THESIS OF

Austin Hall for the degree of Master of Science in Water Resources Engineering presented on June 30, 2015.

Title: Drop it like it's Hot: Combining DTS and Temperature Modeling to Evaluate Stream Restoration on the Middle Fork of the John Day River.

Abstract approved:

____

John S. Selker

Temperature is a key factor for salmonid health and is an important restoration metric on the Middle Fork of the John Day River in northeast Oregon. In the past century, dredge mining, deforestation, and overgrazing have degraded stream habitat and resulted in greater daytime stream temperatures in the region. Recent restoration efforts have focused on mitigating these anthropogenic disturbances by reestablishing floodplain connections, replanting riparian vegetation, and improving instream habitat features and sediment. To evaluate these restoration projects, the Middle Fork of the John Day River was designated as an intensively monitored watershed in 2008, setting the stage for a 10-year temperature monitoring study. Temperatures measured during the summers of 2013 and 2014 add to the wealth of high resolution distributed temperature sensing (DTS) data collected by Oregon State University and serve as the first post-

restoration data for a 2012 restoration project. Utilizing these data in coordination with the model, Heat Source, temperature change from two large restoration projects was quantified.

Results from the study emphasize the significance of stream area and riparian vegetation on stream temperatures on the Middle Fork. Phase 2 of the Oxbow Tailings Restoration, completed in 2012, filled over a channel used for past dredge mining activities, reducing stream surface area and restoring the bifurcated channel to its historic south path. Findings show that this project has buffered daily stream temperatures, leading to decreases in maximum and daytime temperatures and increases in nightly temperatures for early August. Maximum and afternoon temperatures were shown to decrease by 0.65 °C and 0.91 °C, respectively, while nightly temperatures increased 0.85 °C.

Continuing immediately downstream of the Phase 2 project, Phase 3 is currently in its final stages of construction. Objectives of Phase 3 seek to increase stream meanders, restore vegetation, and reconnect the stream to the adjacent valley and Ruby Creek tributary. Projecting future temperatures shows that the longer, wider restored channel increases afternoon temperature by 0.53 °C. Unlike Phase 2, changes to maximum and nightly temperatures were negligable. Altering the design width and vegetation for the restored channel revealed strong linear correlations to stream temperature, providing a simple tool that can be used to estimate temperature difference for future areal and shading scenarios.

Drop it like it's Hot: Combining DTS and Temperature Modeling to Evaluate Stream Restoration on the Middle Fork of the John Day River

by
Austin Hall

A THESIS

Submitted to

Oregon State University

in partial fulfillment of

the requirements for the

degree of Master of Science

Presented June 30, 2015
Commencement June, 2016

Master of Science thesis of Austin Hall presented on June 30, 2015.

APPROVED:

Major Professor, representing Water Resources Engineering

Director of the Water Resources Graduate Program

Dean of the Graduate School

I understand that my thesis will become part of the permanent collection of Oregon State University libraries. My signature below authorizes release of my thesis to any reader upon request.

Austin Hall, Author

ACKNOWLEDGEMENTS

Thanks for the countless contributions from current and past researchers, management, field helpers, interns, and mentors who shared time on the Middle Fork of the John Day River. Without your collaboration, this project would not have been possible. The Confederated Tribes of the Warm Springs Reservation of Oregon (CTWSRO), Oregon Watershed Enhancement Board (OWEB), National Oceanographic and Atmospheric Administration (NOAA), Freshwater Trust (FWT), and Bureau of Reclamation (BOR) provided the funding and direction that made this project possible. Thank you to the United States Forest Service for your flexibility and for complying with data requests and to researchers at the University of Oregon, especially Pat McDowell and James Dietrich, whose data contributions greatly improved the quality of my work.

I thank my advisor, John Selker, for his calm and insightful inspiration and for giving me more trust and confidence than I deserved! Thanks for the field support, contagious enthusiasm and receptive presence through my years at Oregon State. Thanks for great advice on defining the goals of graduate school and for making my move to Oregon possible. I would also like to thank Mousa Diabat, whose work paved the way for stream temperature modeling on the Middle Fork of the John Day River. Thank you for your patience and collaboration during the project and for mentoring me and teaching me how to use Heat Source model.

Thanks to my family for supporting me and especially to my sister, Lisa, who scouted out a career path for me and for breaking in the office at Gilmore 208 before I got there. Thanks to my office mates/friends for letting me by myself and for sharing great memories and office traditions together. And finally, thanks especially to the interns who had to put up with me for the weeks on the Middle Fork!

TABLE OF CONTENTS

TABLE OF CONTENTS (Continued)

Page

TABLE OF CONTENTS (Continued)

Page

LIST OF FIGURES

LIST OF FIGURES (Continued)

LIST OF FIGURES (Continued)

LIST OF TABLES

LIST OF APPENDIX FIGURES

LIST OF APPENDIX FIGURES (Continued)

LIST OF APPENDIX TABLES

Chapter 1: Introduction

Temperature is an important indicator of stream health and is a primary water quality metric in river restoration in the Pacific Northwest. As the longest undammed tributary of the Columbia River, the John Day River in Northeast Oregon holds crucial habitat for anadromous spring Chinook and summer steelhead, species that use the headwaters for spawning and juvenile rearing. Despite providing lower temperature tributaries and high quality habitat required by cold-water salmonids, the Middle Fork does not support the historic runs it once did (R. C. Wissmar, 1994). Anthropogenic disturbances have elevated stream temperature maxima and reduced annual fish counts to a fraction of their original numbers. In 1998, water quality issues related to temperature qualified sections of the Middle Fork of the John Day River as an impaired water, placing it on the 303 (d) Threatened and Impaired Waters List under the Clean Water Act (Crown 2010). This led to the development of Total Maximum Daily Loads (TMDLs) for the John Day Basin, setting limits for allowable heat loads for the river.

Large fish kills in the last decade highlight the sensitivity of stream health to temperature in the Middle Fork, an area where summer stream temperatures typically reach or exceed the incipient limits for native salmonid species. In the summer of 2007, temperatures exceeding 25° Celsius caused the death of 120 salmon, 50% of the estimated population on the headwater reaches (Huff, 2010). Another fish kill occurred in early July, 2013 when a rapid temperature increase on the Middle Fork of the John Day River was responsible for the loss of an estimated 183 wild Chinook salmon. These fish kills set a priority for stream temperature in restoration, reaffirming the previously established TMDL designation.

1.1 Middle Fork of the John Day River

The John Day River spans 457 undammed km from the Blue Mountains to the Columbia River Gorge. Tributary to the John Day River, the Middle Fork of the John Day River is a 4th-6th order stream originating near the town of Austin and continuing 117 km where it meets North Fork of the John Day River. The headwaters of the Middle Fork flow through narrow constrained alluvial valleys and wide alluvial meadows with sedge and grass-lined streambanks with scattered deciduous shrubs. The stream is largely void of pole sized trees in the open valley sections. The upper reaches of river hold vital habitat for bull trout, redband trout, and Pacific lamprey and is used by threatened summer steelhead and spring Chinook salmon for spawning and juvenile rearing. Streamflows range from peak flows of 21.1 m^3/s in April to September low flows of 0.91 m^3/s at the USGS gaging station at downstream in Ritter, OR. Elevations range from 1,250-1,000 m with an average stream gradient of 0.0035. Peak average daily summer air temperatures range from 4-30° C with minimal precipitation.

1.2 Restoration on the Middle Fork of the John Day River

The 1980 Northwest Power & Conservation Act directed funding from Bonneville Power Administration with the objective of "protecting, mitigating, and enhancing" fish habitat along effected basins of the Columbia River, including the John Day River basin. Since then, over 20 projects have taken place on the MFJDR in an attempt to improve fish habitat and water quality on the river.

In 2008, the Middle Fork was designated by Oregon Watershed Enhancement Board (OWEB) as part of the Intensively Monitoring Watershed (IMW) network, initiating a 10-year monitoring study to track restoration projects and their effects on the river. In coordination with this study, the United States Bureau of Reclamation conducted several reach assessments to assess existing conditions along the stream. The findings of the study showed water quality, habitat quality, channel condition and dynamics, and riparian/upland vegetation were either at risk or at unacceptable risk. Restoration projects before and after this assessment have focused on improving hydraulic and ecosystem processes for summer steelhead, spring Chinook salmon, and bullhead trout. Past strategies to address these goals included the restoration of flow to historic channels and nearby floodplains as well as the additions of large woody debris, gravel spawning areas, and native vegetation plantings in and along the river. Cattle grazing restrictions have also been implemented to protect bank structure and improve stream vegetation.

In the past decade, major reconstruction projects have been completed on the Middle Fork of the John Day River including large-scale projects on the Galena, Forrest, and Oxbow conservation properties. In 2006, the Middle Fork John Day River Channel Relocation and Riparian Restoration was completed, diverting flow from an altered stream section used for pasture in the 1900s to its historic path, reconnecting the stream to its floodplain. In 2010, engineered log jams were placed in sections of the stream on the Forrest property to create habitat and thermal refuge for fish. By 2011, the first piece of a multiphase project known as the Oxbow Tailings Restoration Project was completed downstream on the Oxbow Conservation Area, adding large woody debris to the south channel. In the following year, phase two of the project was completed, modifying the path of the Granite Boulder Creek tributary and filling in a channelized section used in historic mining operations while redirecting streamflow to the historic south channel.

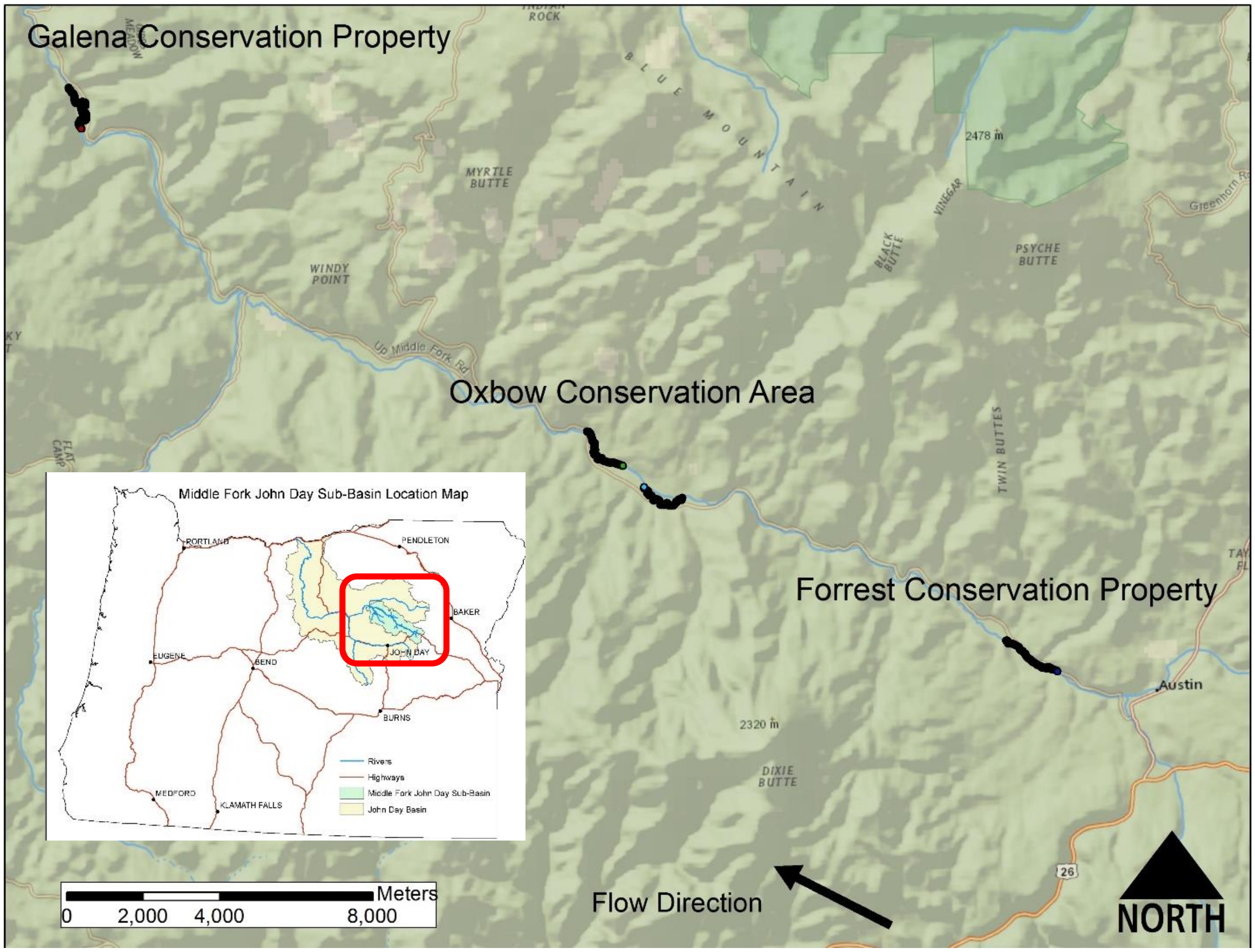

Figure 1.1: Conservation properties on the Upper Middle Fork of the John Day River. These sites encompass the restoration projects monitored by the IMW.

While the goals of these projects have sought to address specific deficiencies in the stream ecology has there been measureable success? This question often remains unanswered as funding is allocated to tangible project aspects without consideration of monitoring (Kondolf 1995). Restoration success then becomes more subjective than scientific relying on perceived changes to the biology of the river. Whether the metric is temperature, fish counts, or bank stability, sufficient data must be collected before and after the project is implemented. To capture the climatic variability it is recommended that monitoring take place several years before a project is implemented and continue for a decade after restoration to allow the effects take place (Kondolf, 1995).

Since the formation of the Middle Fork of the John Day Intensively Monitored Watershed (IMW), a wealth of data has been gathered at three conservation properties in the region. Unique from other restoration efforts, the IMW allocated funds for a 10-year monitoring study with the intent of tracking stream changes after completed projects. Researchers at Oregon State University have been involved in this monitoring phase, placing instrumentation in the river and adjacent valley to better understand the physical interactions of the stream.

In 2014, the seventh year of temperature monitoring was completed, adding to a high-resolution database of summer low flow temperatures collected across Forrest, Oxbow, and Galena conservation properties. Temperatures were recorded during 1-2 week peak heat, low flow periods in order to capture high stress conditions for salmonid species. Unique from conventional point temperature measurements, the methods employed throughout the study utilize distributed temperature sensing (DTS) technology. Using fiber optic cables, it was possible to record temperatures continuously in both spatial and temporal domains, data that are informative for understanding thorough physical interactions within the stream and its surroundings (Selker et al. 2006). The quality of these data provides the foundation for comparing pre-restoration baseline temperatures to stream temperatures after restoration.

Stream temperature data collected with DTS in the summers of 2013 and 2014 provide the first post-construction data for the Phase 2 Oxbow Conservation Area Tailings Restoration, completed in 2012. By removing an approximate 1,000 m channelized section of the Middle Fork that was created from dredge mining activities in 1939-1943, flow was rerouted to its natural meandering south channel, restoring floodplain connectivity within the valley. Granite Boulder Creek, a cold water tributary that flowed into this channelized section, was then extended 300 m reconnecting it to the south channel. Vegetation plantings with exclusion fences were also implemented as part of this restoration, though an adequate time has not allowed for full growth potential.

Monitoring data from downstream portions of 2013 and 2014 also corresponds to a section of river which is currently in construction during Phase 3 of the Oxbow Dredge Tailings Restoration project. The objective of Phase 3 seeks to reconstruct 1,700 m of river channel while removing the original channel, also the product of dredge mining in 1939-1943. Ruby Creek tributary, often dry in summer months, is also to be reconstructed for a 130 m section. Extensive tree planting and fencing are among the goals in an effort to minimize stream temperatures despite a 300 m stream length increase.

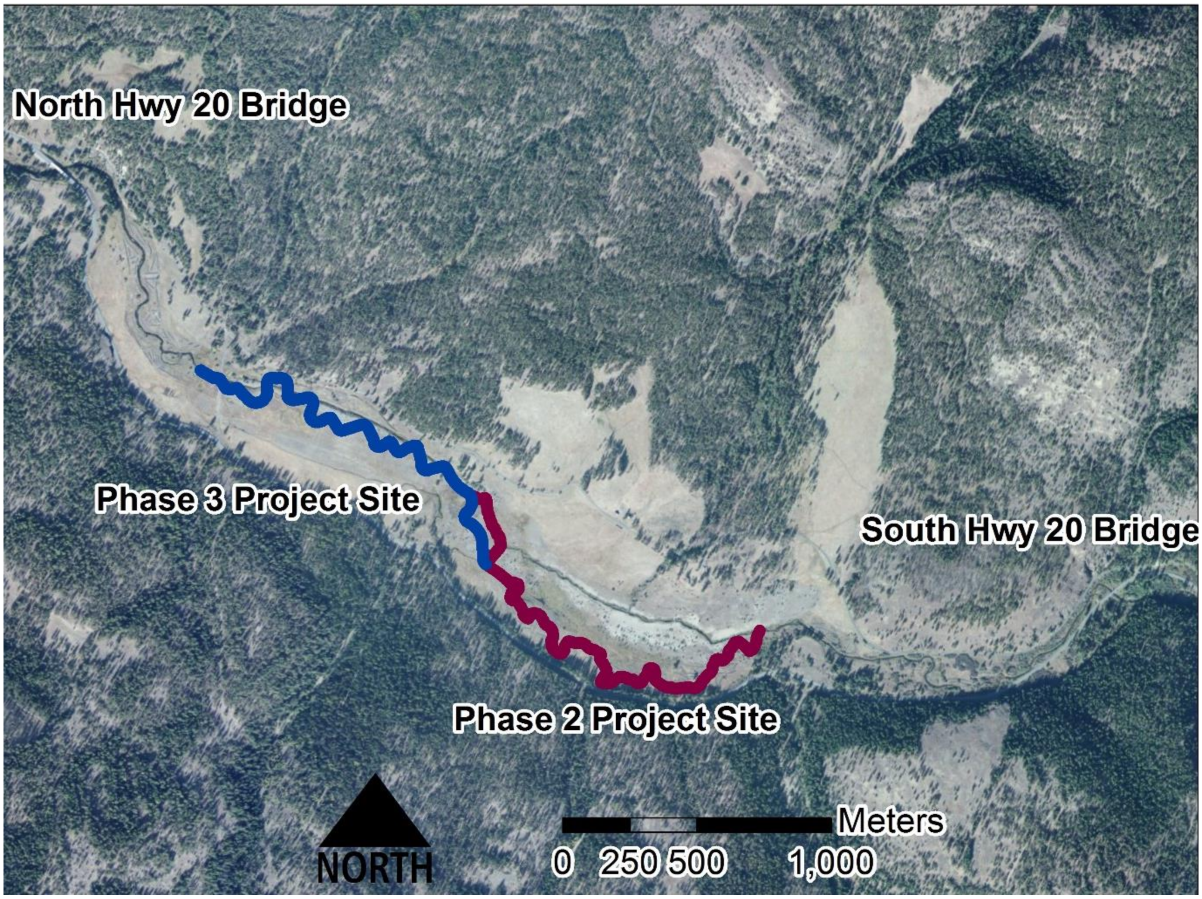

Figure 1.2: Phase 2 and Phase 3 Oxbow Conservation Tailings Restoration projects, located on the Oxbow Conservation Area property

1.3 Scope of Research

The purpose of this study is to validate the two Oxbow Conservation Tailing Projects on the Middle Fork of the John Day River as they relate to temperature and establish simplified trends to inform future stream restoration projects. Using high resolution continuous temperature monitoring data and deterministic modeling, the objective is to gain insight into physical processes controlling stream temperature on the Middle Fork and determine which projects are most effective at reducing temperature and why.

Validation of these two projects was undertaken by combining direct physical observations of stream temperature with modeled temperatures using the energy balance model, Heat Source (M. Boyd and Kasper 2003). Using the wealth of data collected from remote sensing, onsite weather, direct field measurements, and calibration, temperatures from before restoration were recreated at fine (5 m) resolutions under the same climatic and flow conditions. Using this approach, it becomes possible to estimate temperature changes from before and after restoration. The goals for this approach are three-fold for each restoration scenario.

1. Use high resolution temperature data to compare temperatures from before and after restoration and use these data to calibrate Heat Source stream temperature models for each reach
2. Apply these models to recreate stream temperatures under equivalent flows and climate conditions
3. Statistically compare directly measured/modeled post-restoration temperatures to modeled and measured historic data

1.4 Hypothesis and Scientific Questions

Several scientific hypotheses have been formed in conjunction with new monitoring data collected in 2013 and 2014. These questions seek to answer the valuable question “is stream restoration working on the Middle Fork of the John Day River?” By addressing the Phase 2 and Phase 3 Oxbow Conservation Area Tailings restorations and investigating the application of proper temperature instrumentation, three hypotheses have been developed. These hypotheses are addressed in individual chapters throughout this thesis.

1) Has Phase 2 channel reconstruction led to decreased stream temperatures on the Oxbow Conservation Property as the result of reduced exposed stream area and increased flow to the South Channel? (Chapter 3)
2) Will Phase 3 channel reconstruction will lead to increased stream temperature as the result of increased stream area and length? How can future vegetation mitigate temperature increases? (Chapter 4)
3) Can fiber optic cable selection bias temperature measurements on the Middle Fork of the John Day River? (Chapter 5)

Chapter 2: Background on Temperature and Restoration on the Middle Fork of the John Day River

2.1 Temperature and Fish Health

Water temperature is responsible for regulating fish metabolism and controls the amount of dissolved oxygen in a stream (Bell 1991; Oregon DEQ 1995). It has also been shown to define fish distribution along a stream reach. At temperatures exceeding 25° C, Chinook salmon and other cold-water species are unable to survive (Bell 1991). For the Columbia River and its tributaries, temperature has long been identified as one of the greatest factors affecting salmonid habitat quality and reproduction. Though temperature limits vary among salmonid and trout species and life stage of the fish (egg, smolt, juvenile, adult), general ranges have been identified in the context of the Columbia River basin. These ranges are broken down based on exposure time and their physical effects on the fish. Instantaneous (>32° C) and incipient (22°-25° C) limits lead to rapid or immediate death via physical degradation of the fish while sub-lethal limits (17.8°-22° C) lead to increased disease susceptibility and reduced metabolic function (Anderson et al.; Boyd & Kasper, 2003, Brett, 1952, McCullough 1999). In eastern Oregon, temperatures rarely exceed the instantaneous thermal limit. It is common for temperatures to reach incipient levels creating the risk of fish mortality after a period of hours to days. Two of the most temperature sensitive fish species found on the headwaters of the Middle Fork of the John Day River are Chinook salmon and native bull trout (Oregon DEQ 1995). Addressing temperature requirements for these species will improve stream health for other aquatic organisms as well. General established incipient temperature limits for these two species and for steelhead have been tabulated in Table 2.1.

Thermal limits for cold-water fish species also depend on an acclimation period where sudden shifts can lead to die off from thermal shock (McCullough, 1999). On the Middle Fork of the John Day River, rapid temperature fluctuations recorded during low flow years in 2007 and 2013 led to large scale salmon die offs on the river (Huff 2009).

Table 2.1 Incipient thermal limits for three common cold-water fish species on the Middle Fork of the John Day, adapted from ODEQ 1994[1]

Species	**Incipient Temperature Limit, C**
Chinook Salmon	25°
Steelhead	21°-26°
Bull Trout	19°-21°

[1]Adapted from ODEQ, 1994

2.2 Thermal Refugia on the Middle Fork

On the Middle Fork of the John Day River, summer stream temperatures often reach and exceed incipient mortality levels for cold-water salmonid and trout species. Despite water temperatures in excess of 25° C, substantial salmonid populations still exist within its stream reaches. At these high thermal levels, native fish species depend on isolated cold areas known as thermal refugia for survival (EPA 2012/Torgerson). Several studies have been conducted exploring the presence and importance of thermal refugia (Nielson et al., 1994; Torgerson, 1995; ODonnell, 2012) on stream reaches with the conclusion that areas 1-3° C cooler than ambient stream temperatures consistently held higher fish concentrations. On the Middle Fork of the John

Day River, both surface and streambed temperature sensing have been utilized to map potential cold-water upwellings. In 1997, Torgerson utilized forward-looking infrared (FLIR) to identify cold patches and establish fish correlations to these areas. In his work, he identified the importance of large-scale refugia for Chinook salmon. O'Donnell expanded on this work in 2012, conducting longitudinal subsurface temperature measurements using fiber optic distributed temperature sensing techniques. In the study, groundwater and tributary refugia surveys revealed maximum subsurface cold patches 1.28° C below than ambient stream temperatures and tributary fed cold patches of 0.03° to 2.31° C below ambient temperatures.

Another potential source of thermal refugia is from hyporheic zones along the stream, defined as areas where the mixing and exchange of instream water occurs beneath or alongside the stream bed. Despite the established floodplains found on the Middle Fork of the John Day River, hyporheic flow was found to be absent at the reach scale (Wright, 2005, Beschta & Baxter, unpublished). Streambed composition was found to be largely homogeneous, further explaining the lack of hyporheic flow. Additional findings from a recent high resolution distributed temperature sensing technology (DTS) study in 2009 showed no conclusive evidence of hyporheic exchange on upper reaches of the Middle Fork (Huff, 2009).

2.3 Stream Temperature and Heating

Stream temperature is a well understood physical parameter defined by heat and mass transfer. The fundamentals of heat transfer are governed by the laws of thermodynamics which describe the conservation of energy and the one-directional flow of energy from higher to lower gradient. Mass transfer defines the physical movement, hydraulically, within a stream system. In the absence of mass transfer, water temperature will change in time proportional to its rate of energy gain or energy loss. This process, described by equation 2.1, is a function of the stream's geometry, the volume of water, and physical properties of water at that temperature (Brown 1969; Diabat 2014).

$$\frac{\delta T}{\delta t} = \frac{A * \Phi\, Total}{\rho_{\,w} * C_w * V_w} \qquad (2.1)$$

A=Stream surface area, m^2
Φ Total=Sum of heat flux into the stream, Watts/m^2
$\rho_{\,w}$ =Density of water, kg/m^3
C_w=Specific heat capacity of water, J/(kg C°)
V_w=Volume of water (m^3)

In the context of a flowing stream, temperature will change according to stream velocity and the rate of dispersion. The general advection dispersion equation for temperature in the absence of heat transfer then takes the form of equation 2.2, where velocity and dispersion are also determined by the geometry of the stream.

$$\frac{\delta T}{\delta t} = -U * \frac{\delta T}{\delta x} + D_L \frac{\delta^2 T}{\delta x^2} \qquad (2.2)$$

U=Stream advection, m/s
D_L=Dispersion, m^2/s

For any stream, both heating and mass transfer are present leading to the complete form of the heat and mass transfer equation (2.3).

$$\frac{\delta T}{\delta t} = -U * \frac{\delta T}{\delta x} + D_L \frac{\delta^2 T}{\delta x^2} + \frac{A * \Phi\, Total}{\rho_w * C_W * V_W} \quad (2.3)$$

The total energy flux (Φ Total) for a stream can be divided into five components: solar shortwave radiation, longwave radiation, streambed conduction, convection between the water-air surface, and evaporation. The summation of these transfer mechanisms lead to a change of stream temperature where net positive energy into the stream results in an increase of water temperature (Boyd & Kasper, 2003).

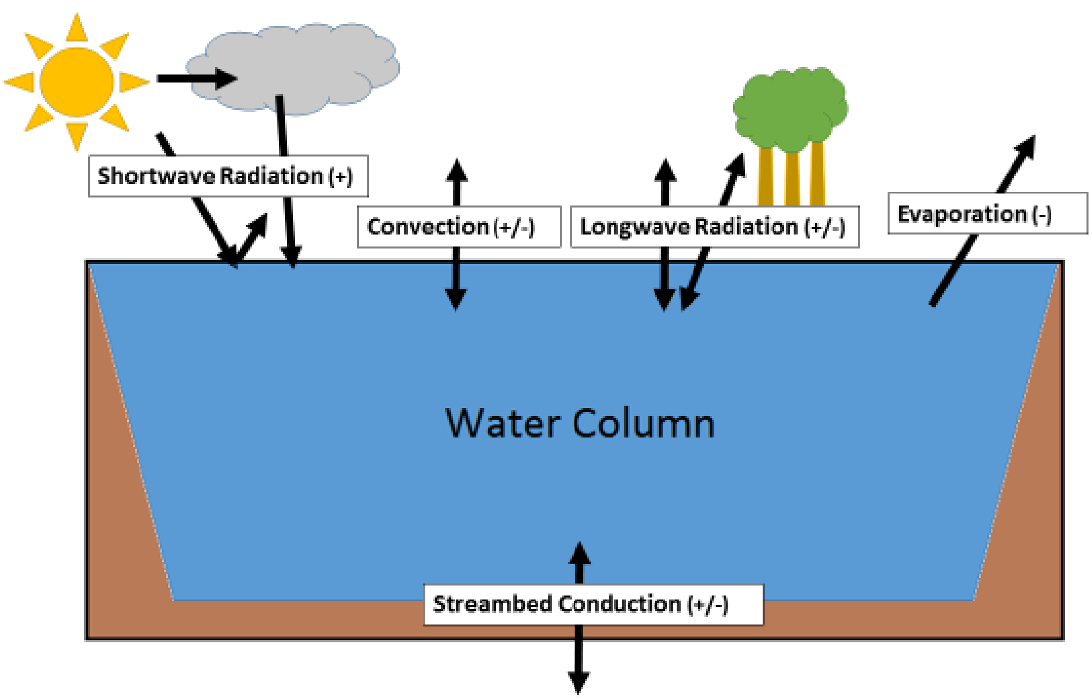

Figure 2.1 Stream heat flux mechanisms and directionality

$$\Phi\ Total = \Phi\ Solar + \Phi\ Longwave + \Phi\ Convection + \Phi\ Evaporation + \Phi\ Bed\ Conduction \quad (2.4)$$

For streams with sparse streamside vegetation, the largest heat source controlling stream temperature is shortwave solar radiation (Brown 1969, Beschta 1997). For unshaded reaches, as much as 90% of incoming radiation can be transferred into the stream (Beschta 1997). The magnitude of solar radiation is controlled by the position of the sun, atmospheric conditions, and the degree of penetration into the stream's water column. As direct beam solar radiation approaches the earth's surface, a percentage is transferred into a diffuse component, scattering as it passes through the atmosphere. On the Middle Fork of the John Day River, measured solar radiation values often exceed 900 W/m^2 for clear sunny days. The influence of riparian shading in reducing shortwave solar radiation has been studied extensively in the Pacific Northwest. Conclusions indicate that riparian vegetation can greatly reduce summer stream temperatures as well as improve bank stability (Beschta 1997). Even at scales as low as 150 m, maximum stream temperature has been found to decrease with the addition of shade (Johnson 2004).

Longwave radiation, described by the Stefan-Boltzmann Radiation law, is emitted as a function of temperature for all terrestrial bodies. Within a stream system, total longwave radiation can be positive or negative and is determined by the difference of atmospheric radiation and stream back radiation. Land features such as vegetation also contribute longwave radiation, reflecting radiation back into the water column (Boyd & Kasper, 2003). Emitted longwave radiation is responsible for stream cooling during nighttime periods.

Evaporation occurs by the release of latent heat as water changes from liquid to gas form. Often the largest dissipater of heat from the stream (Parker and Krenkel, 1969, Boyd and Kasper, 2003), evaporation is a function of vapor pressure deficit between the air and water surface and the wind speed. Because of this, dry days with low vapor pressure exhibit high rates evaporation.

Rates of evaporation are often the most difficult parameter to estimate due to the heterogeneity of climate conditions along a stream reach (Benyahya et al. 2010). Past studies on the Middle Fork of the John Day River indicate that evaporation is a significant component of the stream's energy balance in the summer, varying with wind direction, stream incision, and stream bank gradient (Benner, 2000). Two alternate evaporative methods, mass transfer and Penmen combination, both characterize the relationship of wind speed and evaporation empirically using Dalton-type equations for the wind function which take the form of $f(w) = a + bw$ (2.5). The coefficients a and b are then determined by a linear fit of experimental evaporation data. The evaporation rate per unit area as a function of the wind function and vapor pressure deficit becomes:

$$E = f(w) * (e_s - e_a) \qquad (2.6)$$

The variation of the wind function coefficients is apparent in literature values which were derived primarily for lake and reservoir environments. Few studies, however, have focused on the wind function for river settings which are physically different systems. Average wind function coefficients from Benner's 2000 study for the Middle Fork of John Day River indicate higher values than the other studies, defining the wind function as $f(w) = 4.00 * 10^{-9} + (2.36 * 10^{-9})w$ converted for equivalent units of mb^{-1}.

The remaining heat fluxes, streambed conduction and convection, generally contribute less to the total heat budget of a steam. Convective or sensible heat losses are due to temperature differences at the air-water interface. Convection is proportional to evaporation by the Bowen ratio and subject to the same considerations of wind functions (Boyd and Kasper 2003).

Streambed conduction occurs at the alluvium-water interface and is a function of temperature gradients and the thermal conductivities of water and the river sediment. Past work in quantifying bed conduction was studied by Brown in 1972. By installing thermocouples at 1 cm intervals in the bed material, Brown found that bed conduction was responsible for absorbing 20% of incident solar radiation at his study stream (Brown 1972). These findings are consistent with later research showing that bed conduction is responsible for buffering daily stream temperatures (Sinokrot and Stefan 1993).

2.4 Modeling Stream Temperature

Stream temperature modeling can be conducted empirically through regression and deterministically for a range of time scales and distances (Stefan and Preud'homme 1993; Morrill, Bales, and Conklin 2005; Wunderlich and Authority 1972; Sinokrot and Stefan 1993) Both model strategies offer useful insight for predicting stream temperature and each comes with its limits, advantages and demands. Regression models require minimal inputs, but are limited in output resolution and unable to describe the effects of local physical processes. Deterministic methods model the physical heating of the stream, providing control and insight of processes controlling stream temperature

One regression-based model by Mohseni, Stefan, and Erickson (1998), established a non-linear trend based on observed air temperatures to predict weekly stream temperatures in the contiguous United States. Another regression model, NorWest, is based on the spatial analysis of thousands of instream measurements collected in the Northwest United States and has been successfully utilized (r^2=0.91, RMSE=1.0° C) to predict stream temperatures for 1-km scales in the region (Isaak et al. 2011). Such models are often useful in predicting medium to large scale stream temperature changes due to climate variation and warming air temperatures.

Deterministic models, by contrast, function by incorporating the physical heat transfer process that occurs within a stream. Though they demand extensive input data, deterministic models offer the most complete interpretation of stream temperature and allow for analysis and exploration of individual stream temperature drivers. The limits of scale for deterministic models are set by the quality and rigor of spatial and temporal inputs. Deterministic models have been used to quantify the shading effects of streamside vegetation (Brown 1971; Beschta 1997; Diabat, 2014), to estimate the effects altering stream surface area (Brown 1971; Sinokrot and Stefan 1993) and calculate and quantify groundwater inflows and hyporheic zones (Huff 2009; O'Donnell 2012). With adequate data, it has been possible to study the relative contributions of each heat flux on the stream's energy budget as well as predict temperatures on a meter and hourly scale (Boyd 1996). Like regression based models, deterministic models have also been used to model stream temperature changes resulting from potential climate change scenarios focusing on decreased streamflow and increased air temperatures (Diabat 2014). Because of their basis on physical processes, deterministic models are particularly useful in describing physical modifications from restoration.

Deterministic models are used extensively in state agencies such as the Oregon Department of Environmental Quality (ODEQ) as the basis for developing allowable TMDLs for impaired waterways in the region. ODEQ maintains and utilizes Heat Source, a deterministic model developed at Oregon State by Matthew Boyd in 1996. Since its release, Heat Source has been updated (current version 8.0.8) improving its application and input flexibility. Rather than simplifying physical stream processes, Heat Source was developed to incorporate high resolution data, taking advantage of modern GIS, aerial imagery, and remote sensing. Improvements to data quality from LiDAR and new stream temperature collection methods, such as DTS or FLIR, have helped further facilitate advances and improvements in model resolution. An important component of Heat Source is its coordination with the extension 'TTools,' a plugin for ArcGIS that allows for vegetative and topographic sampling from digital elevation maps and land use surveys. While limited to modeling the heat and mass transfer equation in one dimension, the model has been shown to accurately model stream temperatures in advection dominated, non-stratifying systems (Boyd & Kasper, 2003). Because of its scientific physical basis, proven utility, and adequate output resolution, Heat Source has been adopted for modeling stream temperatures of the Middle Fork of the John Day River restoration.

Past stream temperature modeling campaigns on the John Day River have explored heat loading in order to establish Total Maximum Daily Loads (TMDLs) and to explore the effects of climate change and restoration practices on the river. These efforts utilized deterministic modeling in order to quantify physical processes controlling the energy fluxes into and out of the stream. In 2010, Oregon DEQ released John Day River Basin TMDL report. Contained within this report are model results that show the expected heat loading over the John Day River, Middle Fork of the John Day River, and North Fork of the John Day River, an extent covering 723 stream km. While its results provide practical insight about large scale heating processes, the scale of model inputs and the scope of the study limits its applicability at the reach-scale. Key findings from the TMDL report indicated that under pre-anthropogenic conditions, the Middle

Fork of the John Day River could be restored to temperatures below the current impaired levels (Crown 2010).

Another study (Diabat 2014) explored the projected influence of climate change on stream temperatures for the Middle Fork of the John Day River. This study builds on 2002 stream inputs and results derived in the 2010 TMDL report, applying a model under altered climatic inputs. Considered in the analysis is the variation of air temperature and timing, flow, and riparian vegetation at model scales ranging from 100 m to 500 m. Findings from this study emphasize the importance of riparian vegetation in buffering stream temperatures, demonstrating the effects of shading in mitigating the effects warmer air temperatures.

Chapter 3: Exploring Temperature Change after Phase 2 Restoration

3.1 Introduction

Since 2010, sections of the Middle Fork of the John Day River located on the Oxbow Conservation Area have been part of a multiphase stream restoration known as the Oxbow Tailings Restoration Project. The goals of this project are to improve instream fish habitat and water quality by removing mining tailings, adding wood structures, and planting riparian vegetation. Completed in 2012, Phase 2 of the project modified the path of Granite Boulder Creek tributary and filled in a 1,050 m channelized stream section used in historic mining operations from 1939-1943. In doing this, flow from the previously bifurcated channel was rerouted to its natural meandering south channel, reducing stream surface area from 13,500 m^2 to 8,000 m^2 and restoring floodplain connectivity to the valley. Vegetation plantings with exclusion fences were also implemented as part of this restoration, though significant increases in effective shade have not yet resulted.

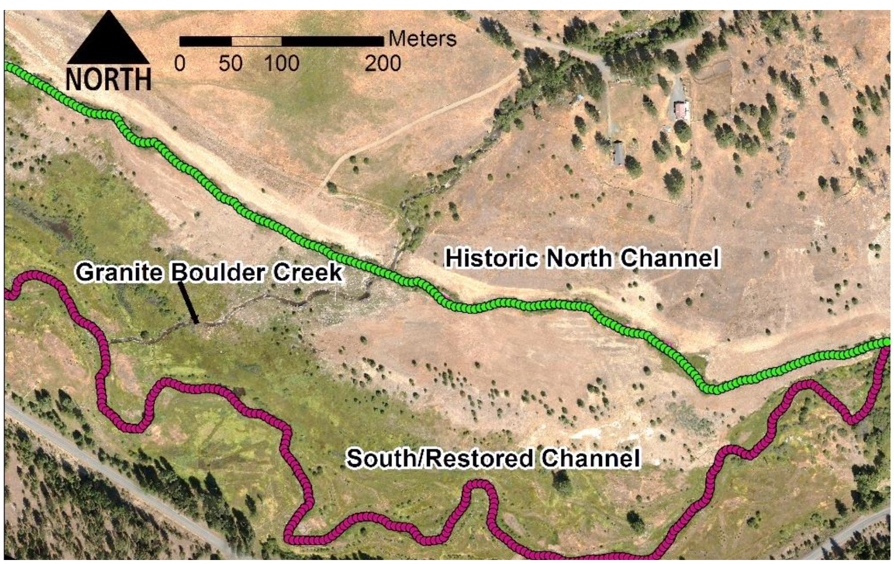

Figure 3.1: Map highlighting the work of the Phase 2 restoration project. The historic divergence of the bifurcated channels is depicted on the right of the map.

3.1.1 Scope of Phase 2 Study

The purpose of this study is to estimate the temperature effects of the Oxbow Phase 2 Tailings Project channel restoration on the Middle Fork of the John Day River. Stream temperature data collected in the summers of 2013 and 2014 provide the first post-construction data following the project's completion. Temperatures were recorded during 1 to 2 week peak heat, low flow periods in an effort to capture high stress conditions for salmonid species. Unique from conventional point temperature measurements, the study utilizes distributed temperature sensing (DTS) technology. Using fiber optics, it was possible to record longitudinal temperatures continuously in both space and time, data that is informative for understanding thorough physical interactions within the stream and its surroundings. The quality of this data provides the foundation for comparing pre-restoration baseline temperatures to stream temperatures after restoration.

Validation of the Phase 2 project was conducted by combining direct measurements of stream temperature after restoration with modeled historic temperatures using an energy balance approach through the deterministic model, Heat Source (Boyd & Kasper 2003). Using the wealth of data collected from remote sensing, onsite weather stations, and direct field measurements, temperatures were recreated at fine resolutions under equivalent 2014 climatic and flow conditions. To address the question of project efficacy with regard to stream temperature, the following objectives were developed:

1. Successfully calibrate a high resolution stream temperature model using distributed temperature sensing data

2. Apply this model to recreate stream temperatures under equivalent flows and climate conditions for the historic pre-restoration channels
3. Statistically compare post restoration temperatures to modeled historic temperatures to quantify the effects of the project.

3.2 Methods

Methodology for quantifying stream temperature change after Phase 2 covers the experimental data collection design and the Heat Source model application. This section outlines the protocols for data collected from distributed temperature sensing (DTS), onsite weather stations, transect surveys, streamflows, and GPS. It also describes model setup and calibration.

3.2.1 Study Site

Within the last century, sections of the Middle Fork of the John Day River on the Oxbow Conservation Property were significantly altered from anthropogenic use. After the discovery of gold in the 1860s, reaches were placer mined and later dredge mined, leading to stream channelization and floodplain degradation littering valleys with tailings and upturning spawning gravels (McDowell 2001). The land surrounding the river, much of which is still privately owned, was subject to overgrazing and logging causing bank erosion, reductions in stream shade and habitat, and channelization. These actions degraded the river's ecosystem, and have led to higher stream temperature maxima on the Middle Fork.

The experimental installation site of the Phase 2 project is centered at 44°38'41.96"N, 118°39'33.81"W on the Warm Springs Oxbow Conservation Area property, located 14 km downstream of the Bates Campground Bridge. Measured flows at the Oxbow field site ranged from 0.40 to 0.65 m^3/s in early August of 2013 and 2014. Granite Boulder creek, located in the middle of the study site, is a cold-water tributary responsible for supplying 0.12-0.18 m^3/s to the base flow of the stream during the same period. DTS monitored stream reaches are found throughout the Oxbow Conservation Area beginning at the Upper Middle Fork Rd (Hwy 20) upstream bridge, moving downstream to the northern Hwy 20 Bridge.

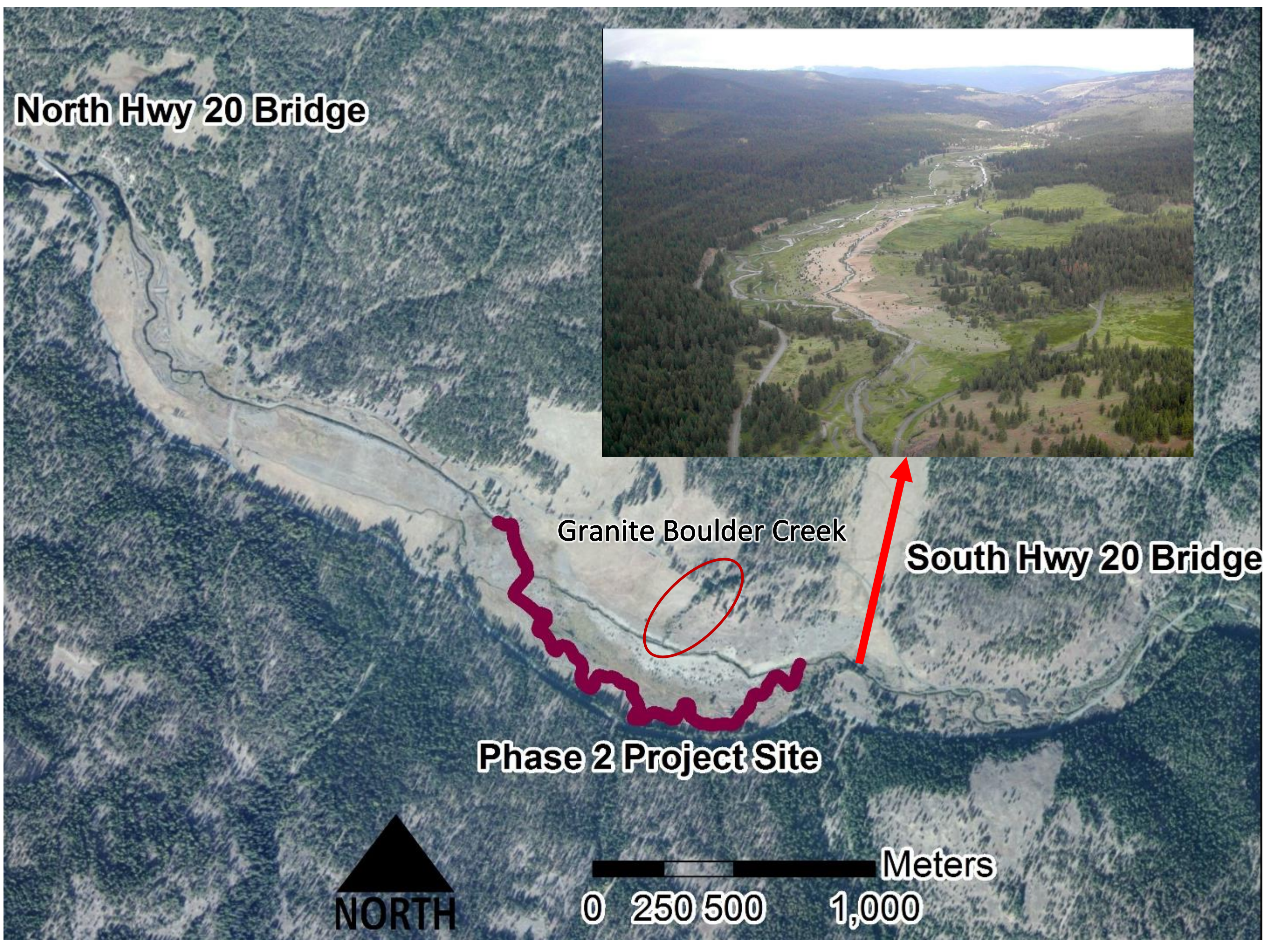

Figure 3.2: Oxbow Conservation Area on the Middle Fork John Day and overview of the Phase 2 project site, prior to restoration. Photo Credit: Warm Springs 2009 Management Plan

3.2.2 DTS Monitoring Field Methods

For 2 weeks in the summers of 2013 and 2014, over 16 km of the Upper Middle Fork were monitored, adding to a 7-year temperature dataset collected by researchers at Oregon State University. Data were collected using distributed temperature sensing technology (DTS), allowing for the measurement of continuous longitudinal temperatures across reaches spanning several km. While providing extensive temperature coverage at affordable cost, installation of DTS at this scale is extremely labor intensive, requiring additional experimental design consideration and careful installation maintenance during the recording period.

3.2.2.1 DTS Equipment

A 4-channel Gemini 5100 Distributed Temperature Sensing unit was utilized in this experiment using a single ended approach (1m spatial resolution at and <0.2°C error for 2 km www.sensortran.com). 5-minute average temperatures were collected on a 15 minute cycle, providing continuous data along 2 km of fiber optic cable that was laid in the newly restored Phase 2 river channel. The cable used was a 6 mm rugged Kaiphone reinforced cable, which provided adequate durability and flexibility during the recording period. The multilayered cable housed two fibers which were reinforced by plastic, Kevlar, metal braiding, helical metal tube, and a white high-density polyethylene exterior coating.

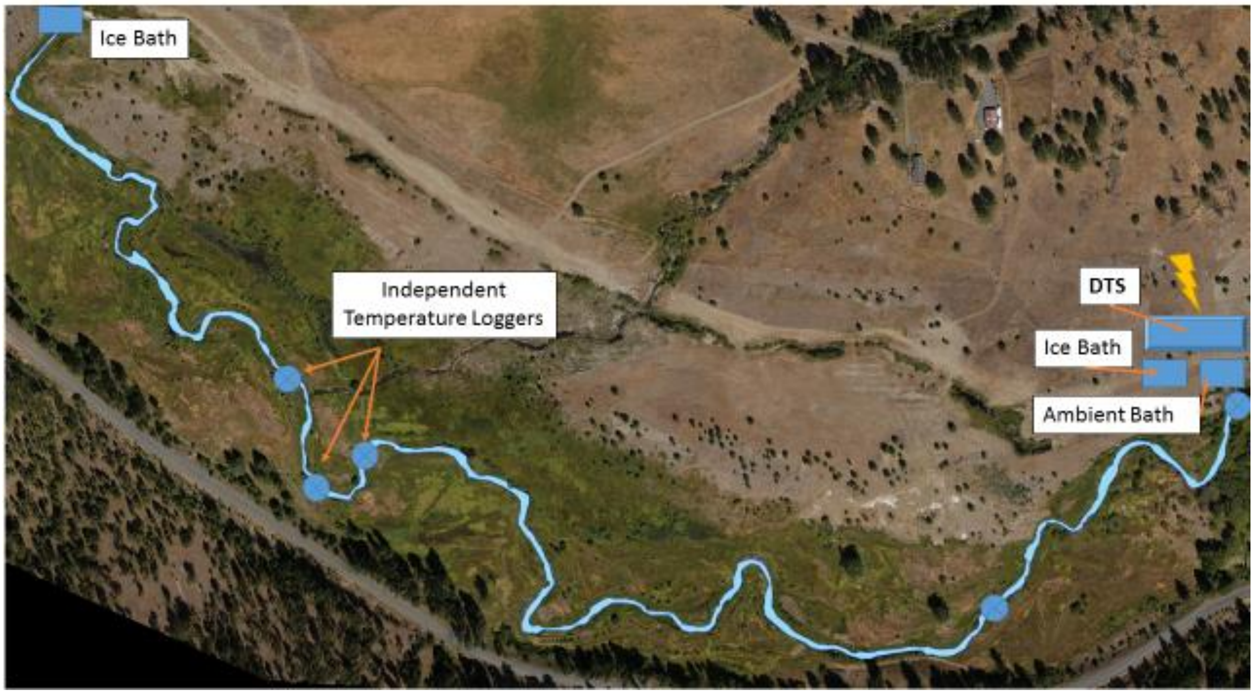

Figure 3.3: Map depicting the 2014 DTS field installation on the restored Oxbow stream reach. Fiber optics were deployed 1,800m downstream of the DTS, measuring temperatures for 11 days in August.

3.2.2.2 Fiber Optic Cable Installation and Calibration

To capture the most representative stream temperature, the fiber optic cable was installed in the thalweg and secured to the streambed every 5 to 10 m using alluvial rocks. As the cable was placed, a high precision RTK TOPCON GR-3 survey grade GPS (10 mm horizontal, 15 mm vertical accuracy) was used to map its location and associated stream depths. At the terminating end of the fiber optic cable, the inner fibers were spliced together to provide double measurements of temperature along the stream. High precision RBRsolo T (accuracy +/-

0.002°C) temperature loggers were embedded within cable sections housed in three controlled temperature baths. Five additional HOBO TidbiT v2 and HOBO U22 loggers (accuracies +/-0.2° C) were secured to the cable in the stream to provide additional independent references for improved calibration and validation.

Following installation, 11 days of temperature data were collected and calibrated. Several modern DTS instrumentation contain in situ calibration routines to allow for on-the-fly calibration of raw data into temperature data (Silixa, Sensortran, Oryx). These routines rely on the accuracy of 2 external probes and can often limit the overall accuracy of the DTS. To improve data quality, manual calibration of the raw data was undertaken, based on the methodology from (Hausner et al. 2011). Matlab code was developed to help facilitate the calibration routine. For more information on data calibration and reference to the utilized code, the reader is referred to Appendix D.

3.2.3 Phase 2 Heat Source Modeling

Heat Source 8.08 was utilized to model post-restoration and baseline conditions on the Middle Fork prior to the Phase 2 Oxbow Tailings Restoration project. This process was completed in three models; one for model calibration and two to recreate temperatures in both the north and south historic channels for 2014 conditions. The historic north channel model recreated temperatures in the old channel with Granite Boulder Creek tributary intersecting 535 m downstream from the north/south channel divergence. The paired historic south channel model was created without Granite Boulder Creek using hourly temperature and flow outputs from the north channel model at the north/south channel convergence. To explore the persistence of any temperature change, the historic south channel model was extended 1400 m downstream to the site of the old bridge (also the terminus of the present/projected Phase 3 restoration project).

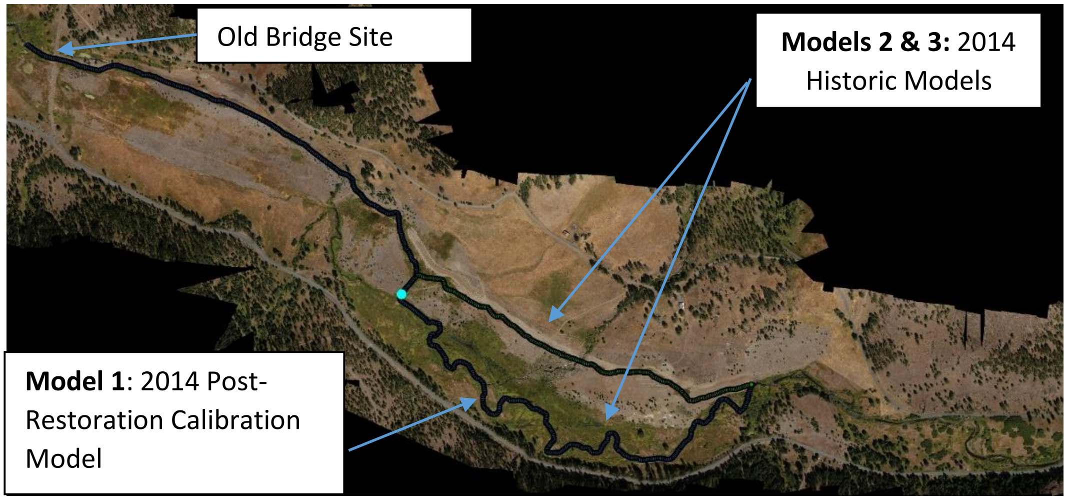

Figure 3.4: Sequence of stream temperature models used for Phase 2 restoration analysis. The south channel model extending to the old bridge site serves as post-restoration data and for calibrating the Heat Source temperature model. Models 2 and 3 cover the historic north/south channels with divided 2014 flow.

3.2.3.1 Model Inputs:

The calibrated Heat Source model was used to simulate temperatures on the restored stream channel from August 3 to August 13, 2014 using a spatial node resolution of 5 meters. This period provided climatic variation which included warm clear sky days as well as cloudy and cool days. The pre-restoration historic north and south channel models were run with identical 2014 climate and base flow conditions. At the divergence, 75% of incoming flow was distributed to the north channel and 25% to the south channel, based on 2011 surveys conducted by O'Donnell (O'Donnell 2012). An alternate set of models was run with a 50% distribution to explore the sensitivity of this distribution.

Explanation of select model spatial parameters, climate parameters, and physics is provided in the following sections with a summary in Table 3.1. For a complete list of model parameter sources and derivations, the reader is referred to Appendix A.

Spatial model inputs were derived from a combination of ground measurements and remotely sensed data. TTools, an extension that works in conjunction with Heat Source, was used to sample stream vegetation, elevation, gradients, topographic shade, and bank top widths from a compiled GIS database (Figure 3.4). These data included high resolution LiDAR with derivative maps of canopy closure (10 m) canopy height (0.5 m), and bare earth (0.1 m) elevations. 2013 structure from motion data (0.1 m) was used for stream bank measurement and for visual validation of GPS and vegetation data. Bathymetry data were derived using measured stream depths and top widths and calibrated with Heat Source's hydraulic modeling component. Streambed composition was determined from pebble counts (Duffin and McDowell, unpublished data) conducted along stream reach.

Figure 3.5: High resolution structure from motion imagery (left) and corresponding 10 m canopy closure and 0.5 m canopy height (right) for the same location on the Oxbow South channel. These data were sampled from the stream centerline using the Heat Source extension, TTools.

Hourly boundary temperatures at the upstream model node were set to measured temperatures collected using distributed temperature sensing. Streamflow was assumed constant for the modeling period and assigned according to synoptic discharge measurements made during the 2014 monitoring period. Typical hourly streamflow measurements recorded at the Ritter USGS gaging station showed little flow variation during late summer, validating this assumption. Minor tributary flows were negligible as minor tributaries ran dry in late summer while Granite Boulder Creek provided ~0.18 m^3/s of flow in the south channel. The temperature of Granite Boulder Creek was calculated using an energy and mass balance approach and compared to a point logger located upstream from its convergence with the south channel. Because data showed that Granite Boulder Creek was warmer at the confluence than at the upstream logger location, calculated temperatures were used for the model. Temperatures sourced from the point logger were used for the historic north channel model. Synoptic discharge measurements revealed an accretion of approximately 0.06 m^3/s of flow between the upstream model boundary and Granite Boulder Creek. Temperature data from nearby shallow groundwater wells on the Oxbow Conservation floodplain were used in conjunction with differences between the unadjusted model and DTS to add this flow as an evenly distributed accumulation for this segment. Hyporheic flow was ignored in all models. While this simplification is sacrifices some model accuracy, previous literature has found no conclusive evidence of significant hyporheic flow at reach and sub reach scales (Huff 2009; Wright 2005). Though flow patterns likely have changed as the result of restoration efforts, hyporheic exchange was not observed to influence stream temperatures extensively in the DTS data.

Synoptic streamflow measurements taken on August 8 and August 9 identify discharge in the Middle Fork during the DTS monitoring period (Appendix Figure 7 and Appendix Table 2). Flow measurements were taken using a Price AA flow meter (instrument accuracy of +/- 3.4% for measured flow velocities (Hubbard, Thibodeaux, and Duong 2015)) at five locations along the Oxbow channel. Granite Boulder Creek was bracketed by two surveys to capture the inflow from the tributary, while other locations were selected at model boundaries and potential sites of flow accretion or withdrawal. These flows were compared and found consistent with independent measurements from the North Fork John Day Watershed Council taken August 4-6, 2014.

Table 3.1: Heat Source inputs and sources for the Phase 2 restoration models

Model Inputs	**Value**	**Procedure**	**Source**
Vegetation	0-32 m	2008 LiDAR-derived imagery	United States Forestry Service (USFS)
Topographic Angle	2-18.4	10m DEM	Oregon Geologic Data Compilation (OGDC)
Stream Elevation	1126-1142 m	2008 LiDAR-derived bare earth imagery	USFS
Stream Width	1-13 m	2013 structure from motion survey	University of Oregon (Dietrich, 2014)
Streambed Porosity	0.29	Gravel Counts	University of Oregon (2008-2011)
Streambed Thermal Conductivity	2.0 W/m/°C	Literature	Thermal properties for basalt, Eppelbaum, Kutasov, Pilchin 2014
Streambed Thermal Diffusivity	0.006 cm^2/sec	Literature	Thermal properties for basalt, Eppelbaum, Kutasov, Pilchin 2014
Bank Angle	0-16	Measured/Calibrated	Stream measurement/ Model Iteration
Manning's n	0.045-0.075	Literature with calibration	Chow (0.04-0.07), Jarrett (0.056-.183)
Boundary Temperatures	13.6-25.3	Measured	2014 DTS Installation
Streamflow	0.41-0.63	Measured	2014 Streamflow Survey
Groundwater	0.03	Measured/Calibrated	DTS, Model Iteration
Tributary Temperatures	10.6-19.0	Measured	North Fork John Day Watershed Council
Weather	-	Measured	Dunstan Weather Station
Wind Sheltering	0.7	Calibrated	DTS-Model Comparison

3.3 Results

3.3.1 Model Calibration

The calibration model was run for 11 days in early August and then compared to temperatures measured by the DTS in the 2014 field campaign. Results indicate that the model was able to recreate temperatures along the monitored stream thalweg at 500 m, 1,000 m, 1,500 m, and at the end of reach. Comparison shows that model-DTS correlation was stronger at night and during periods of low cloudiness when energy fluxes were less variable. For the first 8 clear sky days, mean error for the model was 0.10° C and absolute error was 0.21° C. Modeled stream temperatures consistently over predicted maximum stream temperatures, resulting is modeled downstream temperatures 0.20° C greater than temperatures measured by DTS. There was also increased model error during high variable cloud cover days during a summer thunderstorm system that occurred from August 11-August 13. Mean error and absolute mean error were 0.21° C and 0.27° C respectively for this period. This error can be attributed to the sporadic nature of clouds during this period which was not well captured by the separated weather stations in the neighboring valleys. Further, increases in streamflow from the measured 8.4 mm of precipitation were not incorporated in the temperature model.

A spatial comparison of modeled and DTS temperatures is shown in Figure 3.7 for August 5, a clear measuring day. Analysis of errors at select distances along the cable shows maximum error occurs at the middle of the reach, with a mean error of -0.19 ° C. Higher error at this location can be attributed to simplification of groundwater accretion before Granite Boulder Creek. Vegetation data may also have contributed to this error, as LiDAR data used for the study was collected in 2008.

Table 1.2: Clear Sky Model Results

Location	Mean Error, °C	Absolute Mean Error, °C	RMSE, °C
500 m	-0.12	0.14	0.19
1000 m	-0.19	0.22	0.28
1500 m	-0.11	0.14	0.20
End of DTS	0.10	0.21	0.28

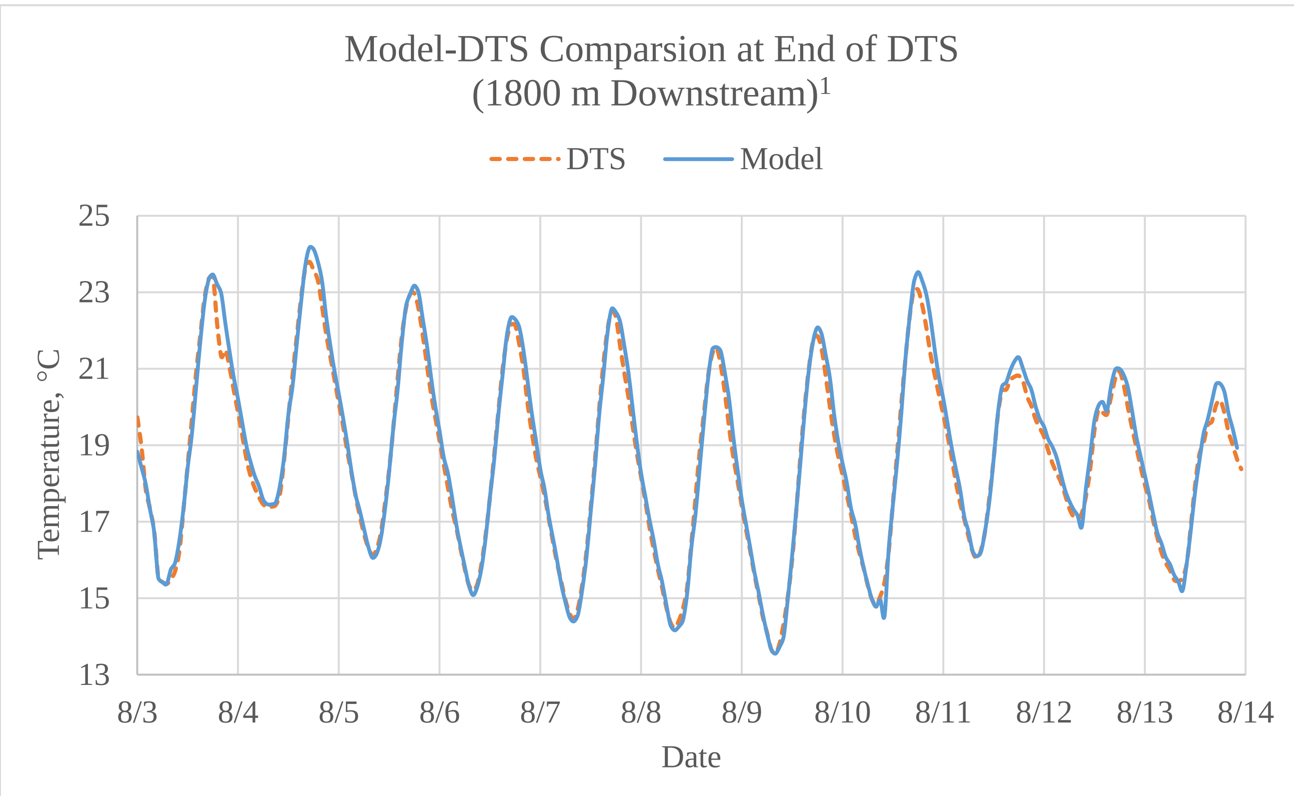

Figure 3.6: Phase 2 Model-DTS Comparison at downstream DTS boundary

[1] Some fluctuations in the DTS data are a product of laser instability and were occasionally present in the in the instrument used in the installation. Most significant is the drop in the afternoon of August 3.

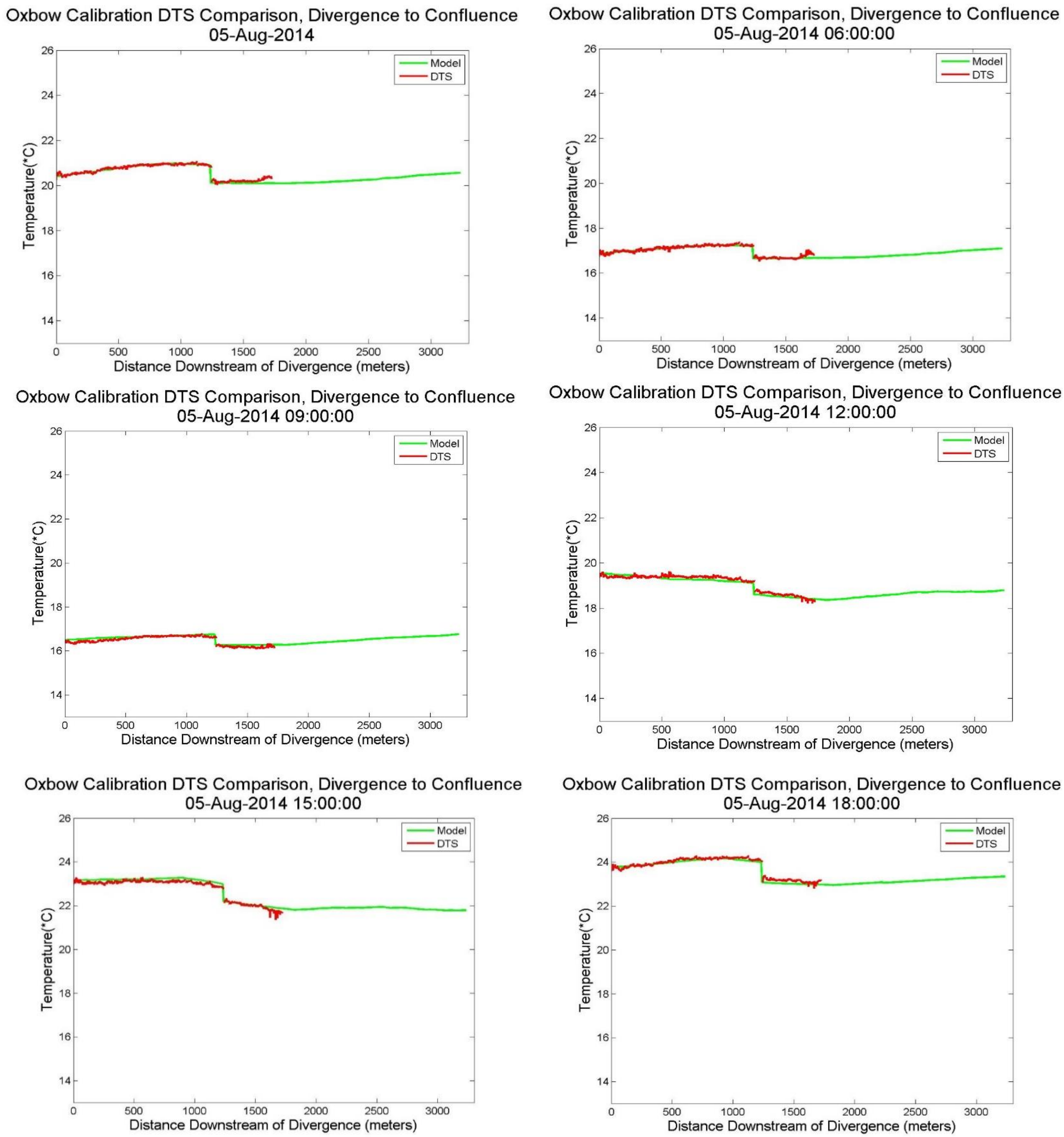

Figure 3.7: August 5 spatial comparison of measured DTS and modeled stream temperatures for select times. The overlapping sections show the spatial fit of modeled and measured data while the extended model provides estimates of temperatures downstream.

3.3.2 Modeled Phase 2 Temperature Change

To quantify the effects of the Phase 2 Tailings Restoration project, modeled temperatures were compared at two locations. The first location was selected at the historic north and south channel confluence to measure immediate effects of the channel reconstruction. A second location was selected 1400 m downstream to assess the persistence of temperature change. To reduce ambiguity, all further comparison of post-restoration stream temperatures refers to modeled temperatures. Though modeled temperatures tended to over predict maximum stream temperatures compared to the DTS, comparing pre and post restoration stream models with equivalent assumptions provides more complete insight into changes to stream heating processes. Additionally, model comparisons refer to differences between the first 8 clear recording days, excluding the stormy data at the end of the monitoring period.

At both the confluence and the downstream location, temperatures exhibited higher nightly temperatures and lower daily temperatures. During peak solar heating from 2:00 PM to 5:00 PM the restored model showed average decreases of 0.91 °C (Range: 0.40° C to 1.29° C) and 0.62°C (Range: 0.18° C to 1.15° C) at the confluence and downstream locations respectively. Average nightly temperatures showed increases of 0.86 °C (Range: -0.11° C to -0.95° C) and 0.72 °C (Range: -0.45° C to -0.96° C) for coolest hours of 2:00 AM to 6:00 AM.

In Oregon and other states in the Pacific Northwest, seven day average daily maximum temperatures (7DADM) are utilized as a standard for water quality compliance for salmon bearing streams. Following this metric, average 7DADM for the warmest consecutive seven days in the monitoring period were reduced from 23.38 °C to 22.73 °C, constituting a 0.65 °C decrease following restoration. Downstream, this translated to a reduction of 0.54 °C from 23.48 °C to 22.94 °C.

Table 3.3: Modeled changes in average nightly, daily, and maximum stream temperatures following Phase 2 restoration.

Location	**Nightly Change, °C (2:00 AM-6:00 AM)**	**Daily Change, °C (2:00 PM-5:00 PM)**	**Change 7DADM, °C**
Confluence	0.86	-0.91	-0.65
Downstream	0.72	-0.62	-0.54

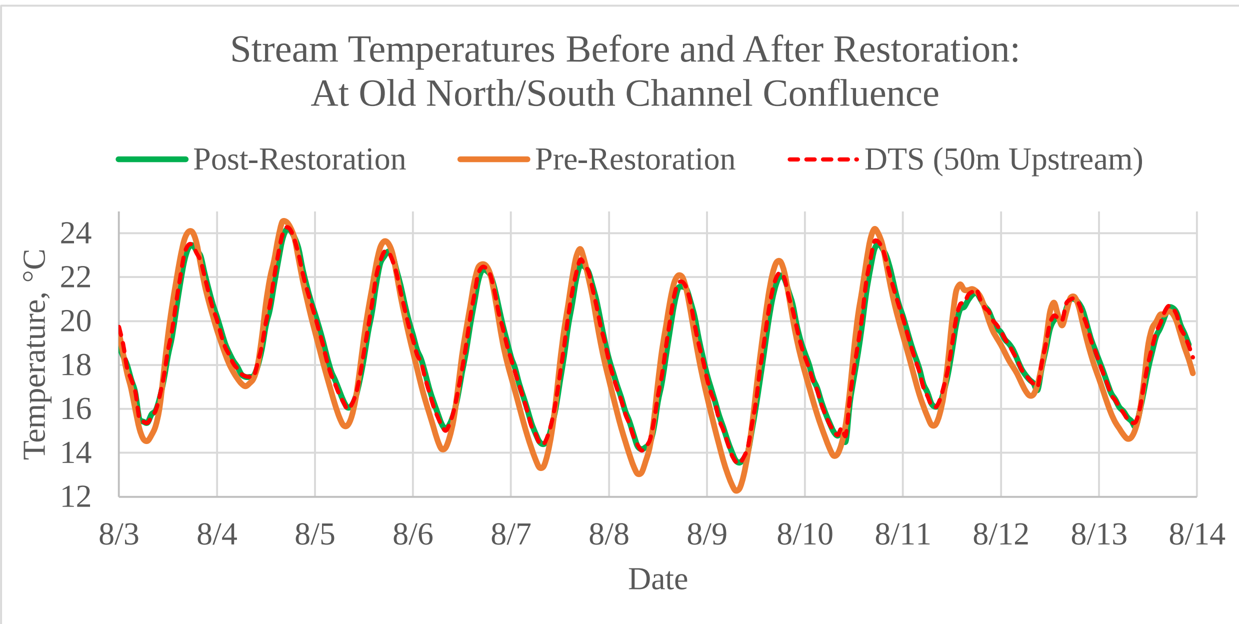

Figure 3.8: Stream temperature comparison immediately downstream of Phase 2 restoration boundary. Changes in stream temperature amplitude are visible on every model day, shown by decreased daily and increased nightly temperatures. DTS data overlaps post-restoration data for calibration reference.

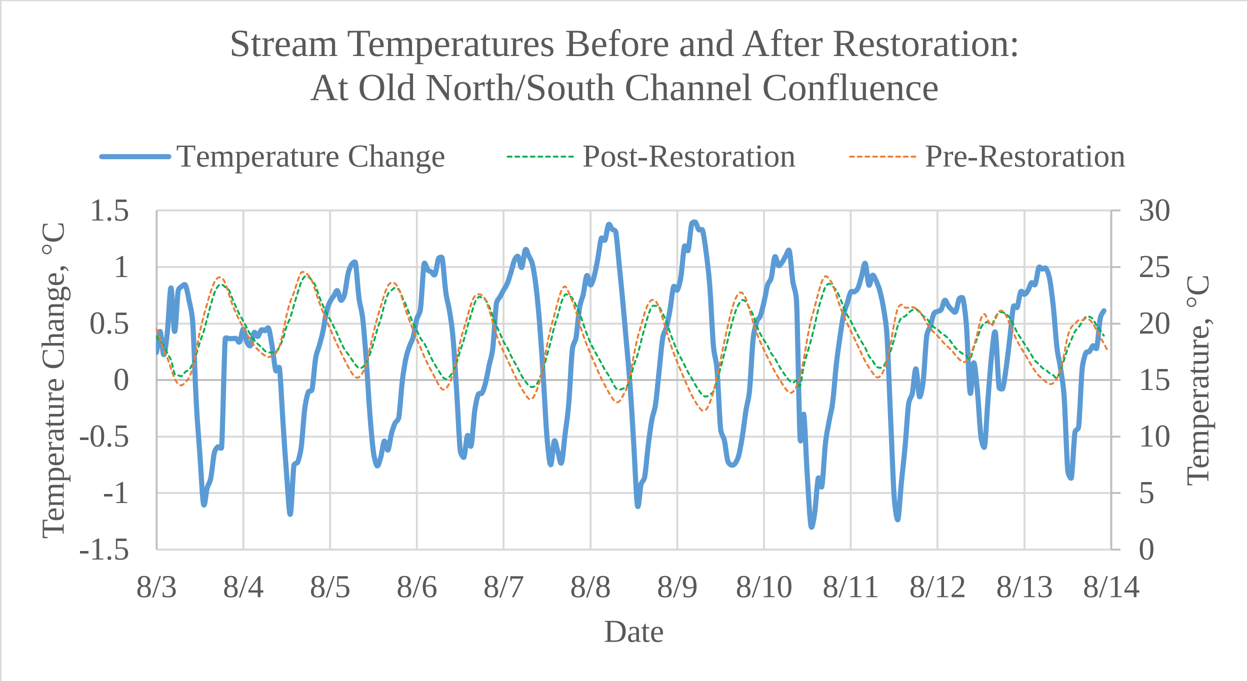

Figure 3.9: Modeled temperature differences downstream of Phase 2 restoration. Greatest temperature differences to do not correspond to hottest periods.

3.3.2.1 Stream Heat Fluxes

The existing restored channel and the historic north and south channels share similar heat budgets for the August 2014 recording period due to comparable channel composition, solar exposure, and riparian vegetation. While the restored channel exhibits a moderate increase in daytime heat energy accumulation compared to that predicted for the historic channels, the combined model heat budgets of the historic channels predicted greater overall downstream heat accumulation. At the peak stream temperature period from 5:00 PM to 6:00PM, modeled restored and historic heat budgets converge, coinciding with a decrease in solar radiation intensity over the stream.

A greater total heat flux was predicted on the modeled restored channel, which increased by as much as 60 W/m^2 (10%) from 12:00 PM to 2:00 PM compared to the modeled historic channels (Figure 3.11). This increase was attributed to less evaporative flux as well as a shift in timing of streambed conduction heating for the modeled restored channel. Increases in temperature for the historic streams during this period resulted in 13-37 W/m^2 greater rates of evaporation. Changes to streambed conduction showed that the modeled restored channel streambed absorbed energy at a 24-40 W/m^2 lower rate than the historic channel models from 12:00 PM to 2:00 PM. However, because the combined historic streams exhibited 40% greater surface area for energy transfer these heat flux changes were insignificant. Additionally, for the shallower historic stream models, less energy was required to heat reduced stream volumes.

Because the streambed material heated more slowly for the deeper restored channel model, it was shown to absorb greater amounts of heat from the stream during hours of peak stream temperature (12-27 W/m^2). This effect contributed to decreases in maximum stream temperature.

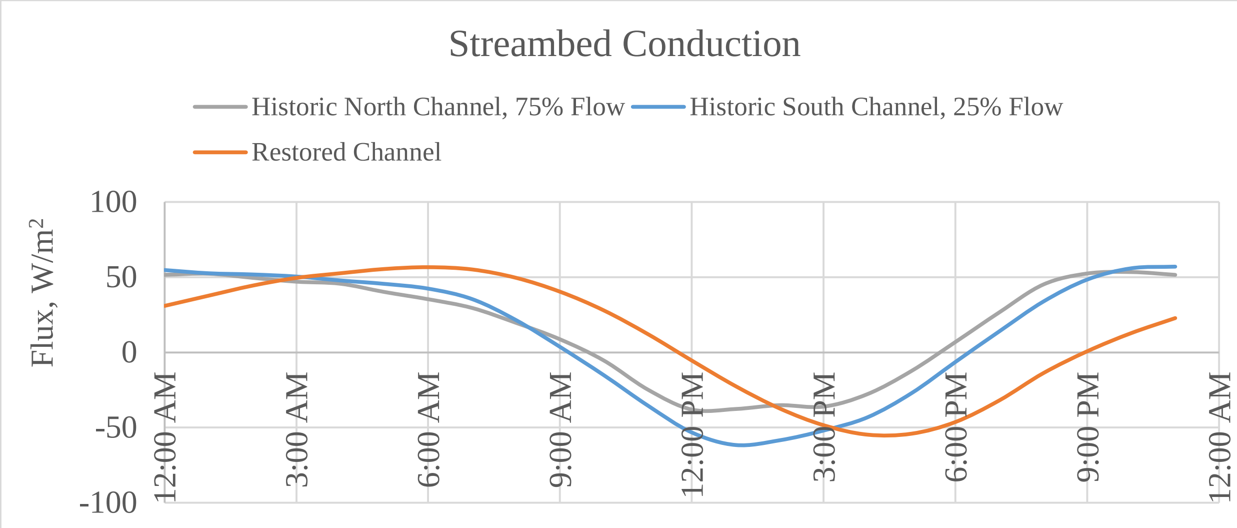

Figure 3.10: The deeper restored channel predicts a shift in streambed conduction heating, contributing the decreases in maximum stream temperature

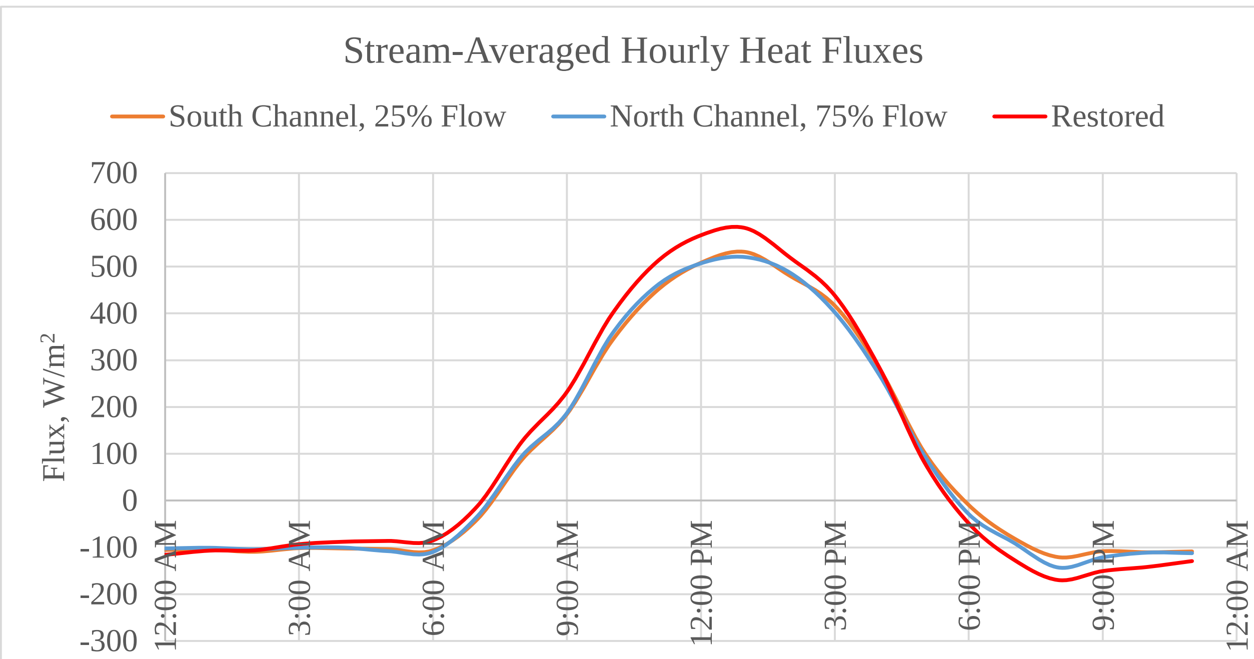

Figure 3.11: Average hourly total stream heat flux for restored and historic stream channels. While the restored channel shows greater total heat accumulation during the day, it is insignificant compared to the combined heating of the historic models.

3.3.2.2 Stream Hydraulics

The hydraulic component of Heat Source predicted stream velocities which were used to approximate residence times over the historic and restored channels. Results indicate that more concentrated flows reduced travel times along the south channel, providing less daytime exposure to solar radiation in a sparsely vegetated reach. The historic north channel exhibited the lowest residence time at 1.25 hours. This conveyance was contrasted by the historic south channel with a residence time of 2.09 hours. The restored south channel showed a residence time of 1.42 hours.

Depths were also 25% lower for the historic channels than for the restored channel, indicating less flow volume in the stream. Reach average depths of 0.41 m were reduced to 0.31 and 0.29 for the north and south channels respectively.

3.3.3 Flow Sensitivity

Streamflow was increased and decreased by 25% to demonstrate the expected effects of the Phase 2 restoration during years with more or less flow. While this does not encompass the range of flows for flood or extreme drought years, it provides insight for typical late summer flows. Altering the range of streamflow by 25% of 2014 flow resulted in increases and decreases in day time and maximum stream temperatures. The model was run for four clear days, August 5-August 9, to determine the maximum expected changes to stream temperature from varied streamflow and compared from 2:00 PM to 5:00 PM and at peak stream temperature periods. Under a 25% flow reduction, the Phase 2 restoration was predicted to reduce 2:00 PM to 5:00 PM temperatures by 1.01 °C and maximum daily temperatures by 0.61 °C immediately downstream of the restoration. Increasing flow resulted in 2:00 PM to 5:00 PM reductions of 0.66 °C and maximum temperature decreases of 0.32° C. At night, temperature differences between the 2014 flow model and the altered flow models were unappreciable, indicating that flow changes had a higher impact on reducing day time temperatures than changing night time temperatures. Further downstream of the project, day time stream temperature change due to restoration is less impacted by streamflow. Decreased flow maximum temperatures were predicted be most alleviated by restoration, with a decrease of 0.84° C.

Table 3.4: Predicted effects of the Phase 2 restoration for 25% varied streamflow.

Location	**Decreased Flow**		**Increased Flow**		**2014 Flow**	
	(2:00 PM-5:00 PM)	**Maximum (5:00 PM-6:00 PM)**	**(2:00 PM-5:00 PM)**	**Maximum (5:00 PM-6:00 PM)**	**(2:00 PM-5:00 PM)**	**Maximum (5:00 PM-6:00 PM)**
Confluence	-1.01° C	-0.61° C	-0.66° C	-0.32° C	-0.91° C	-0.65° C
Downstream	-0.69° C	-0.84° C	-0.54° C	-0.57° C	-0.62° C	-0.54° C

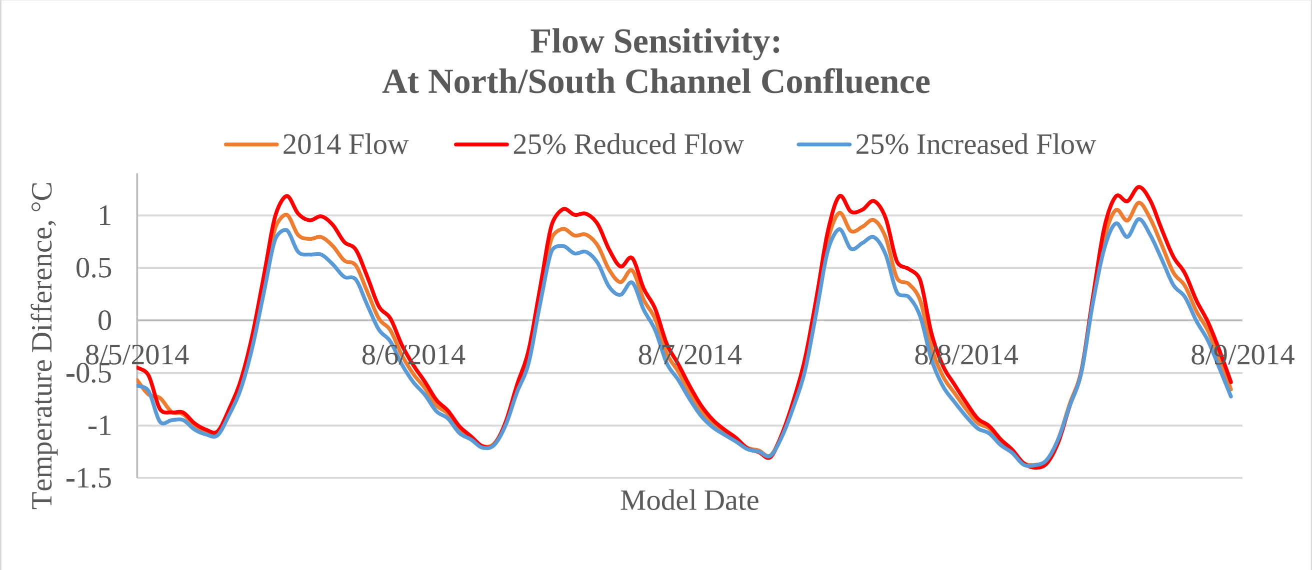

Figure 3.12: Phase 2 effects on stream temperature immediately downstream of the restoration site. While daytime and maximum temperature changes are proportional to flow, nightly temperatures are relatively unchanged.

3.4 Discussion

Effective long-term project planning with an intensive monitoring component can help to ensure that sufficient baseline data are collected several years prior to restoration. However, when projects are added, designed, and implemented in several phases as was the case on the Oxbow conservation property, thorough baseline monitoring is not always available. Even when spatial data exists for both the pre-restoration and the restored streams, varied climate and flow data can confound analysis. In the Oxbow Tailings Phase 2 Restoration project, high resolution DTS temperature were data collected in 2011 during a flood event with early August flows of 2.32 m^3/s. Compared to August 2013 drought flows of 0.66 m^3/s and August 2014 flows of 0.89 m^3/s, pre-restoration temperatures do not represent typical conditions on the Middle Fork and invalidate direct annual comparison between historic and restored streams. This lack of control data necessitated the use of a model to evaluate the Phase 2 restoration.

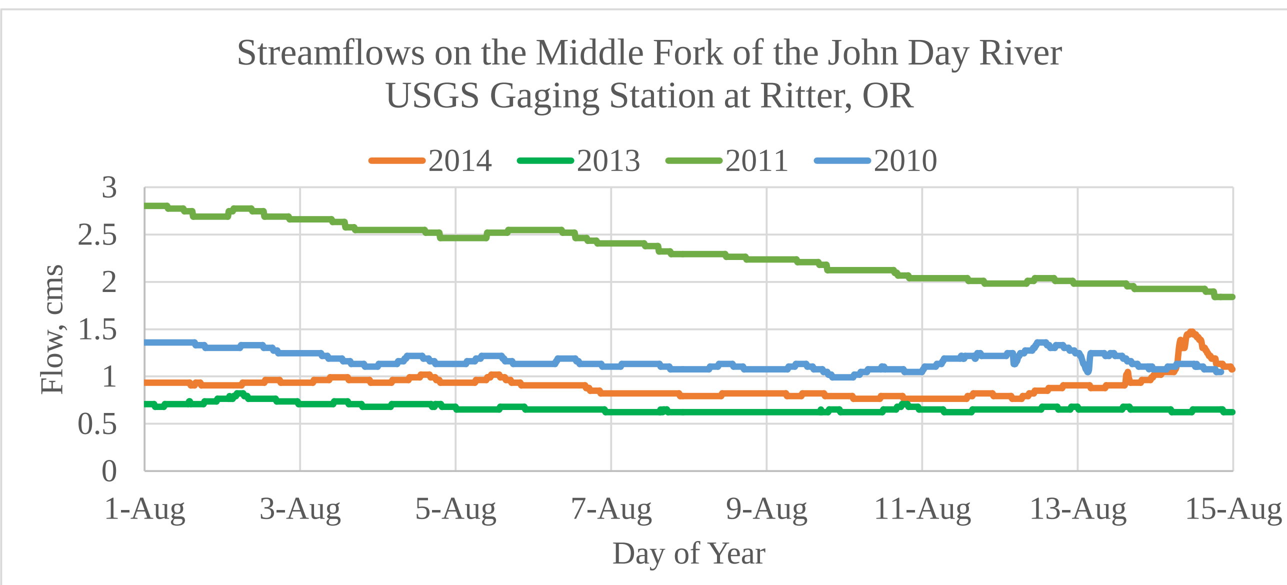

Figure 3.13: Annual streamflow comparison for the Middle Fork of the John Day River, August 1-August 15, measured at Ritter, OR

Results from the Phase 2 stream restoration study demonstrate the utility of a physically based model in providing estimates of stream temperature change after restoration. Recreating existing stream temperatures through the base model quantified underlying stream fluxes controlling stream temperature and provided the comparison of these processes for the historic stream. By adjusting the base model for the pre-restored channel, historic stream temperatures were estimated for equivalent 2014 climate conditions. Comparison of temperatures and energy inputs between these models has shown the effectiveness of stream surface area modifications in reducing both daytime and peak daily stream temperatures for this stream reach.

The removal of the historic north channel equates to a 40% reduction in exposed stream surface area. It also reduced the length of stream 38% from 2,925m to 1,830m. Though residence times were lower for the north channel, less stream surface area has reduced the pathway for shortwave, longwave, and convective heat fluxes to enter the stream. Because stream temperature on the Middle Fork of the John Day River is dominated by shortwave radiation, reductions in stream area correspond to effective reductions of day time stream heating. For 2014 summer conditions, this reduction predicts to average decreases in afternoon stream temperature of 0.91° C (± 0.10) and a decrease of average maximum daily temperatures of 0.65 ° C (± 0.21). The errors for these estimates are derived from measured and modeled downstream conditions and do not incorporate the errors of the DTS instrument itself, which was accurate to 0.2° C.

Flow increases and decreases will affect the magnitude of temperature changes due to restoration. However, future conditions will more than likely include increasing years of summer low flow conditions, validating the importance of this study’s findings. For 25% decreased flows, afternoon temperatures were reduced by an additional 0.10 ° C, while changes to maximum temperatures were negligible. Increasing flow showed restoration was less effective in changing afternoon and maximum temperatures, demonstrated by the respective 0.25° C and 0.33° C changes.

A unique feature of this restoration is the enduring nightly increase in stream temperature which, combined with lower daytime temperatures, provided an overall buffering of diurnal temperatures. This change can be explained by changes in heat flux and the effects of Granite Boulder Creek on the stream reach.

Decreases in stream surface area reduced the pathway for energy to be emitted from the stream through evaporation and longwave radiation, resulting in decreased rates of cooling for the restored channel. Concentrating streamflow from two channels to one channel also contributed to decreased rates of temperature change, with the new channel requiring more energy to change the temperature of the deeper water column. These changes are demonstrated in the general heat transfer equation: $\frac{\delta \mathrm{T}}{\delta t} = \frac{-\boldsymbol{A} * \Phi_{Total}}{\rho_{w} * C_{w} * + \boldsymbol{V_w}}$.

Temperatures cool across all but the south pre-restored channel due to high upstream boundary temperatures and the inflow of Granite Boulder Creek. Increased rates of evaporation and low flows emphasize these changes compared with stream sections downstream where changes are less pronounced. The majority of stream heating occurred on the south channel where high residence times and low flows provided increased relative heat transfer into the stream. Weighting both the north channel and south channel temperature changes by their flow rates shows downstream temperatures are ultimately controlled by the north channel and the cold-water flow contributions of Granite Boulder Creek (Appendix Figure 11). Adding the heating effects of the south channel reduced the ability of the Granite Boulder Creek to cool stream temperatures, leading to higher daytime temperatures downstream of the confluence.

3.4.1 Model Limitations and Additional Uncertainty:

Outputs from a physically based deterministic model such as Heat Source are limited by the quality and resolution of input data. Even with extensive field campaigns, accurately defining spatially and temporally varying parameters is not always feasible. On the Middle Fork of the John Day River, it was found that there is a high degree of variability in microclimates from one valley to the next. Air temperatures at the Forrest property weather station (10.2 km SE) were found to be as much as 8° C cooler for clear nights compared with temperatures recorded at the Dunstan weather station (9.8 km NW). Further, shortwave radiation data indicates the variable nature of cloud cover on less clear days. Due to the inability to quantify climate variability on the stream reach scale and the unpredictability of atmospheric emissivity during cloudy periods (Boyd & Kasper 2003), a higher degree of uncertainty exists for non-clear sky periods. Previous evaporative studies on the Middle Fork of the John Day River (Benner, 2000) also indicate that wind speed and direction were unique across most study sites and influenced largely by stream banks and streamside vegetation. Due to the inability to model this heterogeneity, these factors were estimated through model calibration.

To model stream temperatures on the Middle Fork of the John Day River several assumptions were required. These include simplifications for data inputs as well as Heat Source methodology. While vegetation on the Middle Fork provides low levels of effective shade for the stream, LiDAR-derived vegetation data was collected in 2008 and may be a slight underestimate of current conditions. Stream boundary base flow, hyporheic flow, and groundwater flow were assumed constant in temperature and flow magnitude throughout the study. While DTS temperature data does not provide strong evidence for variability in these parameters, some fluctuation is likely. Additionally, because synoptic discharge measurements did not reveal flow losses, hyporheic flows were represented as shallow groundwater inflows.

3.5 Summary and Conclusion

Modeled stream temperatures suggest that Phase 2 of the Oxbow Tailings Restoration was effective in reducing stream temperatures downstream of the project. Filling over the dredge-mined channel resulted in a stream area reduction of 40%, effectively scaling down the amount of heat energy received by the stream. Because minimal vegetation exists along the stream, this reduction in stream temperature was directly related to the amount of shortwave solar radiation entering the water column. In addition to reducing overall stream surface area, Phase 2 concentrated flow volumes into the south channel, increasing flow depths and decreasing the rate of temperature change along the reach.

Phase 2 was shown to alter temperatures at three distinct periods throughout the day, described by a dampening of diurnal temperatures. As the result of decreased energy loading, maximum temperature decreases of 0.91° C were observed directly downstream of the north/south channel confluence during peak midday heating. Maximum 5:00 PM to 6:00 PM evening stream temperatures were also shown to decrease by an average of 0.65° C for the restored channel during clear sky conditions. The third temperature change was observed at night, when temperatures were shown to increase an average of 0.86° C.

Changes in heat budgets alone did not describe the changes in temperatures throughout the day. While changes in streambed conduction, longwave radiation, and evaporation were observed between the restored and existing channels, cold-water inflows were also responsible for cooling the stream. With restoration, the ability of Granite Boulder Creek to cool the Middle Fork was increased. During maximum stream temperature periods, Granite Boulder Creek was found to be the greatest determinant of downstream temperatures providing 25% flow contributions at temperatures 2.5° C below Middle Fork stream temperatures. These differences were 1.7 ° C at night when warmer restored temperatures were described by decreased energy emitted from the stream.

Chapter 4: Predicting the effects Phase 3 Channel Reconstruction

4.1 Introduction

Stream temperature is a limiting factor for salmonid species on the Middle Fork of the John Day River where summer temperatures often meet or exceed the thermal incipient lethal limits. Since its designation as a Threatened and Impaired Water under section 303 (d) of the Clean Water Act, extensive efforts have been made to restore the Middle Fork of the John Day River back to its historic state and improve the integrity of the endangered fishery. At the Confederated Warm Springs Oxbow Conservation Property on the upper Middle Fork of the John Day River, a multi-phase restoration spanning several years has been underway. Despite anthropogenic changes beginning in the 1930s, this section of river holds several cool tributaries, features vital for cold-water fish survival. Phase 1 of the Oxbow Tailings Restoration Project began in 2011 with the addition of log structures in the historic south channel. In the following year, Phase 2 was completed, modifying the path of the Granite Boulder Creek tributary and filling in a channelized section used in historic mining operations while redirecting streamflow to the historic south channel.

These projects set the stage for the next phase of the Oxbow Tailings Restoration Project, which seeks to reconstruct a stream section downstream of the Phase 2 project, also the product of past dredge mining practices. Phase 3 involves the creation of 1,700m of meandering river channel with the objectives of enhancing fish habitat, restoring wetlands, and improving connection with Ruby Creek tributary. Extensive tree planting and fencing are included in the design in an effort to reduce stream temperatures despite a 300 m stream length increase.

4.1.1 Stream Temperature and Stream Temperature Modeling

Flow characteristics, channel morphology, and near stream attributes such as riparian vegetation all control the influence of atmospheric inputs into the stream, the primary driver of stream heating (Sinokrot and Stefan 1993; M. S. Boyd 1996; George W. Brown 1969). Understanding the influence of each of these parameters can help establish restoration priorities for temperature and predict changes to the stream system.

The influence of riparian shading in reducing shortwave solar radiation has been studied extensively in the Pacific Northwest. Conclusions indicate that riparian vegetation can greatly reduce summer stream temperatures as well as improve bank stability (Beschta 1997). Even at scales as low as 150 m, the addition of shade has been shown to reduce maximum stream temperatures (Johnson 2004). The influence of solar radiation and the ability for streamside vegetation to mitigate its heating effects is directly controlled by the air-water interface of the stream. Brown reiterated this fact in his research, stating the correlation between stream surface area and volume to stream temperature (Brown 1972).

Physically-based deterministic models coupled with high resolution monitoring data are useful for recreating historic stream temperatures and quantifying the effects of restoration. Particularly when limited data and variable climate conditions mask short-term changes, stream temperature models can provide an effective means for comparison. Another important restoration application of stream temperature modeling is predicting the effects of future management scenarios. By employing the same process-based approach, one can predict the effects of changes due to channel reconstruction, altered stream vegetation, and varied surface area on stream temperature.

4.1.2 Scope of Study

The goal of this study is to quantify projected temperature changes from the Phase 3 project and to identify effective restoration strategies to inform future efforts. By combining high-resolution monitored temperature data with a stream temperature model, a comparison can be made between the straight existing channel and the future restored channel. Temperature data collected in 2013 and 2014 using distributed temperature sensing (DTS) technology serves as validation data for the model, informing inputs of uncertain physical parameters like evaporation and stream hydraulics. Rather than recreate historic temperatures as was demonstrated previously, the Phase 3 calibrated model is applied to project stream temperatures for the future designed channel. The objectives for this study focus on the quantifying the effects of altering stream area and stream length, aspects that are slated to increase as the result of restoration. Select scenarios are also modeled to predict temperature mitigation for future riparian vegetation growth. The developed model seeks to answer the following questions:

1) How will the Phase 3 channel reconstruction affect stream temperature under equivalent 2014 climate and flow conditions?
2) How will vegetation mitigate stream temperature increase on the Middle Fork?
3) How does stream surface area affect the river's temperature and heat budget?

While an objective of this study is to predict the temperature effects of the Phase 3 restoration, the absence of as-built future channel hydraulic data and bank surface widths limit the exactness of this comparison. As a result, the modeled unmodified restored channel likely represents a wider stream than what is to be constructed. Nevertheless, by modifying stream widths, a range of expected temperature changes for various surface areas can be created which can be used to validate restoration when current channel data is available.

4.2 Methods

Phase 3 methodology describes the DTS monitoring field campaign conducted in August, 2013 and the stream temperature model setup, calibration and application for the Oxbow Phase 3 restoration project. Data collected during this period includes longitudinal stream temperatures in addition to stream depths and associated locations mapped using high precision GPS.

Analysis of the Phase 3 restoration project was conducted by combining direct stream temperature measurements with the deterministic model, Heat Source (ODEQ, 2012). Remote sensing, onsite weather stations, and direct field measurements were all used to source inputs for a stream temperature model with 5m spatial resolution. This model was calibrated with 2013 climate and DTS data collected prior to restoration and then applied to the same channel and to the expected restored channel under equivalent 2014 climate and flow conditions. Further exploration of channel modifications assume 2014 climate conditions for equivalent comparison. The following procedure was developed to explore temperature changes due to Phase 3 and surface area modification:

1. Successfully calibrate a high resolution stream temperature model using distributed temperature sensing data collected in 2013
2. Apply this model to predict stream temperatures under equivalent 2014 flows and climate conditions for the existing and planned restored channels
3. Compare both channels with existing vegetation and improved vegetation scenarios

4. Explore the effects of surface area modifications on the restored Phase 3 channel

4.2.1 Study Site:

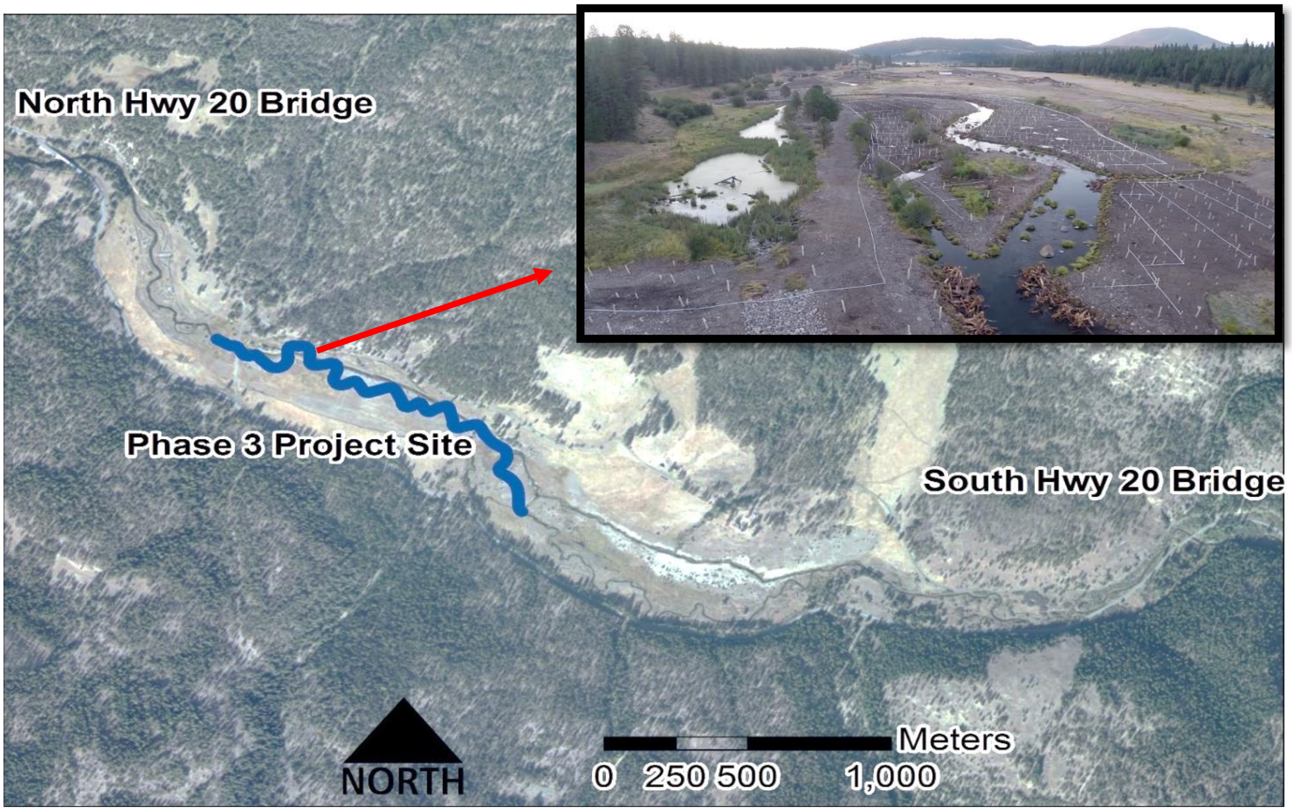

Figure 4.1: The Middle Fork of the John Day on the Oxbow Conservation Area and Phase 3 project site, currently under construction. Photo Credit: Brian Cochran, 2014

The experimental installation study site is centered at 44°38'41.96"N, 118°39'33.81"W on the Confederated Warm Springs Oxbow Conservation Area property located between river km 14 and river km 20 as measured downstream from the Bates Campground Bridge. The Oxbow valley meadow drains an area of 500 km^2 with measured summer streamflows on the downstream river section of ~0.65 cubic meters per second. The average stream gradient for the existing channel is steeper than the upstream river section with an average value of 0.005 compared with 0.0035.

4.2.2 DTS Monitoring Field Methods

Stream temperature data collected in the summers of 2013 and 2014 provide pre-construction data for the Phase 3 Oxbow Conservation Area Tailings Restoration. While data in 2013 provides complete coverage of the project site, temperatures recorded in 2014 only provide data upstream of the project due to the ongoing channel construction that summer. Temperatures were recorded during 1 to 2 week peak heat, low flow periods in an effort to capture high stress conditions for salmonid species.

4.2.2.1 DTS Equipment

A 4-channel Gemini 5100 Distributed Temperature Sensing unit (1m spatial resolution at accuracies +/- 1°C for distances under 10 km) was used to collect 8 days of consistent temperature data in early August 2013, adding to the long-term dataset and providing validation for the stream temperature model. 3-minute average temperatures were collected on a 9 minute cycle, providing continuous temperature data for 4 km upstream of the DTS and 2 km downstream. Downstream DTS measurements were collected using two fiber optic cables installed in the left and right sections of the channel while the upstream fiber optic cable was placed in the channel thalweg.

The cable used in the monitoring study was a 6 mm rugged Kaiphone reinforced cable which provided adequate durability and flexibility during the recording period. The multilayered cable housed two fibers that were reinforced by plastic, Kevlar, metal braiding, helical metal tube, and a white high-density polyethylene exterior coating. This cable was adopted to reduce solar radiation bias and cable breaks during the installation.

4.2.2.2 Fiber Optic Cable Installation

The cable was deployed upstream and downstream of the DTS and secured to the streambed every 5-10 m using alluvial rocks. Following the installation of cable, a high precision RTK TOPCON GR-3 survey grade GPS (10mm horizontal, 15mm vertical accuracy) was used to map its location and associated stream depths. At the ends of the fiber optic cable, the inner fibers were spliced together to provide double measurements of temperature along the stream. At the midpoint of the 4-km section, the two 2-km fiber optic sections were spliced together, extending the monitoring coverage. Four controlled, independently measured baths were maintained during the experiment to provide reference temperatures for post-experiment data processing. Fiber optic cable was placed in 25-30 m coils in each of the baths which were independently monitored with HOBO TidbiT v2 and HOBO U22 loggers (accuracies +/-0. 2°C). One ambient temperature bath and one ice bath were located at the site of the DTS, while the other two ice baths were placed at the upstream downstream project terminus. Five additional HOBO TidbiT v2 and HOBO U22 loggers (accuracies +/-0. 2°C) were secured to the cable in the stream and attached to shaded enclosures to provide external references for improved calibration and validation.

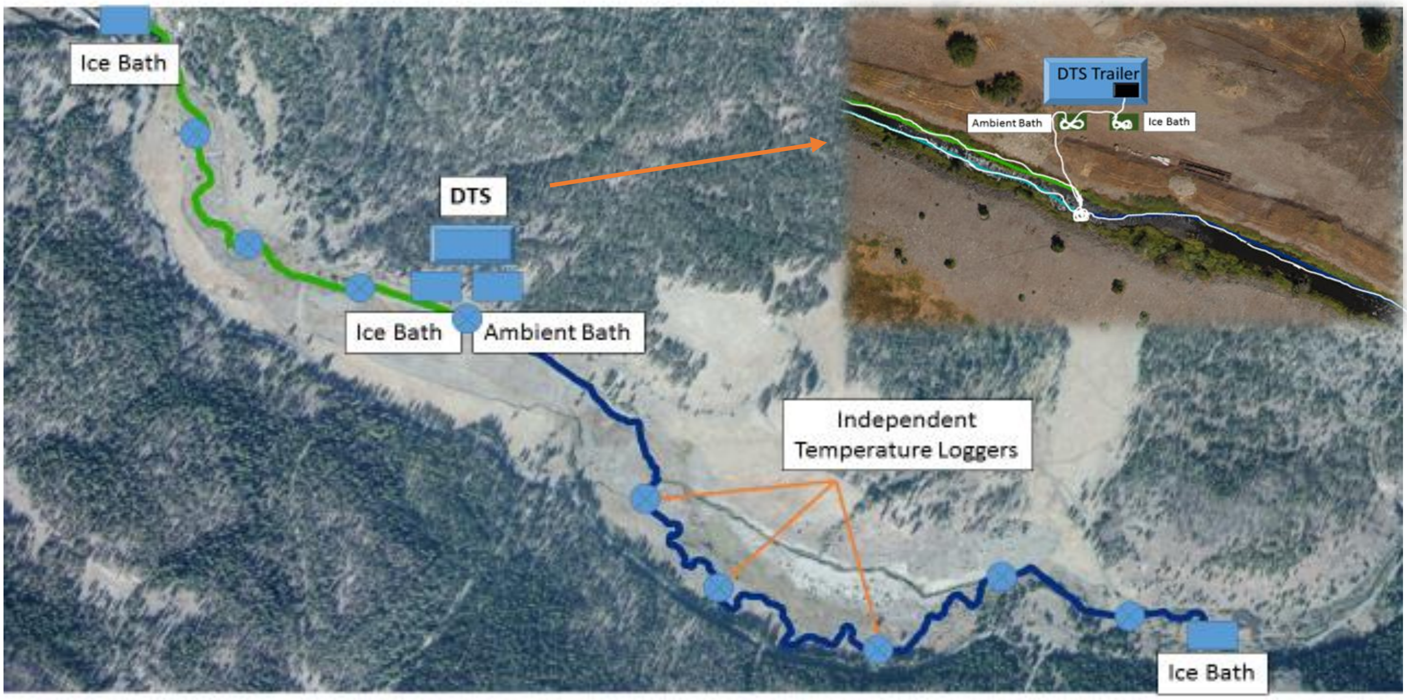

Figure 4.2: 2013 DTS Monitoring Field Installation. Two cable sections extend upstream (NW) and downstream (SE), providing 6 km of stream coverage for model calibration. Map is not to scale.

DTS data calibration and post processing was completed after the monitoring period to convert raw signal data into temperature profiles. Adopting the methodology from (Hausner et al. 2011), MATLAB code was developed to facilitate calibration, incorporating the reference temperatures and cable positions. For more information, the reader is directed to Appendix D.

4.2.3 Phase 3 Heat Source Modeling

Heat Source 8.0.8 (Boyd et al. 2012) was adopted to model and compare stream temperatures at 5m spatial resolution on the Phase 3 restoration site. Two distinct models were developed to provide coverage of the existing pre-restoration channel and the planned Phase 3 design channel. While the stream temperature model developed for Phase 2 adequately modeled stream temperatures on the upstream Oxbow reach, stream geometry and wind sheltering required modification for the less vegetated downstream Phase 3 model. Model calibration was conducted by comparing DTS temperatures collected in 2013 to temperatures modeled on the existing channel under 2013 climate and flows. Following calibration, the existing and planned Phase 3 channel models were run for 2014 climate conditions and compared at the downstream project terminus.

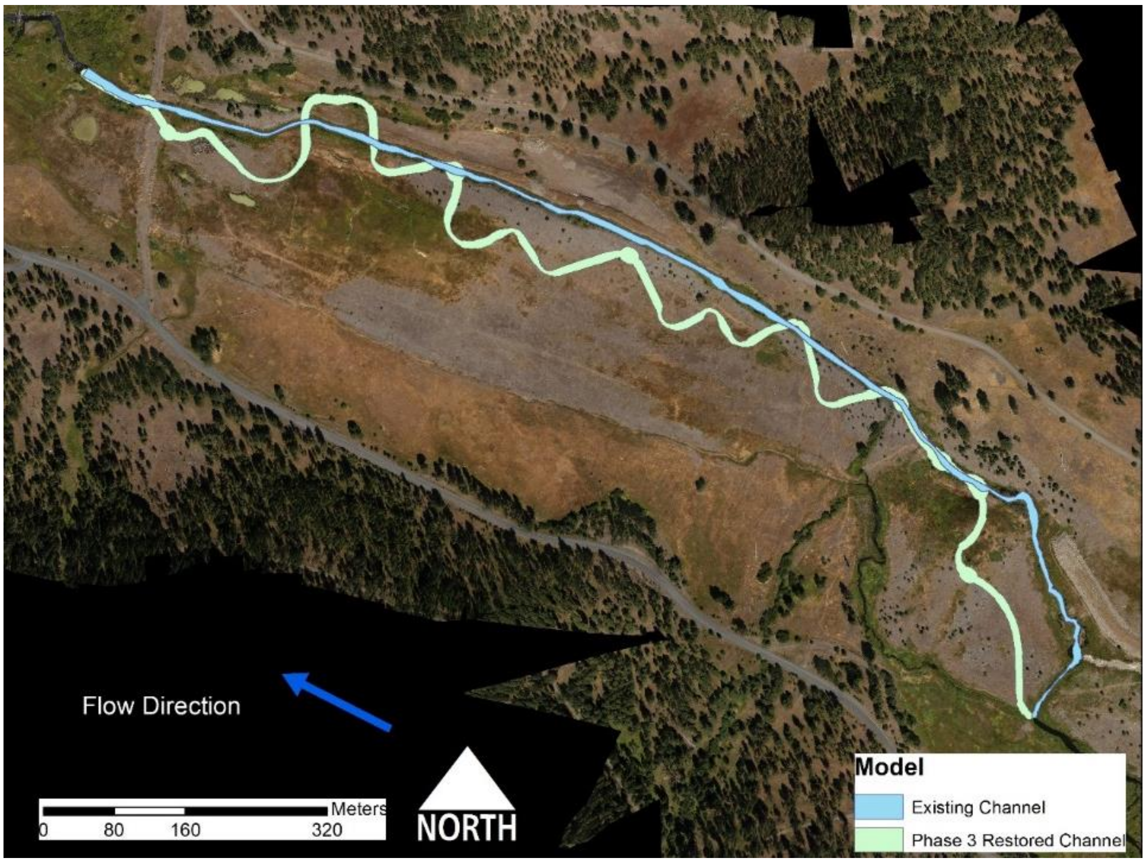

Figure 4.3: Top view of modeled existing and restored Phase 3 stream channels

.

To improve riparian shade along the restored channel, the Phase 3 design calls for the addition of tree plantings, seeding, and browse fencing. For the study, the term effective shade is used to represent to the reduction in shortwave solar radiation due to topographic features and vegetation. Effective shade is defined as the ratio of the difference in potential and received solar radiation at the stream surface divided by potential solar radiation above shading features. To explore the effects of the potential vegetation growth, the 2014 restored Phase 3 channel model was modified, replacing existing native grass that previously provided low effective shade with 5 m high, 50% dense foliage. This vegetation type was sampled from USFS-derived, LiDAR canopy data which exists on a downstream section of the Oxbow Conservation Area property to simulate potential and feasible restored vegetation. Two alternate vegetation scenarios were also run to explore the effects of 10 m, 50% dense foliage and to see how effective a fully matured black cottonwood grove (20 m high, 75% density) would be in reducing stream temperature. Vegetation simulations were modeled with a 1m buffer from the stream bank where no vegetation was defined. Vegetation simulations are summarized in Table 4.1 below.

Table 4.1: Existing and restored channel simulations exploring non-vegetated and vegetated streams

Model	Vegetation	Climate Year
Calibration	Existing	2013
Existing Channel A	Existing	2014
Existing Channel B	5 m, 50% Density	2014
Phase 3 Design Channel A	Existing	2014
Phase 3 Design Channel B	5 m, 50% Density	2014
Phase 3 Design Channel C	10 m, 50% Density	2014
Phase 3 Design Channel D	20 m, 70% Density	2014

Shortwave solar radiation is the primary driver of stream temperature for the Middle Fork (Diabat 2014; Crown and Butcher 2010; Benner 2000). Because the amount of radiation entering the stream is proportional to the stream's surface area, it was of interest to explore the relationship between and temperature and channel area. Heat Source does not require top width as an input. Rather, it calculates top width as part of its hydraulics package using stream flow, bank angle, and bottom width. To accomplish the desired increase in surface area, bottom widths were adjusted to stimulate changes in top width. Hydraulic model outputs of stream top widths were then used to redefine vegetation along the stream, which was resampled prior to running the heat transfer component of Heat Source. Three additional scenarios were run to explore the effects of surface area on stream temperature. Two models simulated 50% and 100% increases to the stream's bottom width, while the third reduced current bottom widths by 50%. Corresponding changes to surface area are tabulated in Table 4.2.

Table 4.2: Restored channel simulations for varied stream surface area

Model	Vegetation	Surface Area	Climate Year
Phase 3 Design Channel A1	Existing	-27%	2014
Phase 3 Design Channel A2	Existing	32%	2014
Phase 3 Design Channel A3	Existing	67%	2014

The outlined model parameters describe the inputs for the 2013 calibration model of the existing channel in addition to the existing channel and Phase 3 restored channels for 2014 conditions. The 2014 dataset was utilized for restoration comparison to provide equivalent analysis with the Phase 2 restoration study. The streamflow survey conducted in 2014 also provided more accurate inputs and showed stream conditions for that year were closer to typical average annual summer flow values. A complete derivation of model inputs and sources can be found in Appendix D.

4.2.3.1 Spatial Inputs:

Spatial inputs for the existing stream temperature model were collected from ground measurements and sourced from remotely sensed data of the Middle Fork. High resolution imagery created from a 2013 structure from motion survey (Dietrich 2014) was used to map bank widths while 2008 LiDAR provided stream elevations and gradients. Vegetation shading data was sourced from digitized LiDAR-derived canopy height and canopy closure imagery provided by United States Forestry Service in Portland, OR. These data were sampled within a range of 60m from the stream using the Heat Source companion tool, TTools. Channel geometry was sourced from top width measurements and stream depth measurements collected in 2013. Heat Source's hydraulic modeling component was used to calibrate field data and determine equivalent bank width to depth ratios.

Planned channel geometry inputs for the future restored channel were sourced from design data provided by United States Bureau of Reclamation. This included hydraulic outputs from HEC-RAS and a DEM of the planned channel. Restored channel vegetation was established using similar methods as the existing channel with a modified native grass vegetation layer that filled over the existing channel. Potential streamside vegetation was defined based on the model scenario while maintaining existing developed vegetation, consistent with Phase 3 plans.

4.2.3.2 Continuous Data:

Hourly temperatures at the upstream boundary of the current channel were measured by DTS in 2013 and 2014 for the respective models. Streamflows for 2013 were sourced from the North Fork of the John Day River Watershed Council while 2014 flows were measured using synoptic streamflow measurements. Streamflows were 0.60 m^3/s in 2013 and 0.65 m^3/s in 2014. Daily fluctuations in flow were ignored for the study period, a reasonable assumption for late summer flows on the Middle Fork. Flows from the tributary Ruby Creek were included in the model, though flows were minimal at 0.01 m^3/s. dry during the recording period. Hourly meteorological data was provided from the Dunstan conservation property, 9.2 km downstream.

Hyporheic exchange was assumed negligible for the both the restored and existing channel models. Evidence from past studies on the Middle Fork indicates that hyporheic flow is largely absent at reach and sub-reach scales (Huff 2010; Kristopher K. Wright 2005). This assumption can carried over with minimal error for the straight existing channel. Though the increased sinuosity of the design channel carries the potential for promoting hyporheic exchange to buffer temperatures and create isolated refugia, the scale of these features is not expected to dramatically affect the total heat budget (Burkholder et al. 2008). Table 4.3 summarizes key model input parameters for the Phase 3 models.

Table 4.3: Heat Source inputs and sources for the Phase 3 restoration models

Model Inputs	Value	Procedure	Source
Existing Vegetation	0-19.8m	2008 LiDAR-derived imagery	United States Forestry Service (USFS)
Topographic Angle	2.6-7.2°	10m DEM	Oregon Geologic Data Compilation (OGDC)
Stream Elevation	1125-1134m	2008 LiDAR-derived bare earth imagery, BOR HEC-RAS	USFS, Bureau of Reclamation
Stream Width	1-13m	2013 structure from motion survey, BOR HEC-RAS	University of Oregon (Dietrich, 2014), Bureau of Reclamation
Streambed Porosity	0.29	Gravel Counts	University of Oregon (2008-2011)
Streambed Thermal Conductivity	2.0 W/m/°C	Literature	Thermal properties for basalt, Eppelbaum, Kutasov, Pilchin 2014
Streambed Thermal Diffusivity	0.006 cm^2/sec	Literature	Thermal properties for Basalt, Eppelbaum, Kutasov, Pilchin 2014
Bank Angle (Width/Depth)	0-15	Measured/Calibrated	Stream measurement/ Model Iteration
Manning's n	0.045-0.075	Literature with calibration	Chow (0.04-0.07), Jarrett (0.056-.183)
Boundary Temperatures	13.6-25.3	Measured	2014 DTS Installation
Streamflow	0.41-0.63	Measured	2014 Streamflow Survey
Groundwater	0.03	Measured/Calibrated	DTS, Model Iteration
Tributary Temperatures	10.6-19.0	Measured	North Fork John Day Watershed Council
Weather	-	Measured	Dunstan Weather Station
Wind Sheltering	0.7	Calibrated	DTS-Model Comparison

4.3 Results

4.3.1 Phase 3 Calibration Model

To calibrate and compare the Phase 3 restoration models, 2013 DTS data were compared with modeled temperatures on the existing channel. Hourly outputs from Heat Source were compared for two days in August; one clear day and one day with intermittent clouds. Time comparison at the downstream model node reveals mean error, absolute error, and RMSE of 0.09° C, 0.17° C, and 0.05° C respectively. The model was shown to over predict daily maximum temperatures by 0.18 °C during clear sky conditions on August 6. It also shows a slight temporal mismatch of cloud cover on August 7, expected due to the separation distance between the stream and the weather station, located 9.2 km downstream. Spatial comparison of the model to the DTS shows better correlation during the night than the day when solar radiation contributes more energy into the stream. Spatial comparison also reveals that the model is unable to predict temperatures in a pool section in the middle of the channel, which was as much as 0.6°C cooler later in the afternoon.

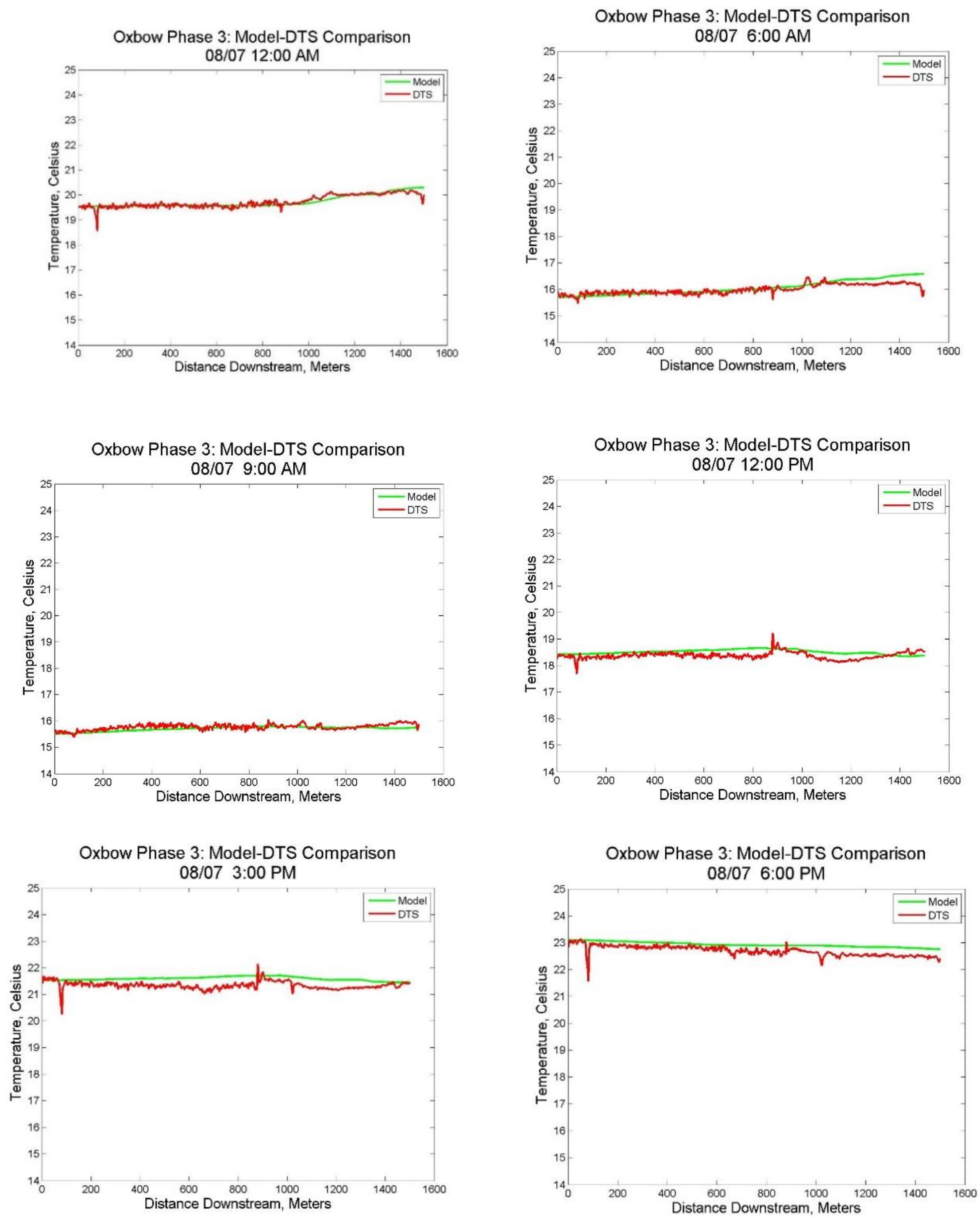

Figure 4.4: Spatial comparison of model with measured DTS data. Model performance is strongest at night and weakest over a deep pool section, apparent at 3:00 PM

4.3.2 Non Vegetated Existing and Restored Channel Comparison

Channel reconstruction is projected to extend the length of the stream 300 m from 1,500 m to 1,800 m, increasing river meanders through the valley floor. Compared to the sedge-lined existing channel, this reconstruction also represents a 70% surface area increase from 10,000 m^2 to 17,000 m^2. Due to these alternations in stream length and geometry, residence times over the reach are projected to increase 25% from 1.24 hours to 1.66 hours.

Results from the Phase 3 model show an overall temperature increase compared to the existing stream model, though this heating was not necessarily tied to maximum daily stream temperatures. Both the existing and projected stream exhibit a positive net heat accumulation during daytime hours leading to maximum stream temperatures and temperature differences occurring at the downstream boundary. It was at this location where channels were compared for the modeling period. For August 3-5, there were notably warmer differences with maximum daily temperature increases of 0.12 °C, 0.17 °C and 0.22 °C for the restored channel. However, other days in the monitoring period showed negligable (<0.1°C) or decreased maximum temperatures. Unappreicable differences can be attributed to the timing of peak stream temperatures which occur later in the evening at 5:00 PM to 6:00 PM, after peak solar radiation emissions into the stream.

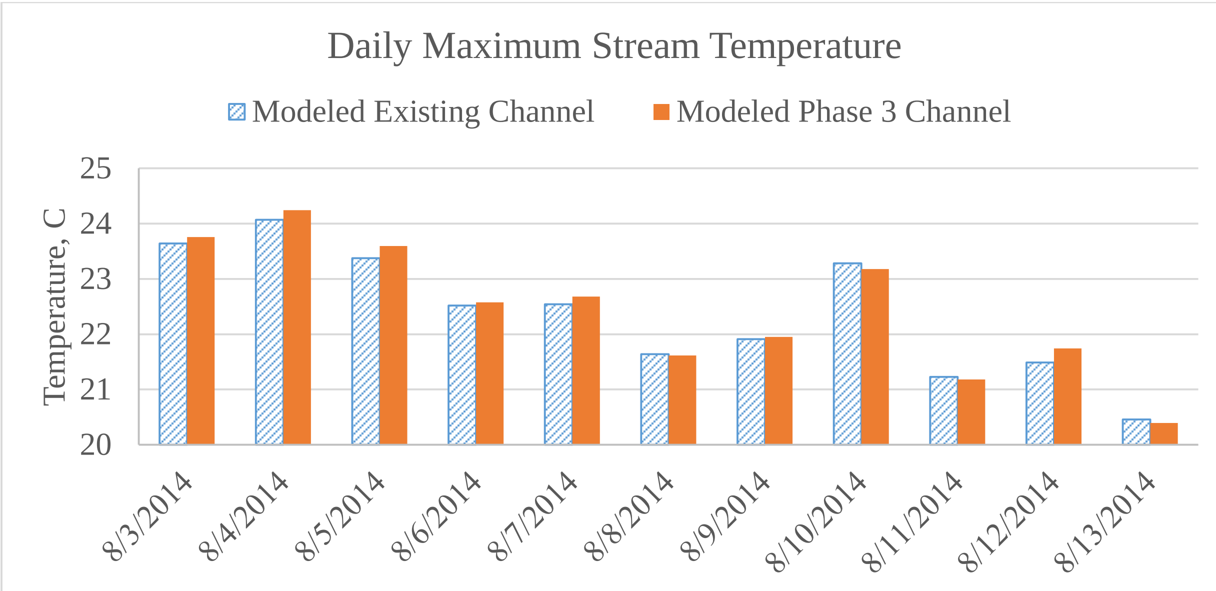

Figure 4.5: Maximum daily temperatures for the existing and non-vegetated stream channels

Comparing hourly temperatures before the daily 5:00 PM to 6:00 PM maximum provides further insight into temperature trends and differences between the two channels. During the day, temperatures diverge downstream as the reconstructed channel accumulates more heat energy than the existing channel. Early in the day from the start of solar loading at 8:00 AM until 4:00 PM, the restored channel showed a consistent temperature increase compared to the existing channel. The largest differences in stream temperature occurred 1 to 2 hours after peak solar loading at 1:00 PM to 2:00 PM, consistent with the streams' residence time. During this period, the downstream boundary was 0.53 °C warmer for the reconstructed channel. After 7:00 PM differences between the two channels were minimal with slight reductions in stream temperatures for the restored channel.

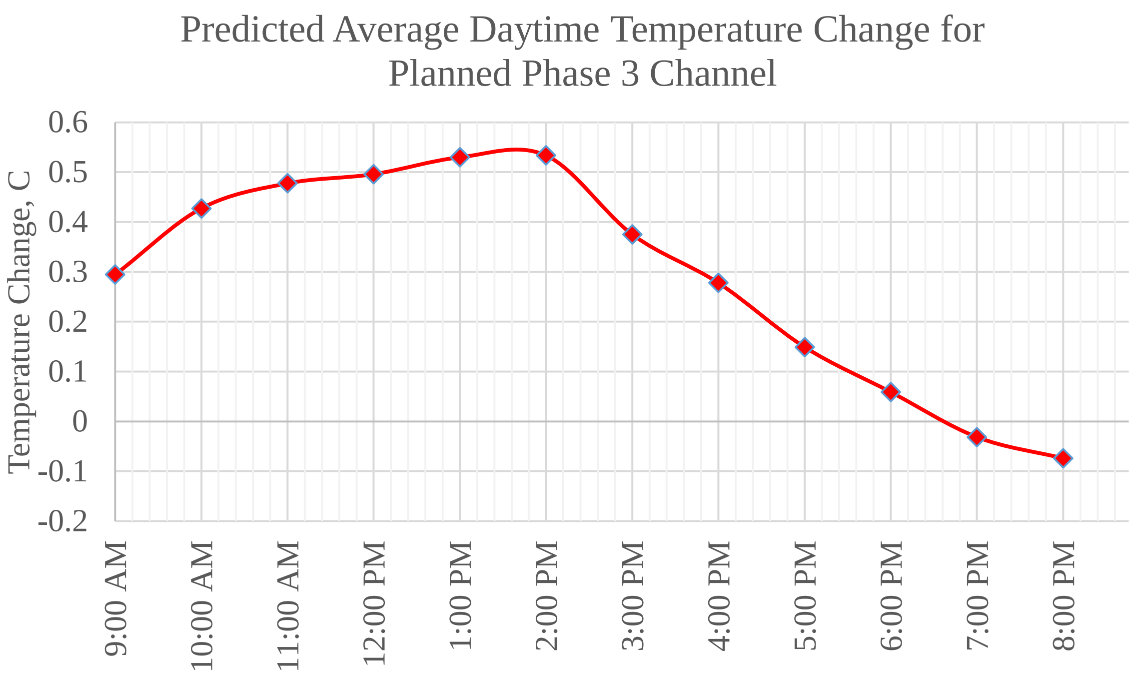

Figure 4.6: Average hourly stream temperature change between the existing and planned, non-vegetated channels. At 6:00 PM, the time corresponding to peak stream temperatures, differences are minor between models.

4.3.3 Phase 3 Temperature Mitigation through Improved Vegetation

The addition of vegetation in the model proved effective in decreasing anticipated stream temperature by reducing the amount of solar radiation received by the stream's water column. For the restored channel, effective shade provided by native grass and stream banks reduced the daily potential solar radiation entering the stream by 5%. Adding the three vegetation scenarios (Table 4.1) raised the daily effective shade to 17%, 34%, and 70% receptively. Hourly effective shade is described for all model scenarios in Figure 4.7.

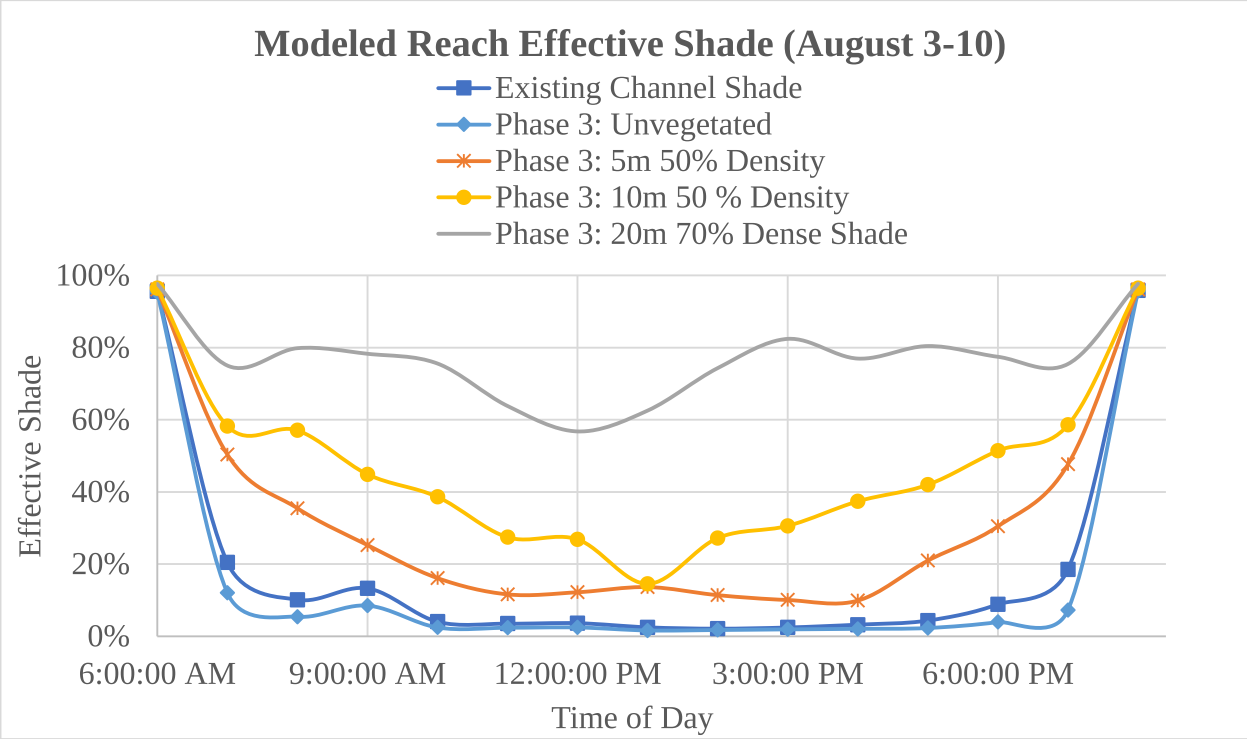

Figure 4.7: Average hourly effective shade for clear monitoring days for non-vegetated and potential vegetation scenarios

Incorporating streamside vegetation provided consistent decreases in expected temperature throughout the day. These changes were apparent in the stream's daily maximum temperature and were most pronounced during hours following peak solar loading from 1:00 PM-5:00 PM. Analysis of vegetated scenario results compares temperatures for both metrics using the restored non-vegetated channel as reference.

The corresponding effects on temperature show that if 5 m high 50% dense vegetation is maintained within 1m of the stream banks, stream temperature increases can be largely mitigated for the restored channel. Average 1:00 PM to 5:00 PM temperatures were reduced 0.32 °C while maximum daily tempratures were reduced by 0.20°C. Doubling the height of effective vegetation to 10m along the reach provided a more pronounced decrease in stream temperatures, reducing

1:00 PM-5:00 PM temperatures by 0.54 °C. This level of shading reduced daily maximum temperatures 0.59°C and delayed the timing of maximum temperature to 7:00 PM. Under the well-developed 20 m high, 70% dense vegetation scenario, channel temperatures were decreased for all hours of the day and the timing of maximum stream temperature was shifted later in the evening to 7:00 PM. Temperatures from 1:00 PM to 5:00 PM for the fully developed canopy are shown to decrease by 1.7°C and while maximum temperatures decreased 0.95°C. For the cloudy period from August 10 to August 11, differences in maximum temperatures are less pronounced.

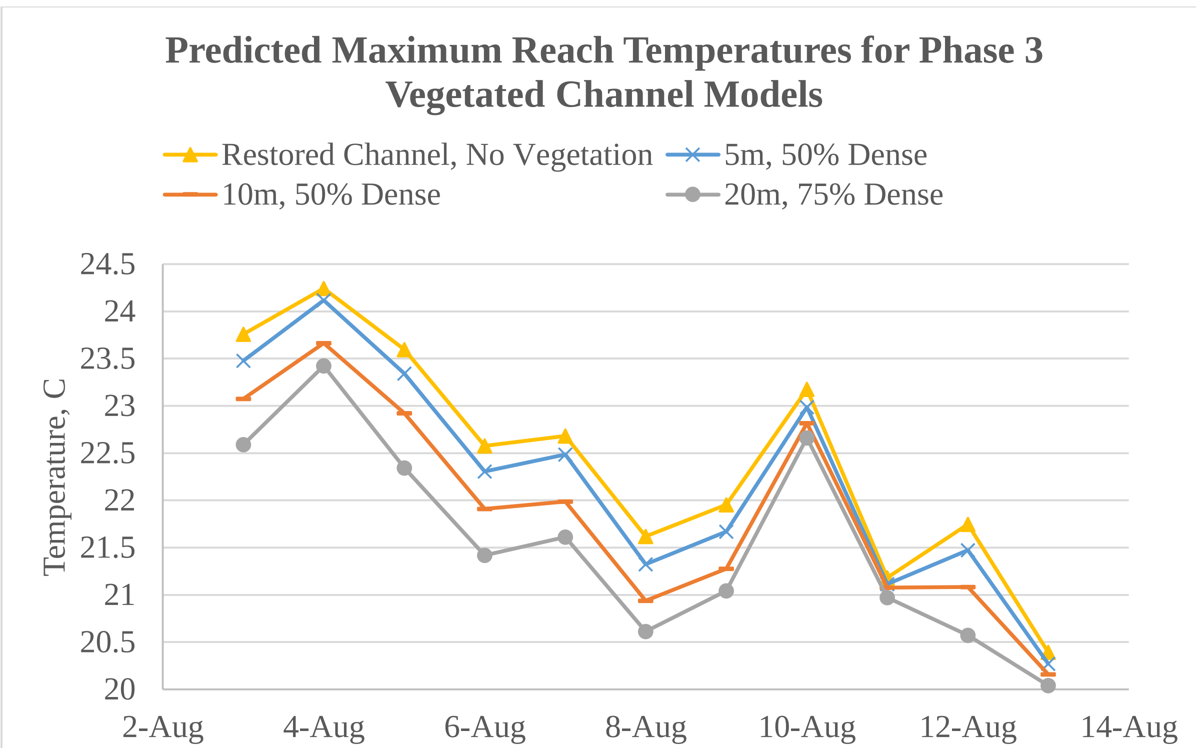

Figure 4.8: Maximum daily stream temperatures for the restored vegetated and non-vegetated models

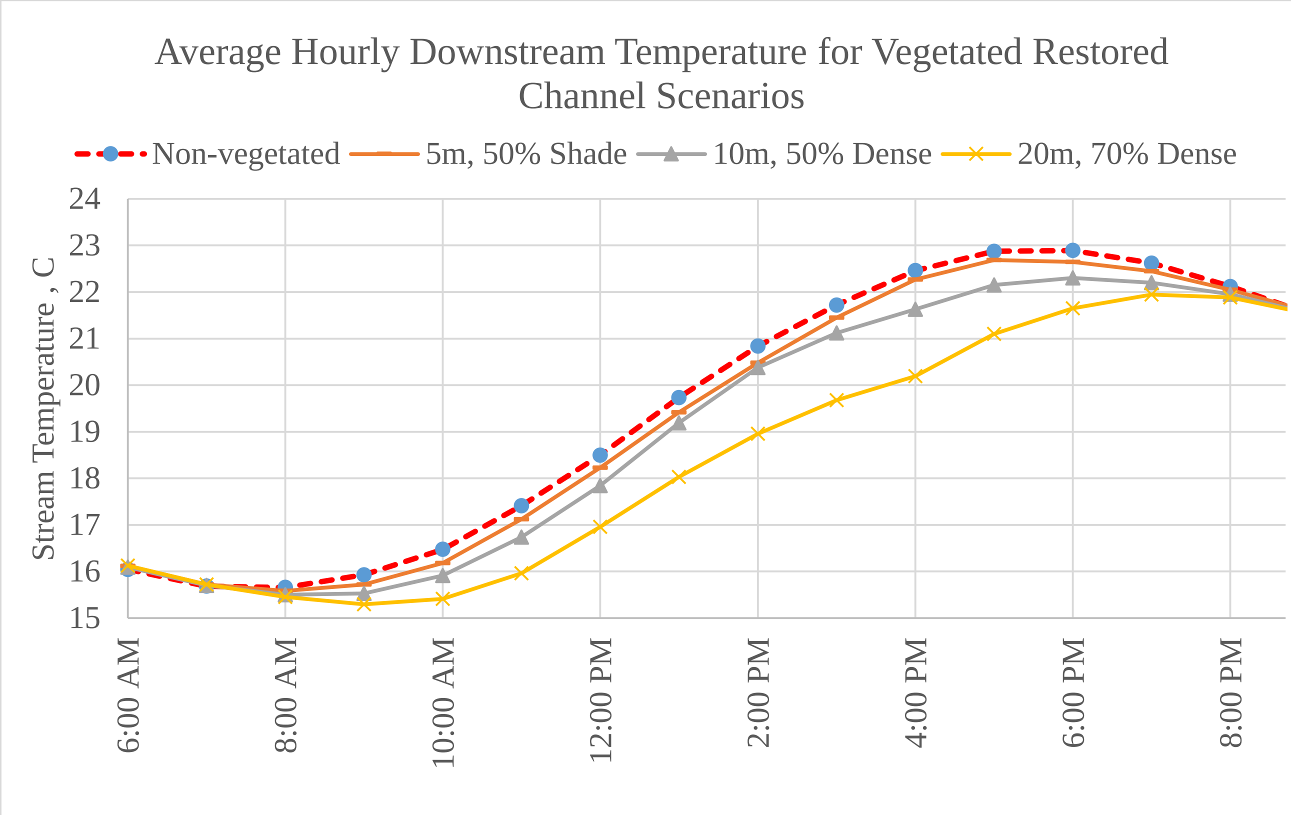

Figure 4.9: Temperatures at the downstream boundary of the restored channel for varied vegetation scenarios

Table 4.4: Maximum and afternoon temperatures and temperature differences between vegetated, restored channel models

Channel	**Daily Effective Shade**	**Daily Maximum Temperature**	**Maximum Temperature Difference**	**1:00-5:00 PM Temperature**	**1:00-5:00 PM Difference**
Restored	5%	22.89	0.00	21.52	-
Restored 5m, 50%	17%	22.69	-0.20	21.26	-0.32
Restored 10m, 50%	34%	22.30	-0.59	20.90	-0.54
Restored 20m, 70%	70%	21.95	-0.95	19.59	-1.7

Comparing temperature changes across the planned Phase 3 restored channel models for different vegetation scenarios revealed a strong linear correlation with daily effective shade. This trend was most linear midday and varied later in the evening as the streams heated at different rates. Averaging daytime stream temperature change from 6:00 AM to 8:00 PM showed stream temperature was directly proportional to incoming shortwave solar radiation. Following the predicted trend, average daytime temperature is predicted to decrease by 0.017 °C per 1% increase in daily effective shade. At hours of peak solar loading, this translated to a reduction of 0.023 °C per 1% increase in daily effective shade.

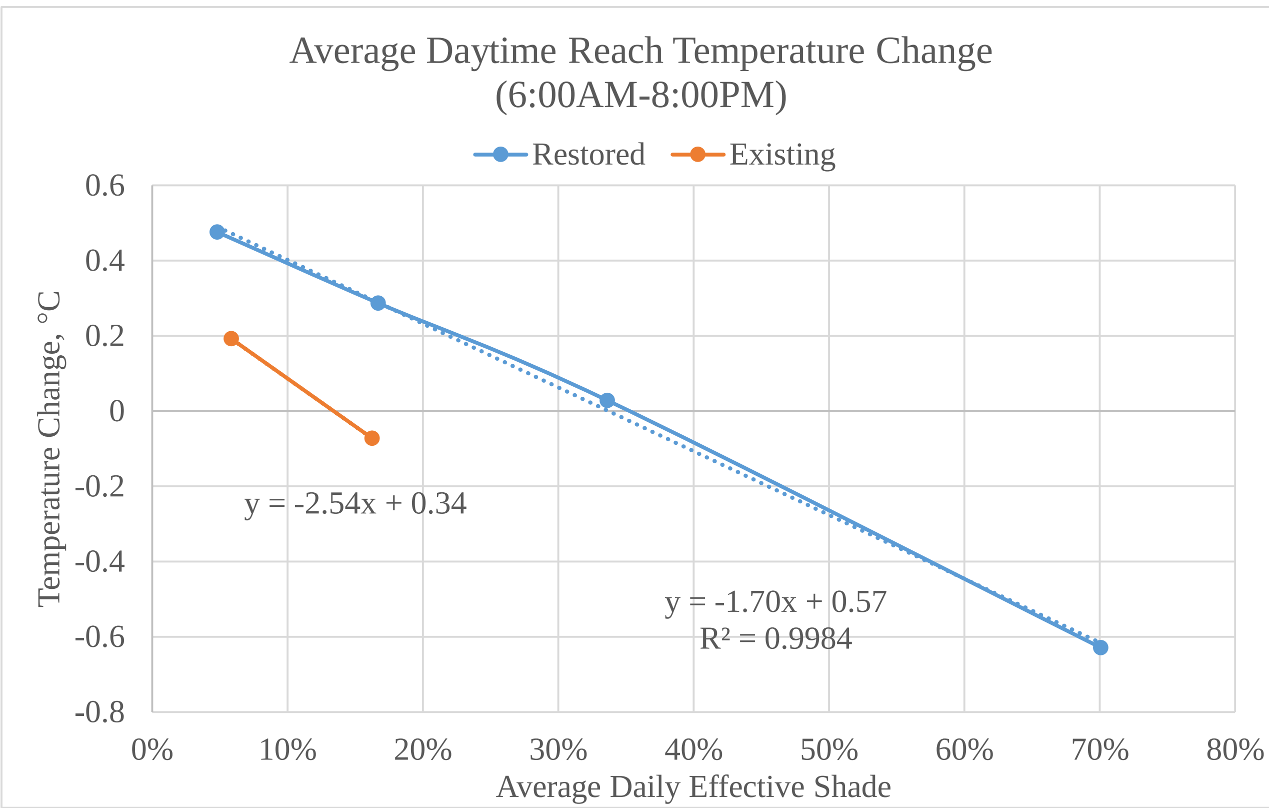

Figure 4.10: Linear trends for temperature mitigation through improved vegetation scenarios

Under a scenario where no channel reconstruction is undertaken, and instead moderate 5 m, 50% dense vegetation is added to the existing channel banks, significant decreases in temperature were observed. From 1:00 PM to 5:00 PM, temperatures on the modeled existing vegetated channel were an average 0.64° C lower than for the modeled unvegetated existing stream. Daily maximum temperatures were also lower, reduced by 0.20 °C . Compared to the planned Phase 3 restored channel, the effects of 5 m, 50% dense vegetation proved more effective in reducing daytime temperatures on the existing channel, shown by a greater 0.26° C decrease in downstream temperatures.

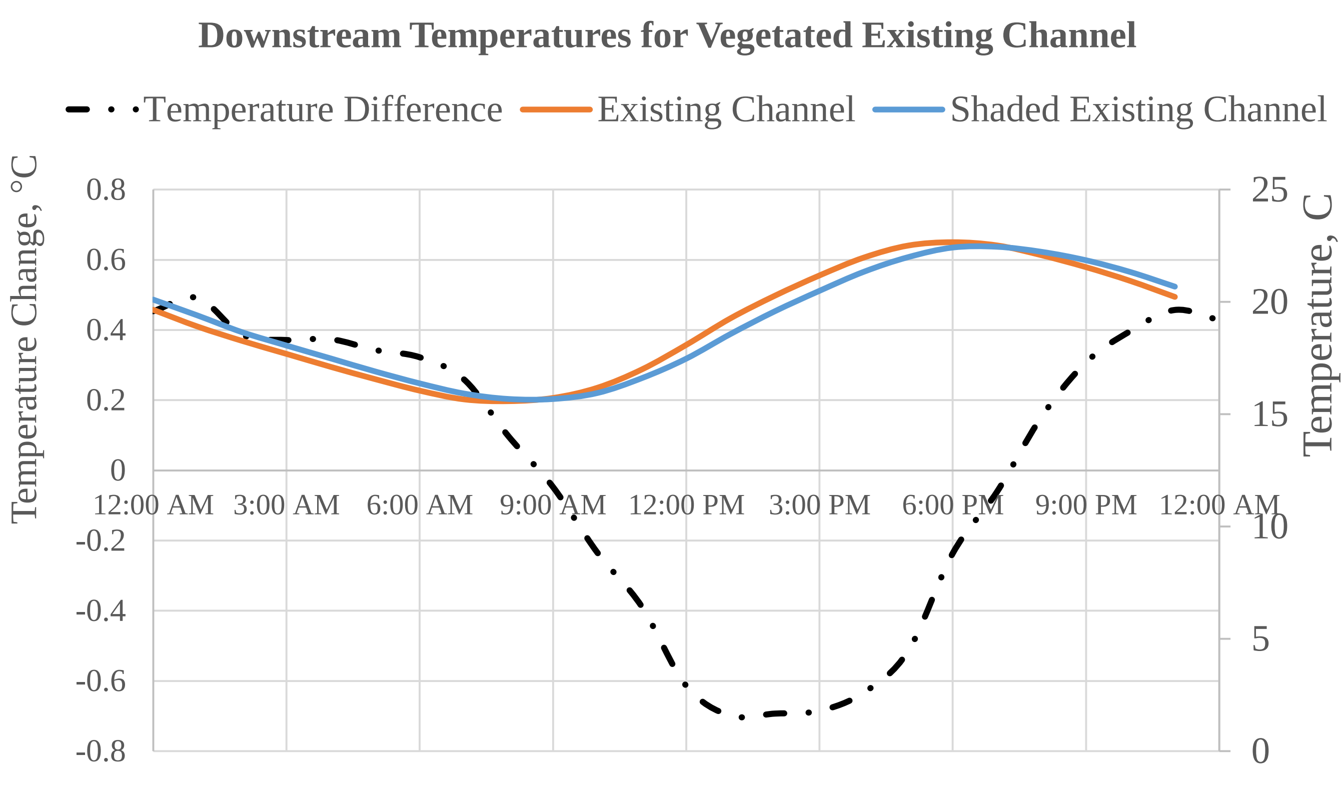

Figure 4.11: Effective temperature decrease for improved vegetation on the existing channel

4.3.4 Phase 3 Areal Study

Results from adjusting the reconstructed channel's surface area reaffirm the stream's sensitivity to shortwave solar radiation. For the existing, minimally vegetated stream, alterations in top width led to proportional changes to stream temperature as well as changes to the stream's residence time. During the period corresponding to solar heating from 8:00 AM to 6:00 PM, stream temperatures were higher for increased area scenarios and lower for the decreased area scenario. Maximum model differences in stream temperature occurred at 2:00 PM while more subtle changes were observed from 5:00 PM to 6:00 PM when stream temperatures were at their maximum. Increasing the new channel's stream surface area from 17,400 m^2 to 23,000 m^2 (+32%) and 29,100 m^2 (+67%) resulted in predicted daily maximum temperature increases of 0.32 °C and 0.78 °C. By decreasing the stream surface area 27% to 12,700 m^2, the daily stream temperature maximum was predicted to drop 0.18 °C. Comparing temperature changes at 2:00 PM across models revealed that temperature was linearly proportional to area. Modeled temperature changes predicted increases of 0.71 °C and 1.41 °C for the wider channels and a decrease of 0.59 °C for the reduced channel. Following solar loading from 7:00 PM until 7:00 AM, steam temperatures in all scenarios converged, indicating that surface area primarily affected daytime temperatures.

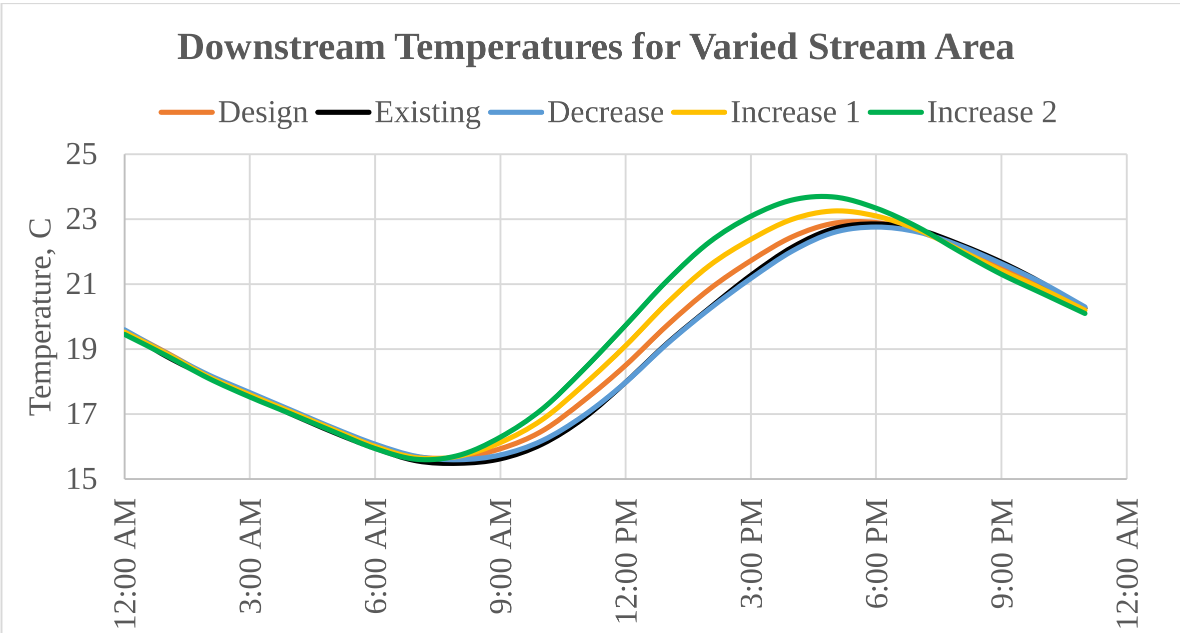

Figure 4.12: Modeled hourly average stream temperatures at the downstream boundary for the existing and restored variable-area channels

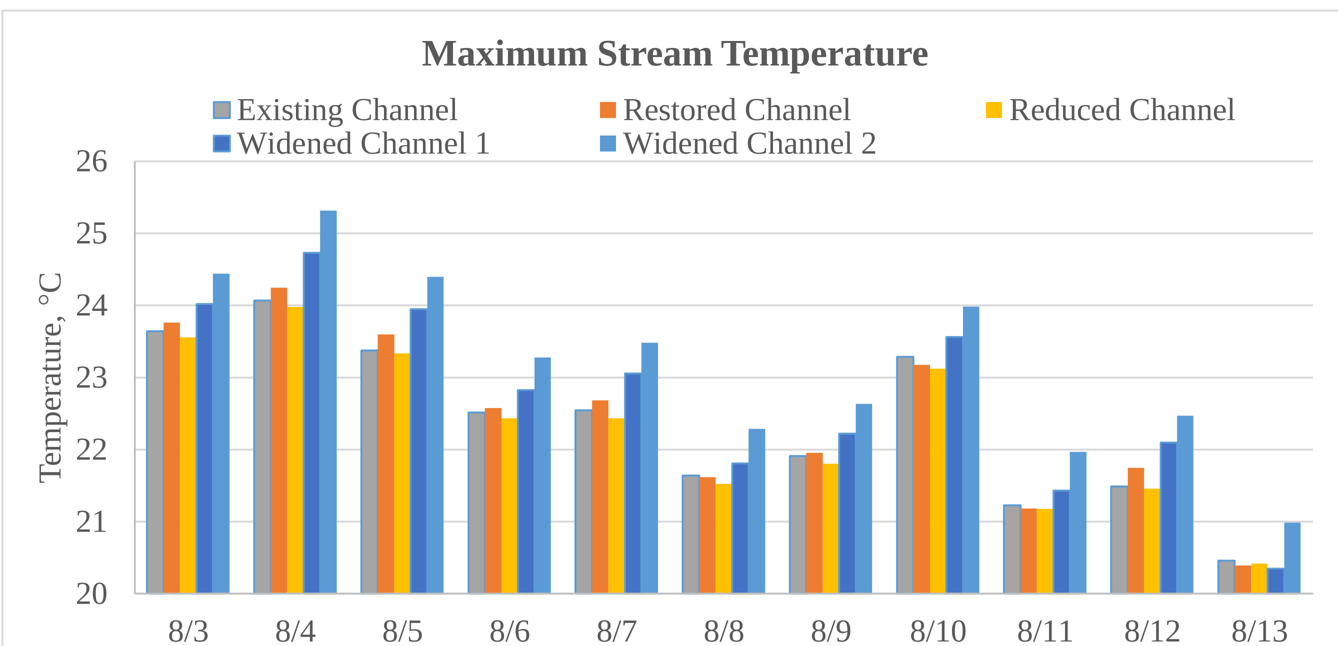

Figure 4.13: Maximum daily stream temperatures for the modeled existing and restored vegetated channels for August 3-August 13, 2014

The models predicted as the Phase 3 stream is widened, water conveyance will be slowed and residence times increased. For stream surface area increases of 32% and 67%, residence times were extended from 1.66 hours to 1.86 hours and 2.04 hours. As the stream is concentrated to a 27% reduced area, residence times are predicted to decrease to 1.44 hours. For the wider stream sections, the time of maximum stream temperature also shifted from 6:00 PM to 5:00 PM.

Table 4.5: Summary of modeled stream temperatures and residence times for the existing and restored channel adjusted area scenarios

Stream Model	Stream Surface Area, m^2	2:00 PM Average (°C)	Daily Average Maximum (°C)	Residence Time (hours)
Existing	10,000	20.2	22.9	1.24
Decreased	12,700	20.2	22.8	1.44
Design	17,400	20.8	23.0	1.66
Increase (1)	23,000	21.6	23.3	1.86
Increase (2)	29,100	22.3	23.7	2.04

Observing temperature changes within each model from the upstream to downstream boundaries revealed a strong linear correlation between stream temperature and stream area. Greatest channel boundary differences occurred between 1:00 PM to 5:00 PM when vegetation was less effective in shielding direct overhead solar radiation. For this period, increasing the stream surface area to 23,000 m^2 (+32%) and 29,100 m^2 (+67%) translated into average increases in stream temperature of 0.64°C and 1.31°C relative to the unaltered channel while reducing the stream's surface area to 12,700 m^2 (-27%) corresponded to a decrease of 0.54°C. The existing channel model followed a similar trend, predicting downstream temperatures 0.48 °C cooler than the planned Phase 3 channel. This temperature was higher than the Phase 3 area trend, partially explained similar stream depth between the Phase 2 and Phase 3 channels.

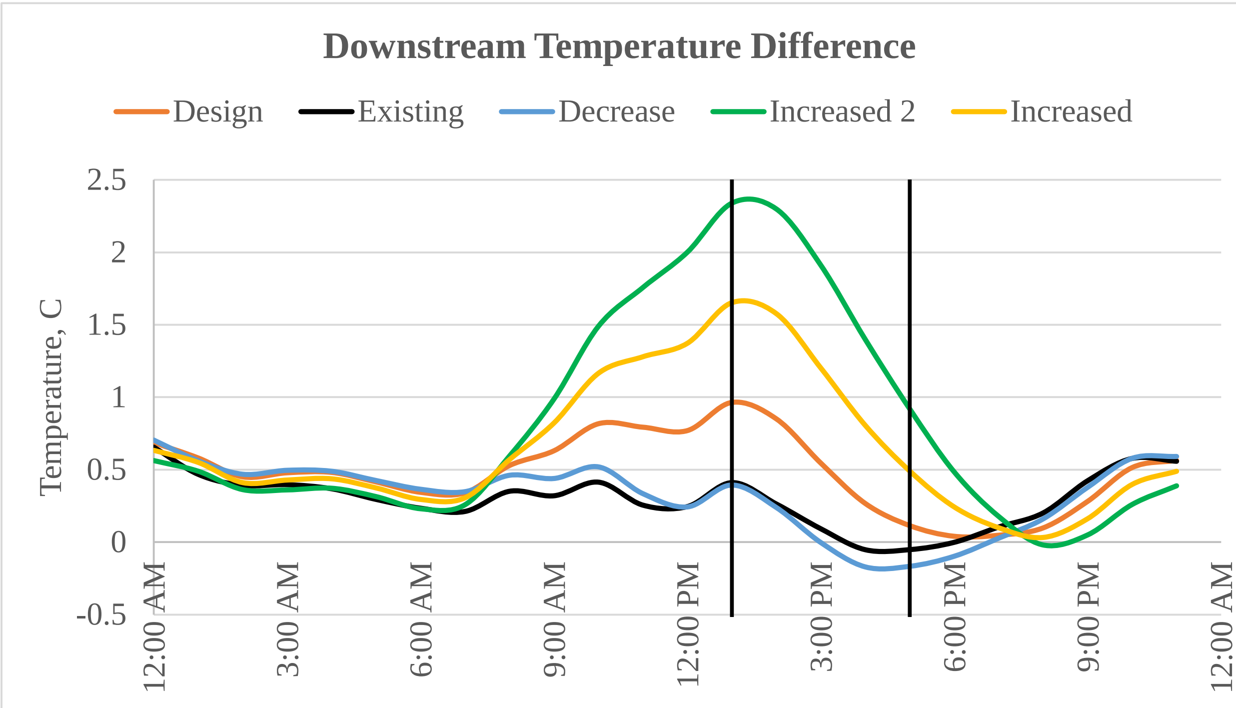

Figure 4.14: Hourly temperature changes across model reaches

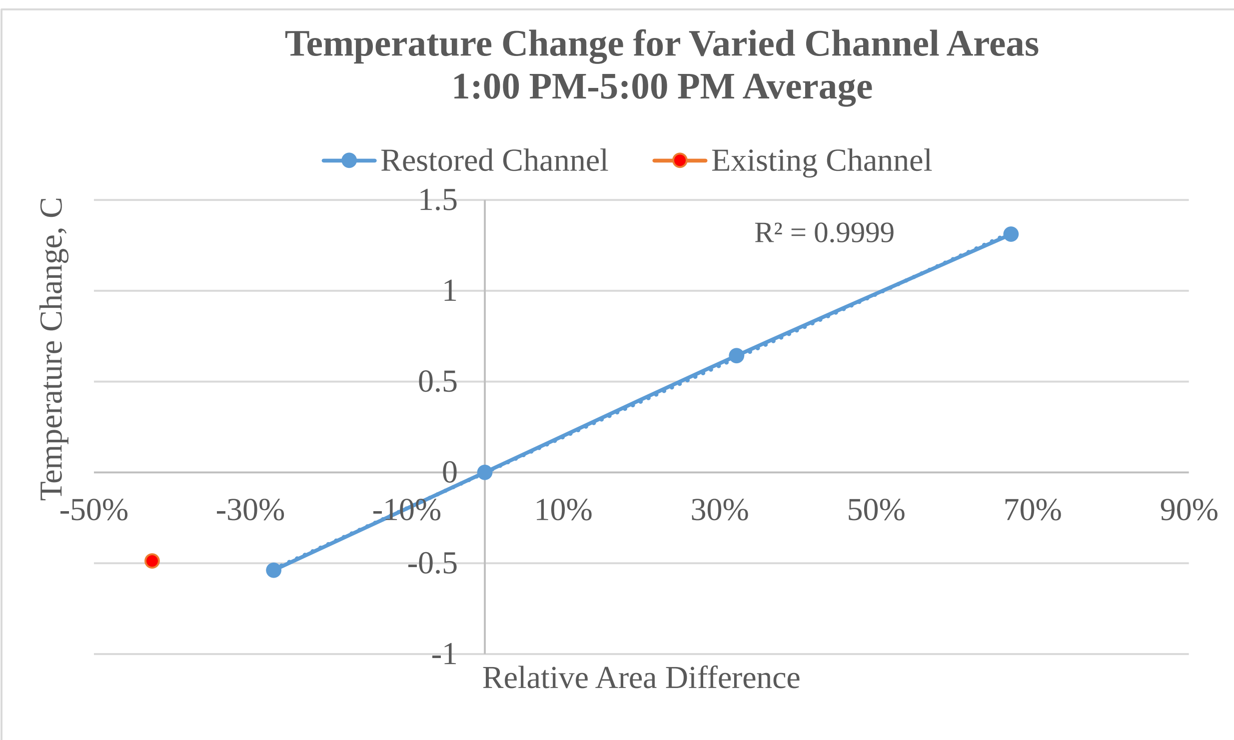

Figure 4.15: Linear temperature change correlation with area for 1:00 PM to 5:00 PM

4.4 Discussion

The channel section described by the existing pre-restoration model is a relatively homogeneous, non-dynamic system. Spatially, this stream exhibits little channel sinuosity and sparse streamside vegetation. By mid-late summer, there is little or no flow accumulation from groundwater or from Ruby Creek. Because of its historical use as a dredge-mining channel, bank geometry is also similar throughout the reach. One unique feature is a 2 to 2.5 m deep pool spanning 200m in the middle of the reach. Though the Middle Fork of the John Day River is a well-mixed river system at reach scale, temperature stratification in features like these are not well modeled by the one dimensional heat and mass transfer equation. As a result, divergences between the model and measured DTS data existed over this section. Despite these discrepancies, modeled and DTS temperatures converged after the pool section. These differences represent a 0.5 to 0.6 C° localized decrease in temperature compared to modeled temperatures, a potential source of thermal refugia for fish.

Application of the calibrated model under 2014 climate conditions shows a consistent heating trend for the anticipated restored channel. While maximum daily temperatures observed at 5:00 PM-6:00 PM were similar for both channels, the reconstructed channel was warmer for all earlier daytime hours. These increases can be attributed to increases in stream surface area in combination with increased residence times from 1.24 hours to 1.66 hours.

Comparing the magnitude of stream heat fluxes, the most pronounced changes were observed in streambed conduction. From early morning to 5:00 PM, streambed conduction was greater in the reconstructed channel showing maximum increases as high as 30 W/m^2 at 12:00 PM. This change can be attributed to changes in stream depth, which is projected to decrease on average from 0.35m to 0.30m between the existing and reconstructed channels. This finding deserves particular consideration on the Middle Fork of the John Day River, where the streambed is composed of large thermally conductive materials. Longwave radiation is also projected to change, driven by differences in stream temperature between the existing and reconstructed channel. As the new channel heats at a greater rate, it emits proportionally greater amounts of longwave radiation, dissipating energy at an additional rate of 12 W/m^2 at 1:00 PM-2:00 PM. Other heat flux changes were negligible between the existing and reconstructed channels with convective and evaporative heat fluxes dissipating 3-4 W/m^2 more for the reconstructed channel.

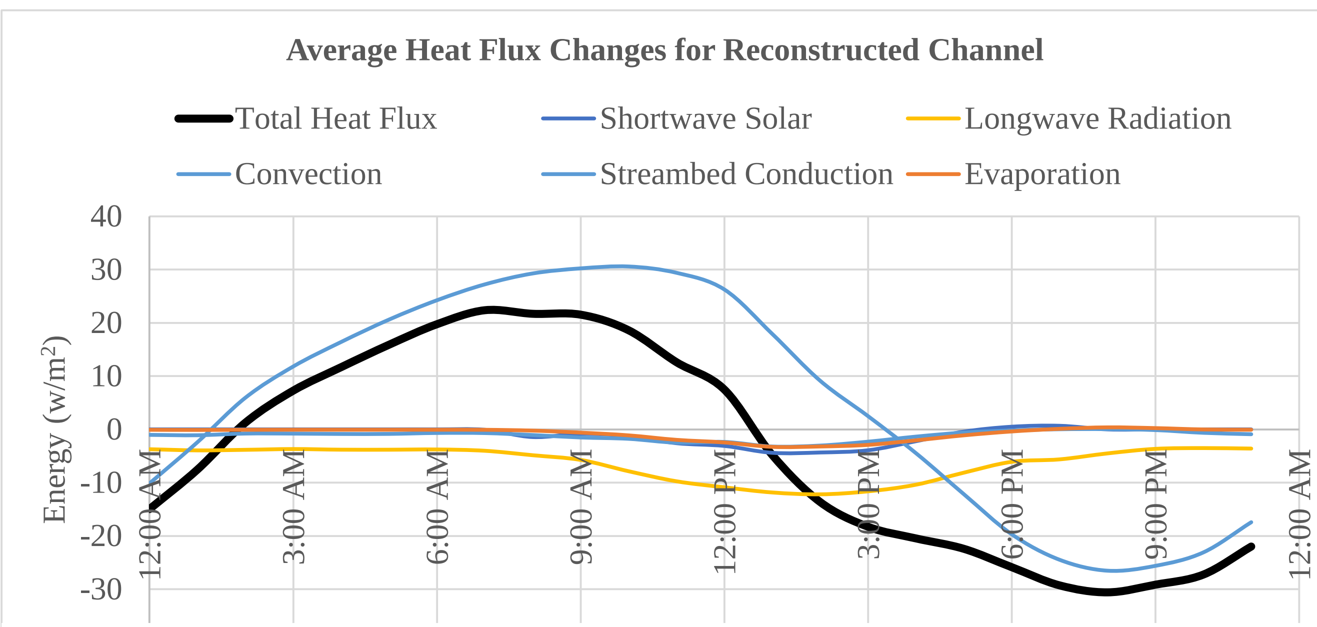

Figure 4.16: Hourly differences in heat budgets between the existing and restored stream channels. Most significant changes are found in stream bed conduction which was shown to vary from differences in channel depths.

Because modeled heat budgets for the existing and planned Phase 3 restored channel are comparable, the main driver of temperature change can be attributed to increases in stream area. As both models share similar shortwave solar radiation-dominant heat budgets, the transfer area into the stream ultimately scales the amount of energy entering the water column. Well-developed sedges line the existing channel, often hanging over and covering portions of the stream. The ability of these plants to block incoming solar radiation is vital for reducing temperatures for a stream dominated by shortwave solar radiation.

Streamside vegetation significantly buffered daytime temperatures for all modeled scenarios. Reiterating the findings of past research (Diabat, 2014; Beschta 1997), limiting the shortwave solar radiation received by the stream effectively reduced temperatures along the reach. By incorporating moderate 5m, 50% dense vegetation in the Phase 3 model, projected temperature increases were significantly mitigated. For this scenario, daily maximum stream temperatures on the restored channel were within 0.03° C of the narrower existing channel. The 0.48° C increase observed earlier in the day between the non-vegetated channels was reduced to an increase of 0.16° C.

Adding 5m high, 50% dense vegetation to the existing channel is predicted to be more effective in reducing stream temperature than it will for the restored planned channel. Comparing shade between the existing and restored shaded channels showed a similar amount of solar radiation was blocked on a daily basis with daily effective shade of 16% and 16.7% respectively. However, on an hourly basis the temporal distribution of received shortwave solar radiation was significantly different between the channels. Early in the day, the existing channel's east-west orientation provides little protection from the rising and setting sun. As the day progresses, the projected solar path of the sun's rays shifts south of the existing and Phase 3 channel, emphasizing effectiveness of shade from vegetation on the south stream banks. Because of the Phase 3 channel's sinuosity, it is projected to receive higher amounts of solar radiation during the warmest times of the day, a consequence of increased north-south channel orientation.

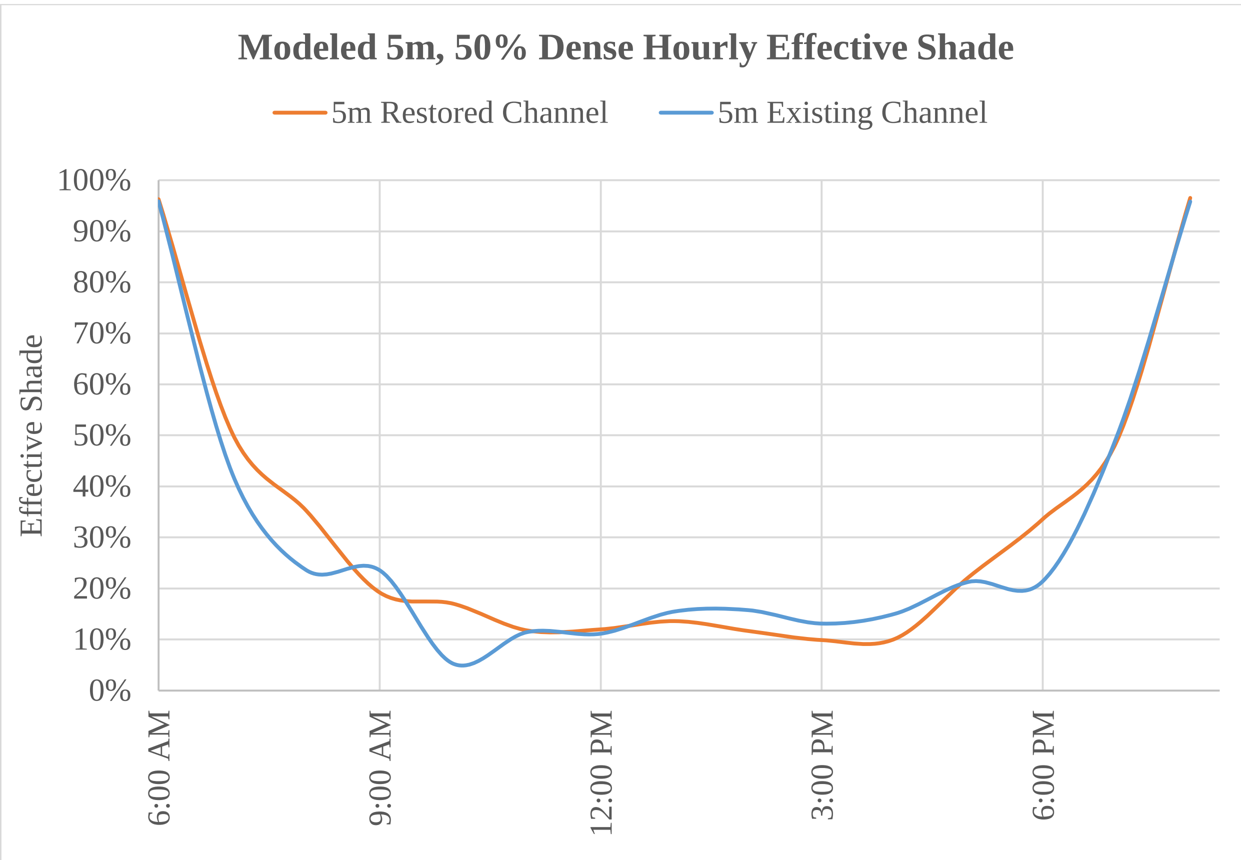

Figure 4.17: Hourly effective shade for restored and existing 5m, 50% dense vegetated stream channels. Key differences in radiation can be observed from 12:00 PM to 5:00 PM, where effective shade is greater for the existing channel

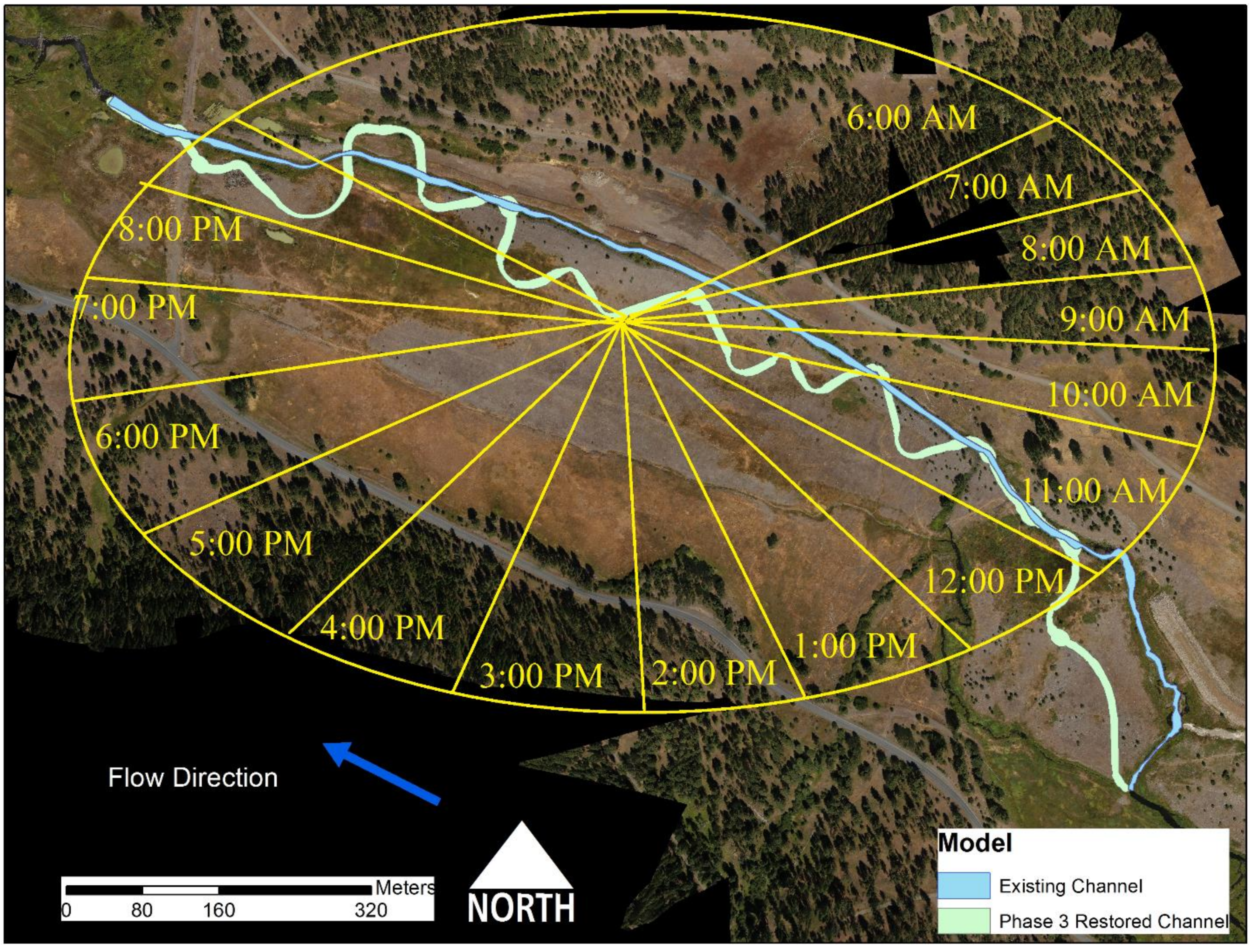

Figure 4.18: Hourly solar path and solar rays in early August[1]. After 12:00 PM, vegetation on the south side of the existing channel becomes more effective in blocking incoming solar radiation.

[1] http://www.sunearthtools.com/tools/coordinates-latlong-sunpath-map.php

Daily effective shade and changes in reach temperature were directly correlated, suggesting the influence of solar radiation on stream temperature in the reach. This trend indicates that to prevent daytime stream heating, vegetation would need to block more than 40% of incoming solar radiation. The most pronounced effects of stream vegetation would be seen in the hours following peak solar loading as maximum temperatures were advected downstream.

The importance stream area was demonstrated by altering bank widths within the planned Phase 3 channel. Changing the stream's surface area through increases to bottom width resulted in changes to channel hydraulics and the stream heat budget. As the stream channel is extended beyond the shading effects of streamside vegetation and banks, temperature increases were more pronounced with more solar radiation contacting the stream.

While the average peak intensity of absorbed solar radiation for the unadjusted channel was 705 W/m^2, the reduced area channel was shown to only receive 701 W/m^2. The intensity of the two enlarged stream sections also increased to 710 W/m^2 and 714 W/m^2, suggesting that existing bank shade was less effective in reducing solar radiation on the wider streams. Increased radiation intensity, combined with increased stream area helped contribute to the non-uniform changes in maximum temperature observed in model results.

By expanding stream area, stream depths were reduced, increasing the amount of solar radiation reaching the streambed during the day. For the 67% larger stream surface scenario, streambed conduction was increased 15 W/m^2. The 27% reduced stream showed a similar trend resulting in streambed heat reductions of 10 W/m^2. While evaporation increased as a function stream area, its changes were less pronounced with 8 W/m^2 increases during the day. The effects of evaporation were minor considering increases in convective heat transfer which increased heat into the stream by 3.5 W/m^2.

Small differences in modeled heat budgets proved insignificant relative to differences in stream surface area, which scaled the amount of energy received by the stream. The proportionality of stream temperature change with area supports this, providing a nearly perfect trend for the non-vegetated channel. Comparing this trend with the trend developed for vegetation shows that the two processes affect temperatures similarly with area as a more sensitive parameter.

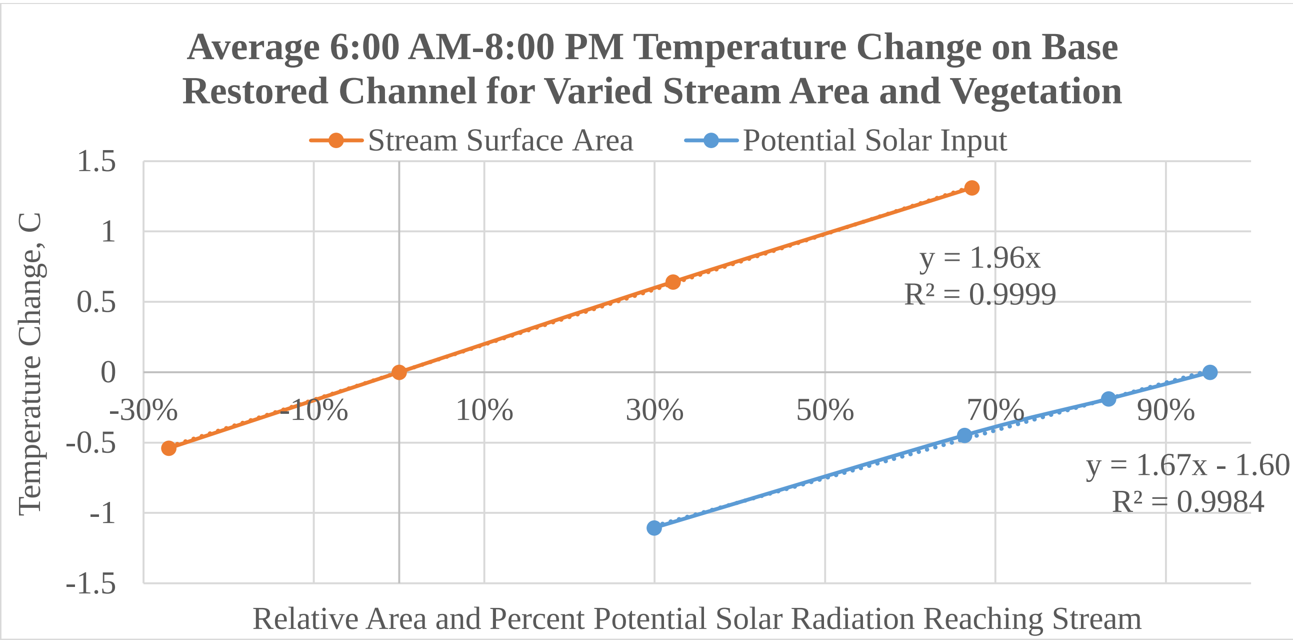

Figure 4.19: Correlation of area and vegetation changes with temperature

Unlike the temperature changes observed upstream in the Phase 2 channel reconstruction, Phase 3 reconstruction and its area and vegetation scenarios had little effect on nighttime stream temperatures. As the sun set, temperatures across all Phase 3 modeled channels converged as reach temperatures were determined by initial temperatures at the upstream boundary. Because residence times remained under two hours, remnants of earlier heating were flushed from the stream system. The largest difference between the stream systems comes from the absence of a cold-water tributary on the Phase 3 stream section. In the Phase 2 stream area Granite Boulder Creek was shown to buffer daytime and nighttime stream temperatures when combined with stream area reductions.

4.5 Conclusion

The results of this study offer insight into the effects of channel surface area and shading on the Middle Fork of the John Day River. These parameters emphasize the influence of shortwave solar radiation on temperature on the stream, particularly during low-flow, high heat conditions. Changes to area and vegetation proved highly effective in controlling temperatures across the reach, scaling the amount of energy absorbed by the stream. If increases are made to the stream's area, as shown by the projected Phase 3 design, temperature is also predicted to increase. Stream hydraulics further emphasize the risks of expanding stream area, predicting increased residence times in a high heat flux environment. Riparian vegetation, even at moderate levels, was demonstrated to alleviate temperature on the reach, further suggesting its importance for future restoration efforts.

Though exact channel geometry of the anticipated restored channel was not available for this study, the varied parameters in this experiment provide a range of expected temperature changes. Due to the strong proportionality of temperature change with area, expected temperature changes can be estimated from Figure 4.19.

Limitations in this analysis come from modeling temperatures in only one spatial dimension. Because both the existing and Phase 3 channel sections incorporate pool features, some degree of stratification is likely to occur. This stratification may hold potential for creating thermal refugia for fish, as demonstrated by the pool on the existing channel. Also, a degree of hyporheic exchange could develop as the result of additional sinuosity, buffering stream temperatures throughout the reach.

Chapter 5: DTS Biases and Insights: Effects of Solar Radiation on Fiber Optic Cable Type

5.1 Introduction

Distributed temperature sensing (DTS) has grown in popularity and has been used in a wide array of hydrologic applications including stream and river environments (O’Donnell 2012; Huff 2009; Selker et al. 2006). Due to the high quality, continuous nature of measurements and affordable deployment costs, DTS offers a replacement for conventional point loggers and forward looking infrared ranging, technologies that provide coverage in only space or time. In areas where elevated temperature poses a threat to water quality as in California and the Pacific Northwest, DTS has been adopted by researchers and agencies as a means for monitoring stream temperature. The Middle Fork of the John Day River, which is located in a dry, arid region of eastern Oregon has undergone several years of DTS monitoring to measure the effects of restoration projects on temperature. Throughout the study, the style of fiber optic cable used has evolved with current cables providing excellent resilience and flexibility. In recent studies, a white plastic sheathed cable was adopted in an effort to reduce solar radiation biases, a potential issue in the shallow, exposed headwaters of the Middle Fork.

Due to differences in albedo, black or dark blue plastic sheathed cables absorb more solar energy, converting that energy to heat. White coated fiber optic cables, though not as resistant to ultraviolet light as conventional black cable types, offer improved reflectivity, lessening the effects of radiative-caused temperature biases. Past research on the effects of solar radiation bias on DTS technology suggests that dark UV resistant fiber optic cables can be affected by shortwave solar radiation, an issue most likely to occur over shallow, slow moving stream sections (B. T. Neilson 2008). The approach of Nielson includes an energy balance for the fiber optic cable, accounting for incoming shortwave radiation and convective energy lost through advection. Findings from this research also indicate that streambed conduction also plays a factor in temperature bias, with differences as high as 0.17° C recorded on the bottom of shallow streambeds compared to shielded thermistor measurements. The effects of bed conduction bias were further explored on the Middle Fork, where vegetation and fine sediment layers were correlated to diurnal reductions in temperatures and 20-40 minutes lags over affected cable sections (O'Donnell Meininger and Selker 2014).

Acknowledging solar radiative bias, other research has sought to exploit differences in fiber optic measurements as the means for quantifying stream shade (Petrides et al. 2011). On the Walla Walla River, a 250 m installation using black and white fibers was installed in the air over a reach vegetated with scattered 2m canopy. Results from the study indicated that vegetation could be identified at 1-m scales from differences in cable measurements, justifying the feasibility of shade estimation for this method.

5.1.1 Scope of Study

To address the potential of solar radiation biases in stream temperature monitoring for a shallow arid stream, two identical high coverage DTS installations were placed in the upstream reach of the Middle Fork of the John Day River on Oxbow Conservation property. For this study, bias was defined as the positive temperature difference between the black and white cables aligned in space and distance. The objectives were to identify the most significant physical parameters that influenced this radiative bias and address if solar radiation bias could have been a significant factor in over-estimating temperatures in past monitoring studies on the reach. Analytical methods were adopted from the work of Neilson et al. (2010) to provide complimentary estimates for this bias by calculating the absorbed radiation per characteristic length of cable.

5.2 Methods

5.2.1 Site Description

The Middle Fork of the John Day River is a 4th-6th order stream located in eastern Oregon originating near the town of Austin. The headwaters of the stream flow through wide alluvial meadows and narrow confined valleys with varying levels of vegetation. The experiment was conducted on the upper reaches of the Oxbow Conservation Property (44°38'41.96"N, 118°39'33.81"W), a confined area upstream of the open valley meadow with 2 to 8 m shrub vegetation and a few scattered stands of cottonwood or pine 20 to 30 m. The streambed is composed of large gravel and cobble. The upper reaches lie at the base of the 60 to 70 m high outcrop, Coyote Bluff. Low summer base flows in 2014 for this reach were measured to be 0.40 m^3/s with an average depth of 0.38m and a depth range of 0.14 m to 1.3 m.

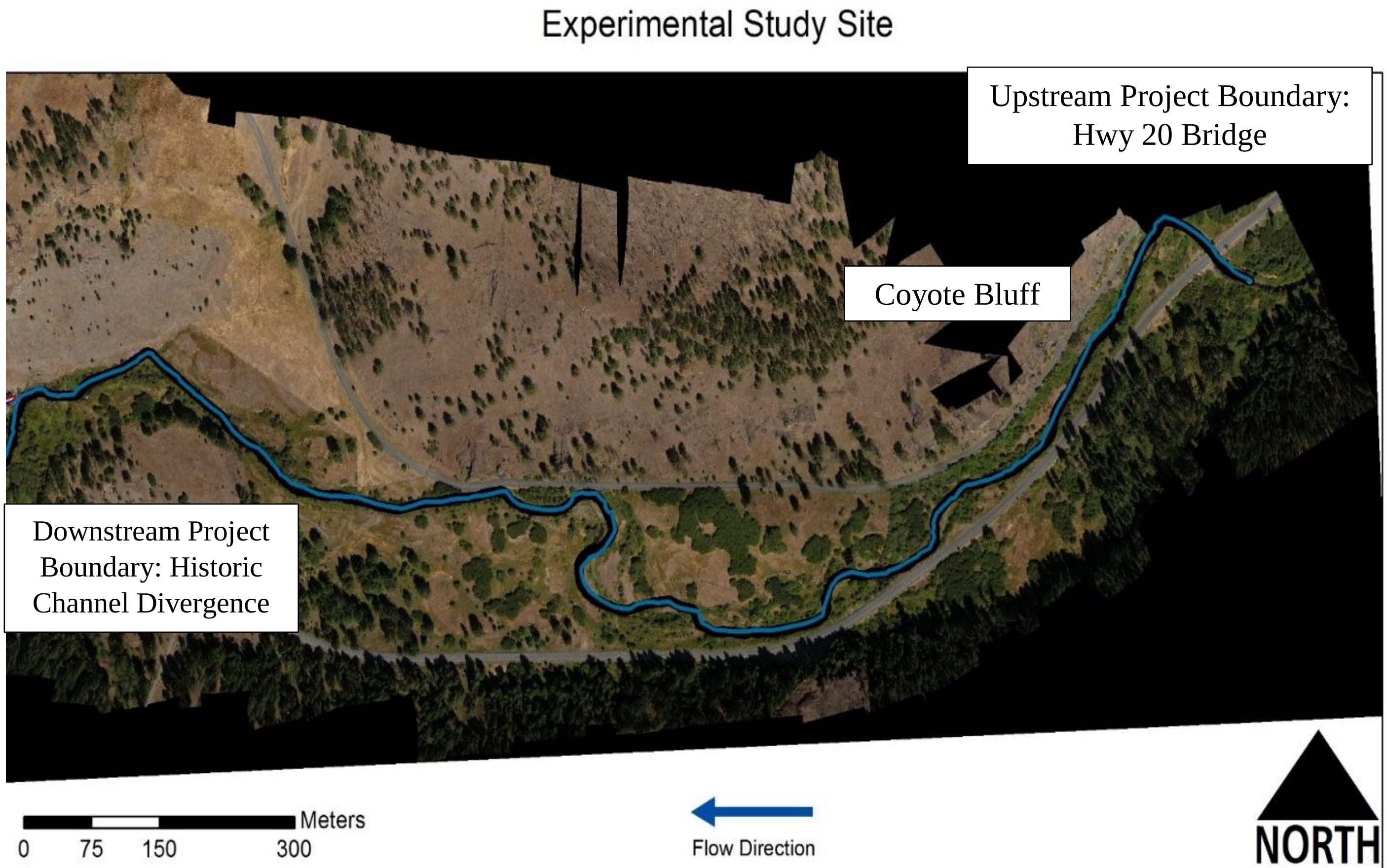

Figure 5.1: Upstream stream section of the Oxbow Conservation Property, site of the black/white fiber optic study

5.2.2 DTS Experiment

One black polyurethane sheathed AFL Flat Drop style fiber optic cable and one round white high-density polyethylene sheathed Kaiphone fiber optic cable were utilized in a DTS monitoring study to investigate the effects of potential radiation bias. Cable geometries were similar with specified cross sectional areas of 30 mm^2 and 28.3 mm^2 and circumferences of 23 mm and 19 mm for the AFL and Kaiphone cables, respectively. The 20% difference in circumference for the black AFL may also have contributed to potential cable temperature bias.

Figure 5.2: Black and white fiber optic cables used in Chapter 4 study. Left: Black 7.8mm x 4.3mm Mini LT Flat Drop Cable with PE jacket and two dielectric strength members. Right: Kaiphone white 6 mm armored white cable with HDPE outer jacket, metal braiding, Kevlar weave and a flexible metal tube. Cable deterioration on white cable is apparent following the experiment.

The cable was deployed over a stream length of 1,800m from the upstream Highway 20 Bridge to the location of the historic north/south channel divergence. This area covered a diverse set of stream conditions with shallow riffles, pools, exposed sections, and regions of varying amounts of vegetation. Both cables were placed in the stream’s thalweg with a minimal distance maintained between the two cables. Temperatures were measured in the summer of 2014 from August 3 through August 13 using a SensorTran 5100 DTS which collected data on a 15 minute cycle with 3 minutes in between black and white cable measurements. Three independently monitored reference baths supplied calibration temperatures to calibrate the raw DTS signal data. RPB Solo T (accuracy ±0.002 °C) thermometers were embedded into these cable sections, recording reference temperatures every minute. The cable location was mapped with a high precision TOPCON GR-3 survey grade GPS (10 mm horizontal, 15 mm vertical accuracy) with depth measurements collected at all GPS locations.

5.2.3 Analytical Methods

Estimates for average temperature bias due to solar radiation were calculated at 12:00 PM using similar methodology to Neilson et al. (2010). Using a simplified energy balance, temperature bias was computed as the difference in absorbed solar radiation and the convective heat losses dissipated by the stream. Weather data were collected at the Dunstan property weather station located 9.2 km away, indicating average noon solar radiation values of 900 W/m^2. Assuming a clear water column, it was assumed that 600 W/m^2 penetrated the 0.35 m water column. Convective losses from the cable were determined by the heat transfer coefficient, derived from the Nusselt number and a characteristic length. The Nusselt number was calculated based on average channel geometry and velocity across the reach for the thermal properties of water at 18°C (Table 5.1), based on average noon stream temperature. The characteristic length was selected to be 0.2 m, a value within the range used by related studies (Read et al. 2014; Neilson et al. 2010), and reasonable for the study site.

Table 5.1: Thermal properties of water for determining convective heat loss from the cable

	Water	Units
Temperature	18.0	^{o}C
Dynamic Viscosity	1.03E-03	N s/m^2
Kinematic Viscosity	1.03E-06	m^2/s
Heat Capacity	4.078	kJ/(kg K)
Thermal Conductivity	0.60	W/(m K)
Prandt Number	6.96	-

5.3 Results

The results of this study revealed consistent daytime temperature biases in the black AFL cable, present during every recording day in the study. This bias scaled with the amount of incoming solar radiation, following a diurnal cycle with peak biases occurring at 12:00 PM to 1:00 PM, the period corresponding to maximum overhead solar loading into the stream. This bias largely subsided by 6:00 PM as the sun was obscured by the adjacent Coyote Bluff cliff system. Leveraging spatial patterns in this temperature bias, it was possible to correlate specific locations of high effective shade as well as the timing of topographic shading on the stream. Slow moving stream sections were also identifiable through spikes in the black cable bias.

Measured average streamwide bias showed that the AFL cable was an average 0.21°C warmer from 12:00 PM to 1:00 PM for August 3-August 9, a period with minimal cloud cover. On the clearest clearest days of August 7 and August 8, this bias was found to be as high as 0.26° C. These values were larger than computed analytical estimates which resulted in lower biases of 0.15° C, likely due to differences in cable circumference and from uncertainty in experimental parameters (characteristic length and average velocity).

Observing temperatures spatially, it was possible to identify two large cottonwood trees along the otherwise shrub-dominated streambanks. As the cable passed under the shadow provided by these trees at 12:00 PM, temperature biases were decreased from 0.25° C to 0.17 °C. A sharp increase in temperature bias of 0.34°C followed by a drop to 0.22°C was correlated to a slow moving pool followed by fast moving riffle section which was responsible for advecting more heat from the cable.

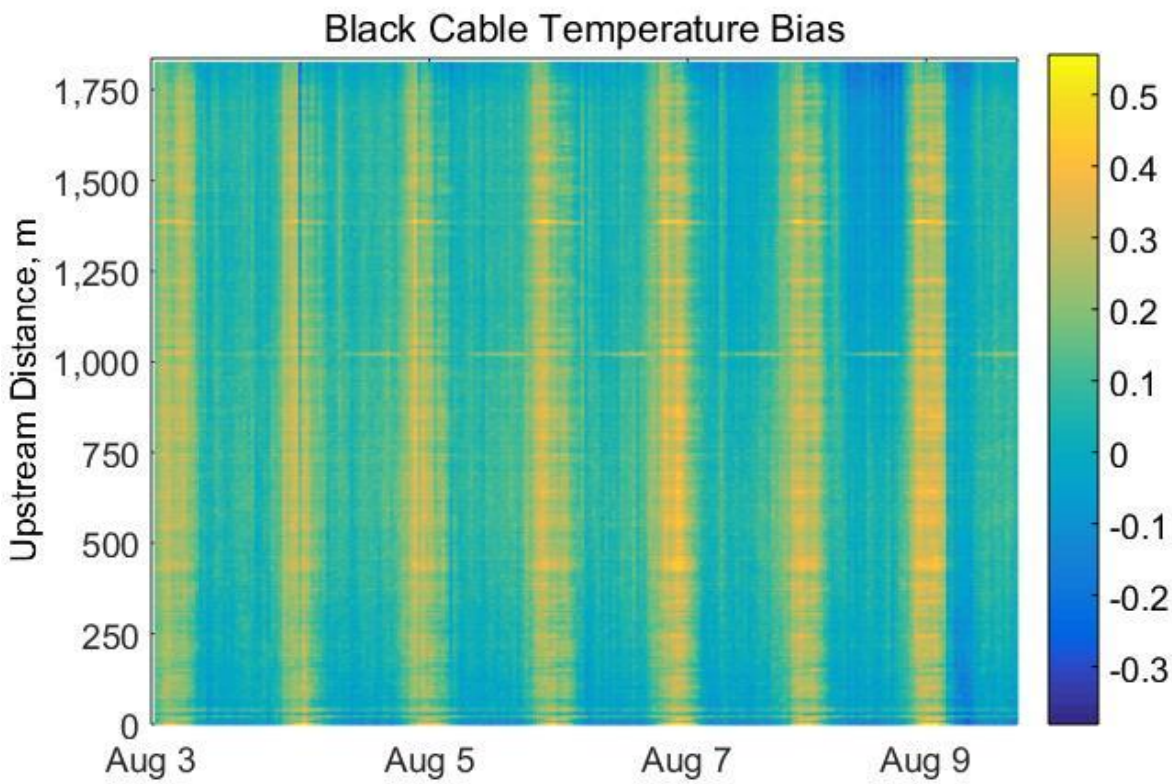

Figure 5.3: Temperature bias for black AFL cable August 3 (12:00 PM) through August 9. Daily biases are as high as 0.34°C in certain locations with temperatures converging at night.

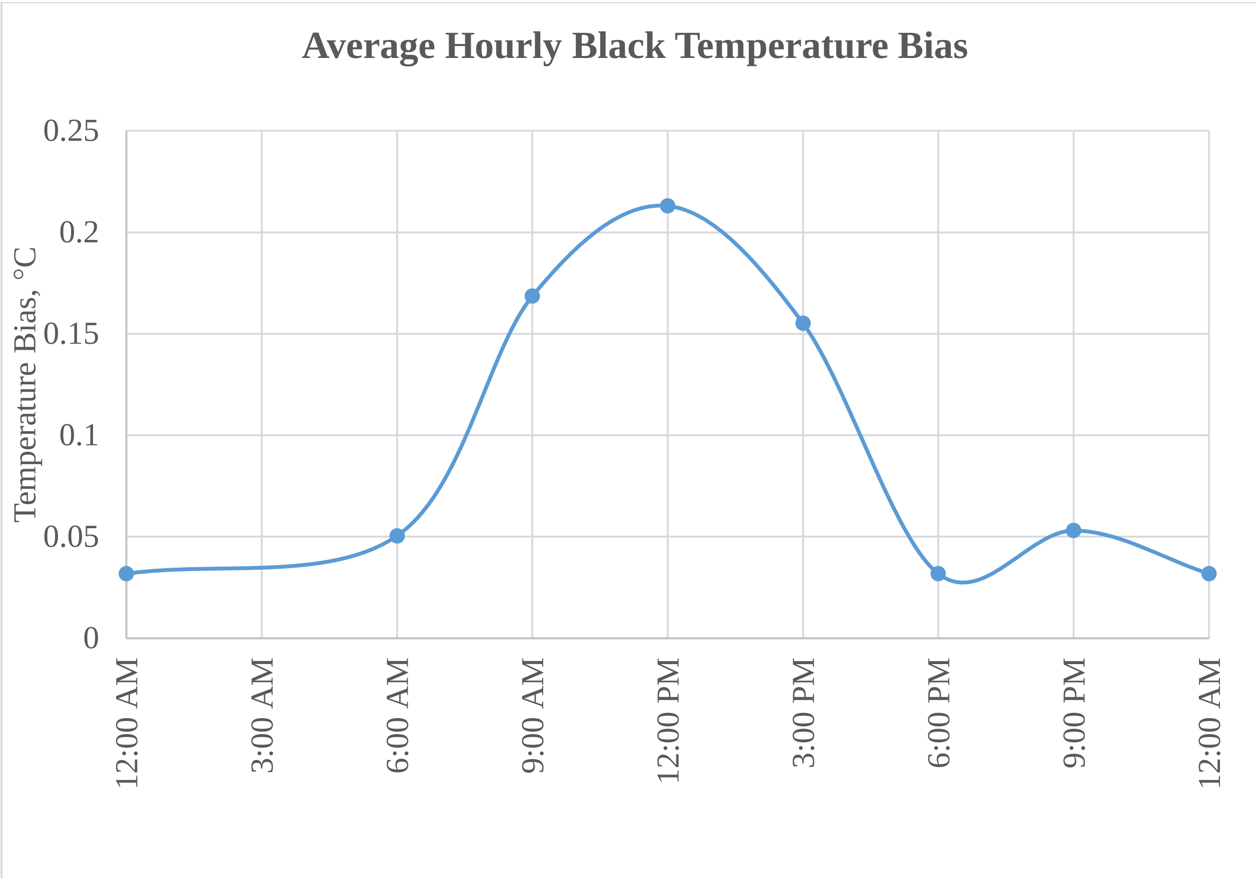

Figure 5.4: Average hourly temperature bias for the black cable. Non-zero nightly biases are indicative of slight differences/errors DTS cable installations.

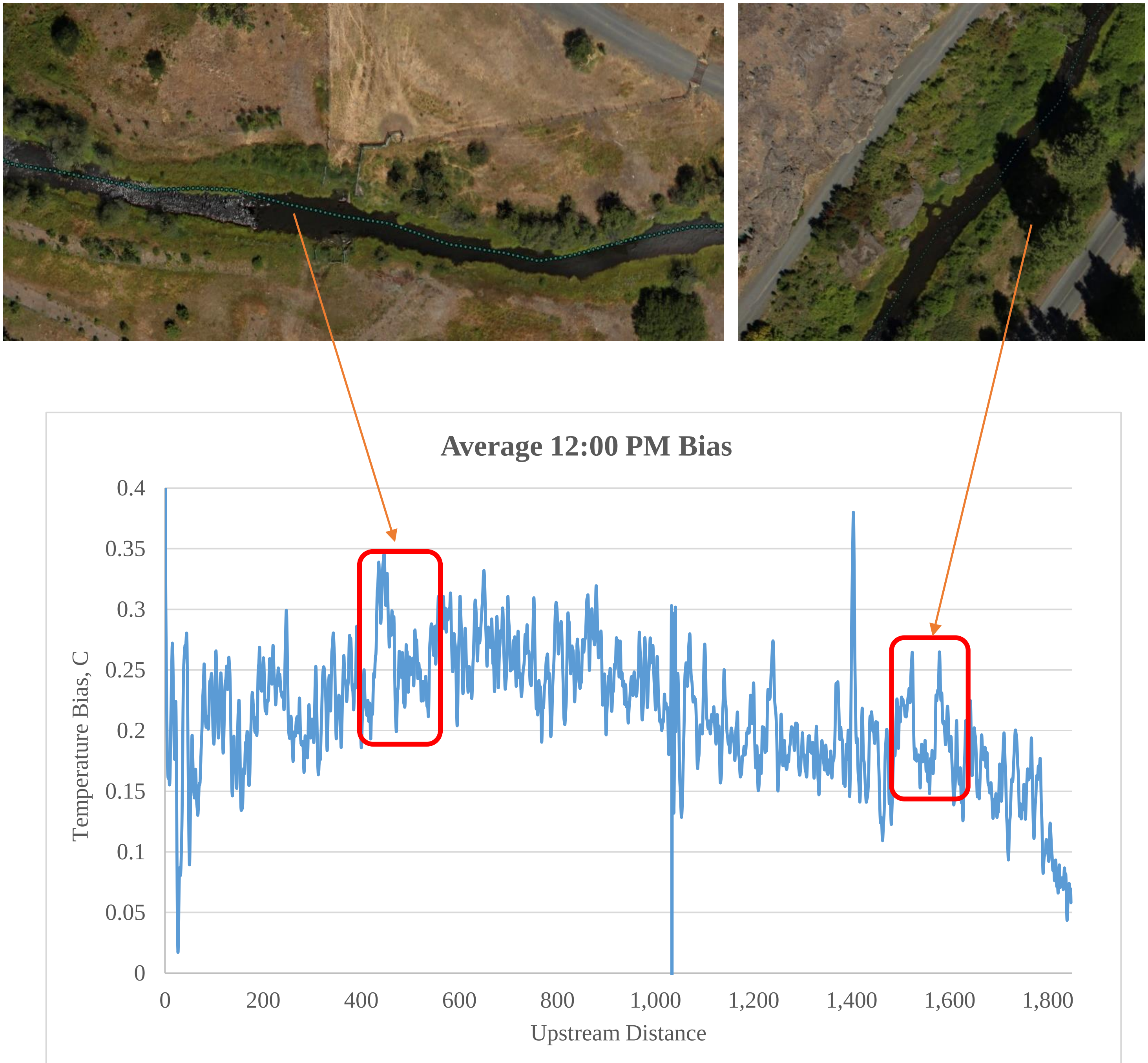

Figure 5.5: Average 12:00 PM black cable temperature bias showing pool and vegetation features. The sharp spike at meter 500 corresponds to a pool section with low advection and higher biases. At meter 1,500, two developed tree stands provide a depression in temperature bias, justifying the potential of DTS for measuring streamside shade.

5.4 Discussion

Recorded and predicted temperature biases indicate the importance of selecting cables with low albedo for DTS temperature monitoring. For the low flowing upper headwaters of the Middle Fork of the John Day River, solar radiation biases are shown to pose a significant concern for data quality, amounting to biases as high as 0.32 °C for the black AFL fiber optic cable compared to the geomtrically simliar white Kaiphone cable. In the context of restoration and stream temperature modeling, the magnitude of this bias may confound observed stream temperature changes and lead to the misinterpreation of project effects.

Differences between predicted and measured biases can be attributed to the assumptions required to estimate the heat absorption of the fiber optic cable. Because no pyrometers were utilized in this experiment, the amount of solar radiation reaching the cable was only estimated, assuming a clear water column and referencing attenuation trends derived by Nielson et al. (2010). Selecting a characteristic length for convective heat transfer was also limited by the range of appropriate values used in previous studies. Nielson (2010) cites potential uncertainty in characteristic length and provides a range of 2 to 20 cm for fiber optic cables in streams while a borehole DTS study by Read (2014) utilizes a characteristic length of 11 cm, representing the diameter of the borehole. Finally, stream velocity used in this study represents the average stream velocity, overestimating the velocity at the streambed. Because of this, estimates for convective heat transfer overestimate the amount of energy dissipated from the cable partially explaining differences between the measured and calculated values.

No effort was made to differentiate the effects of streambed conduction, which likely influenced the magnitude of this error. Because the cables used in the experiment shared similar geometry and composition, it is assumed streambed influences both cables similarly. Collapse of radiative biases correlated with the sun passing behind Coyote Bluffs at 5:30 PM to 6:00 PM indicates that solar radiation played the largest role in observed biases.

At night, when solar radiation flux to stream ceased, a lingering bias was observed for the black cable, averaged to 0.03° C. This bias is likely an artifact from the DTS installation, and does not invalidate the 0.21° C average bias observed midday.

Conclusion

Combining high resolution stream temperature monitoring with stream temperature modeling provides estimates on expected temperature changes following two restoration projects on the Middle Fork of the John Day River. Beyond quantifying stream temperature reduction or increase, this study identifies the key physical drivers of temperature in the region and how they interact with various restoration practices. The headwaters of the Middle Fork are highly sensitive to temperature due to low summer stream flows and long, hot, dry conditions. Due to the river's scale and lack of effective riparian vegetation, solar radiation dominates the heat budget of the stream. Therefore, the most effective restoration practices to reduce stream temperature require focus on reducing solar radiation inputs into the stream.

The importance of reducing stream surface area is suggested by the modeled decreased stream temperatures in the Phase 2 restoration and, oppositely, in the Phase 3 project. By filling in the historic north dredge-mining channel, stream flow was concentrated into the south channel. This alteration buffered stream temperatures diurnally, leading to decreases in the day and increases at night. Causes for these changes are explained by a combination of reduced stream heating during the day and decreased stream cooling at night, factors that were amplified by Granite Boulder Creek, which held a more constant temperature. In the Phase 3 restoration, similar effects on daytime stream temperature are predicted as increased stream surface area results in a shallower stream with wider stream area. Greater predicted heating effects were most pronounced during early afternoon hours, when solar loading was highest. Differences in flow and heating trends between the Phase 2 and Phase 3 channels led to differences in maximum stream temperatures, where the modeled stream expansion of Phase 3 was not shown to change maximum daily stream temperatures. This difference can be attributed to the influence of Granite Boulder Creek, which effectively cools the stream on the Phase 2 channel section. To this end, Phase 2 restoration improves upon Granite Boulder Creek's ability to cool reach temperatures.

Because solar radiation is the leading driver of stream heating, simplified trends were created by observing the effects of vegetation and shade on stream temperature. Changes in near-stream vegetation resulted in proportional changes stream temperature, shown relative to the non-vegetated channel. This trend was even stronger for areal changes, which directly scaled the amount of energy delivered into the stream. Using these trends, it is possible to estimate the effects of channel area modifications on temperature and the potential of vegetation to mitigate temperature increases. Extension of these tools beyond the Middle Fork of the John Day provides useful insight as to how restoration projects might affect temperature on sensitive streams. A complete summary of restoration actions and their effects on stream temperature is provided in the proceeding summary table.

Summary Table: Summary of the effects of restoration activities suggested by DTS monitoring and modeling predictions for August, 2014 on the Middle Fork of the John Day River

Activity	**Example**	**Expected Change on Temperature**	**Comment**
Channel Removal	Phase 2 Oxbow Tailings Restoration	Afternoon decrease of 0.91° C (± 0.10° C), daily maximum increase of 0.65 ° C (± 0.20° C), and nightly increase of 0.86° C (± 0.10° C)	Removing the historic north channel reduced the amount of solar radiation entering the stream, lowering day time and maximum temperatures. Nightly temperatures were also higher as less energy was emitted for the restored stream.
Channel Reconstruction and Remeandering[1]	Phase 3 Oxbow Tailings Restoration	Afternoon increase of 0.53° C (± 0.20° C)	While afternoon temperatures increase, maximum temperatures remain equivalent as the Phase 3 channel dissipates more heat more following peak solar loading
Stream Narrowing	27% Stream Area Reduction on Phase 3 Channel	Afternoon decrease of 0.59° C and daily maximum decrease of 0.18° C	Stream area increases to the proposed Phase 3 channel are projected to cause proportional increases to daytime and maximum stream temperatures. These changes are driven by decreased stream depths and increased surface area for heat transfer. Longer residence times for wider channels emphasize heating changes.
Stream Widening	32% Stream Widening on Phase 3 Channel	Afternoon increase of 0.71° C and daily maximum increase of 0.32°	
	67% Stream Widening on Phase 3 Channel	Afternoon increase of 1.41° C and daily maximum increase of 0.71° C	
Enhanced Riparian Vegetation	Phase 3: 5m, 50% dense canopy	Afternoon decrease of 0.32° C and daily maximum decrease of 0.20° C	Adding shade proved effective in blocking solar radiation, leading to proportional daytime and maximum daily stream temperatures for all modeled scenarios. Modeled shade improvements for the existing channel illustrate the effects of stream orientation combined with vegetation, illustrated by greater stream temperature reductions.
	Phase 3: 10m, 50% dense canopy	Afternoon decrease of 0.54° C and daily maximum decrease of 0.59° C	
	Phase 3: 20m, 70% dense canopy	Afternoon decrease of 1.74° C and daily maximum decrease of 0.95° C	
	Existing: 5m, 50% dense canopy	Afternoon decrease of 0.64° C and daily maximum decrease of 0.20° C	

[1] Modeled Phase 3 stream is a predicted wider channel with the existing hydraulic inputs. As built channel data will provide more accurate estimates following Phase 3 project completion.

It must be acknowledged that temperature is only one metric of stream health and other goals such as stream habitat and hydraulics need also be considered in restoration. The objective of this research is not to grade the projects as successful or unsuccessful. Rather, this research seeks to demonstrate expected changes to one previously identified at-risk metric, one of the stated project goals and an objective of the 10-year intensively monitored watershed study.

Future research for the study can improve upon the quantification of hyporheic flow and pool stratification, factors not effectively modeled in the one dimensional Phase 2 or Phase 3 models. Additional fiber optic studies can help quantify these effects on the new channel, exploiting the differences between a comparable Phase 3 temperature model. Quantification of streambed conduction is also of interest, as it was the heat flux most effected by stream area modification. While modeling efforts on the Middle Fork explore vegetation and stream area independently, a combined trend may be of interest for practitioners to select the most effective combination of both parameters.

Analysis of the Chapter 4 shading scenario results indicates that channel position and orientation play a significant role in how solar radiation is received by the stream. Because of the timing of maximum stream temperatures, minimizing the amount north-south facing stream sections can help reduce additional solar loading during the warmest periods of the day. Both these parameters should be explored in future model scenarios, placing a channel further south in the valley to better utilize topographic shade and by altering the orientation of the stream.

Bibliography

Bell, M. 1991. “Fisheries Handbook of Engineering Requirements and Biological Criteria.” *Reports*, January. http://scholarworks.umass.edu/fishpassage_reports/14.

Benner, David A. 2000. “Evaporative Heat Loss of the Upper Middle Fork of the John Day River, Northeastern Oregon.”

Benyahya, Loubna, Daniel Caissie, Nassir El-Jabi, and Mysore G. Satish. 2010. “Comparison of Microclimate vs. Remote Meteorological Data and Results Applied to a Water Temperature Model (Miramichi River, Canada).” *Journal of Hydrology* 380 (3–4): 247–59. doi:10.1016/j.jhydrol.2009.10.039.

Beschta, Robert L. 1997. “Riparian Shade and Stream Temperature: An Alternative Perspective.” *Rangelands* 19 (2): 25–28.

Beschta, Robert L., and James D. Weatherred. 1984. *TEMP-84: A Computer Model for Predicting Stream Temperatures Resulting from the Management of Streamside Vegetation*. US Forest Service, Watershed Systems Development Group.

Boyd, Matthew, and Brian Kasper. 2003. “Analytical Methods for Dynamic Open Channel Heat and Mass Transfer: Methodology for Heat Source Model Version 7.0.” DEQ. http://www.deq.state.or.us/wq/TMDLs/tools.htm.

Boyd, Matthew S. 1996. “Heat Source : Stream, River and Open Channel Temperature Prediction,” October. http://ir.library.oregonstate.edu/xmlui/handle/1957/27036.

Boyd, Matthew, Dan Turner, and Ryan Mitchie. 2012. *Heat Source* (version 8.0.8). Windows. ODEQ. http://www.deq.state.or.us/WQ/TMDLs/tools.htm.

Brown, George W. 1969. “Predicting Temperatures of Small Streams.” *Water Resources Research* 5 (1): 68–75. doi:10.1029/WR005i001p00068.

Brown, George Wallace. 1972. “An Improved Temperature Prediction Model for Small Streams.” http://ir.library.oregonstate.edu/jspui/handle/1957/299.

B. T. Neilson, C. E. Hatch. 2008. “Effect of Solar Radiation on Fiber Optic Cables Used in Distributed Temperature Sensing (DTS) Applications.” *AGU Fall Meeting Abstracts*.

Burkholder, Barbara K., Gordon E. Grant, Roy Haggerty, Tarang Khangaonkar, and Peter J. Wampler. 2008. “Influence of Hyporheic Flow and Geomorphology on Temperature of a Large, Gravel-Bed River, Clackamas River, Oregon, USA.” *Hydrological Processes* 22 (7): 941–53. doi:10.1002/hyp.6984.

Crown, Julia. 2010. “John Day River Basin TMDL APPENDIX A: TEMPERATURE MODEL CALIBRATION.” Appendix. DEQ. http://www.deq.state.or.us/wq/tmdls/docs/johndaybasin/AppendixATempCalibrationFINAL.pdf.

Diabat, Mousa. 2014. “The Influence of Climate Change and Restoration on Stream Temperature,” May. http://ir.library.oregonstate.edu/xmlui/handle/1957/49288.

Dietrich, James Thomas. 2014. “Applications of Structure-from-Motion Photogrammetry to Fluvial Geomorphology.” UNIVERSITY OF OREGON. http://gradworks.umi.com/36/73/3673086.html.

Eppelbaum, Lev, Izzy Kutasov, and Arkady Pilchin. 2014. *Applied Geothermics*. Lecture Notes in Earth System Sciences. Berlin, Heidelberg: Springer Berlin Heidelberg. http://link.springer.com/10.1007/978-3-642-34023-9.

Hausner, Mark B., Francisco Suárez, Kenneth E. Glander, Nick van de Giesen, John S. Selker, and Scott W. Tyler. 2011. “Calibrating Single-Ended Fiber-Optic Raman Spectra Distributed Temperature Sensing Data.” *Sensors* 11 (11): 10859–79.

Hubbard, E. F., K. G. Thibodeaux, and Mai N. Duong. 2015. “Open-File Report 99-221 Quality Assurance of US Geological Survey Stream Current Meters: The Meter-Exchange Program 1988-98.” Accessed April 16. http://water.usgs.gov/osw/pubs/ofr99-221/ofr99221.html.

Huff, Julie A. 2009. “Monitoring River Restoration Using Fiber Optic Temperature Measurements in a Modeling Framework,” December. http://ir.library.oregonstate.edu/xmlui/handle/1957/13847.

Isaak, D. J., S. J. Wenger, E. E. Peterson, J. M. Ver Hoef, S. Hostetler, C. H. Luce, J. B. Dunham, et al. 2011. “NorWeST: An Interagency Stream Temperature Database and Model for the Northwest United States.” *US Fish and Wildlife Service, Great Northern Landscape Conservation Cooperative Grant. Project Website: Www. Fs. Fed. us/rm/boise/AWAE/projects/NorWeST. Html*.

Johnson, Sherri L. 2004. “Factors Influencing Stream Temperatures in Small Streams: Substrate Effects and a Shading Experiment.” *Canadian Journal of Fisheries and Aquatic Sciences* 61 (6): 913–23. doi:10.1139/f04-040.

Kondolf, G. Mathias. 1995. “Five Elements for Effective Evaluation of Stream Restoration.” *Restoration Ecology* 3 (2): 133–36. doi:10.1111/j.1526-100X.1995.tb00086.x.

Krenkel, Peter A., and Frank L. Parker. 1969. “Biological Aspects of Thermal Pollution.” http://agris.fao.org/agris-search/search.do?recordID=US201300459996.

Kristopher K. Wright, Colden V. Baxter. 2005. “Restricted Hyporheic Exchange in an Alluvial River System: Implications for Theory and Management.” *Journal of The North American Benthological Society - J N AMER BENTHOL SOC* 24 (3): 447–60. doi:10.1899/04-090.1.

Marcus, W. Andrew, Keith Roberts, Leslie Harvey, and Gary Tackman. 1992. “An Evaluation of Methods for Estimating Manning’s N in Small Mountain Streams.” *Mountain Research and Development* 12 (3): 227–39. doi:10.2307/3673667.

Mcdowell, Patricia F. 2001. “Spatial Variations in Channel Morphology at Segment and Reach Scales, Middle Fork John Day River, Northeastern Oregon.” In *Geomorphic Processes and Riverine Habitat*, edited by Joseph M. Dorava, David R. Montgomery, Betty B. Palcsak, and Faith A. Fitzpatrick, 159–72. American Geophysical Union. http://onlinelibrary.wiley.com/doi/10.1029/WS004p0159/summary.

Mohseni, Omid, Heinz G. Stefan, and Troy R. Erickson. 1998. “A Nonlinear Regression Model for Weekly Stream Temperatures.” *Water Resources Research* 34 (10): 2685–92.

Morrill, Jean C., Roger C. Bales, and Martha H. Conklin. 2005. “Estimating Stream Temperature from Air Temperature: Implications for Future Water Quality.” *Journal of Environmental Engineering* 131 (1): 139–46.

Neilson, Bethany T., Christine E. Hatch, Heng Ban, and Scott W. Tyler. 2010. “Solar Radiative Heating of Fiber-Optic Cables Used to Monitor Temperatures in Water: RADIATIVE HEATING ON FIBER-OPTIC CABLES.” *Water Resources Research* 46 (8): n/a – n/a. doi:10.1029/2009WR008354.

O’Donnell Meininger, T., and J. S. Selker. 2014. “Technical Note: Bed Conduction Impact on Fiber Optic DTS Water Temperature Measurements.” *Geoscientific Instrumentation, Methods and Data Systems Discussions* 4 (2): 375–84. doi:10.5194/gid-4-375-2014.

O’Donnell, Tara. 2012. “Evaluation of Stream Temperature Spatial Variation Using Distributed Temperature Sensing,” March. http://ir.library.oregonstate.edu/xmlui/handle/1957/28627.

Oregon DEQ. 1995. “1992-1994 Water Quality Standards Review Issue Papers.” State of Oregon. http://www.deq.state.or.us/wq/standards/docs/temperature/19921994wqStandardsReviewTemperature.pdf.

Petrides, A. C., J. Huff, A. Arik, N. van de Giesen, A. M. Kennedy, C. K. Thomas, and J. S. Selker. 2011. “Shade Estimation over Streams Using Distributed Temperature Sensing: TECHNICAL NOTE.” *Water Resources Research* 47 (7): n/a – n/a. doi:10.1029/2010WR009482.

R. C. Wissmar, J. E. Smith. n.d. “Ecological Health of River Basins in Forested Regions of Eastern Washington and Oregon. Forest Service General Technical Report.”

Read, T., O. Bour, J. S. Selker, V. F. Bense, T. Le Borgne, R. Hochreutener, and N. Lavenant. 2014. “Active-Distributed Temperature Sensing to Continuously Quantify Vertical Flow in Boreholes.” *Water Resources Research* 50 (5): 3706–13. doi:10.1002/2014WR015273.

Ryan Michie. 2009. *TTools* (version 7.56). Oregon DEQ. http://www.deq.state.or.us/WQ/TMDLs/tools.htm.

Selker, John, Nick van de Giesen, Martijn Westhoff, Wim Luxemburg, and Marc B. Parlange. 2006. “Fiber Optics Opens Window on Stream Dynamics.” *Geophysical Research Letters* 33 (24): L24401. doi:10.1029/2006GL027979.

Sinokrot, Bashar A., and Heinz G. Stefan. 1993. “Stream Temperature Dynamics: Measurements and Modeling.” *Water Resources Research* 29 (7): 2299–2312. doi:10.1029/93WR00540.

Stefan, Heinz G., and Eric B. Preud’homme. 1993. “Stream Temperature Estimation from Air Temperature1.” *JAWRA Journal of the American Water Resources Association* 29 (1): 27–45. doi:10.1111/j.1752-1688.1993.tb01502.x.

Te Chow, Ven. 1959. “Open Channel Hydraulics.” http://krishikosh.egranth.ac.in/handle/1/2034176.

Wunderlich, Walter O., and Tennessee Valley Authority. 1972. *Heat and Mass Transfer between a Water Surface and the Atmosphere*. Tennessee Valley Authority, Office of Natural Resources and Economic Development, Division of Air and Water Resources, Water Systems Development Branch.

Appendices

The following appendices provide supplemental data for Chapters 3 through 5. **Appendix A** elaborates on the model inputs and calibration procedures for the Heat Source model utilized in the Phase 2 and Phase 3 restoration analyses. **Appendix B** lists supplemental figures and results not included within the Phase 2 study in Chapter 3. **Appendix C** provides additional figures regarding the Phase 3 study in Chapter 4. Finally, **Appendix D** provides information on the DTS field installation, calibration routine, and includes the sample MATLAB code used to process raw field data.

Appendix A: Heat Source Model Inputs

Appendix A provides more detailed information for the Heat Source model inputs including vegetation, topography, channel geometry, bathymetry, as well as the surveys conducted over the summers of 2013 and 2014. Sampling procedures for remotely sensed data are also described in this section. The data are described in a list-paragraph format, guiding the reader through the inputs, derivations, and data sources for the models. While this section outlines data utilized in the Phase 2 model, procedures for Phase 3 are equivalent.

Spatial Inputs

Vegetation: Vegetation data was derived from 1m sampled LiDAR data produced by Watershed Sciences, LLC, in 2006. Canopy closure (10m) canopy height (0.5m), and bare earth (0.5m) data were obtained from professionally processed raster files received from the United States Forest Service. These data were sampled in a star pattern at each stream node in ArcGIS using Ttools, providing coverage spanning 28m in each direction.

Topographic Shade: Topographic shading was determined in three directions from a 10-meter DEM sourced from OGDC. This DEM provided more complete coverage of nearby mountain features which obscure solar exposure at the beginning and end of the day. (OGDC http://www.oregon.gov/DAS/pages/irmd/geo/sdlibrary.aspx)

Stream Elevation & Gradients: Stream elevation and gradients were calculated from LiDAR-derived USFS bare earth data (USFS, 2008).

Stream Area (Top Width): Stream area was measured from 10cm aerial photography of the stream reach that was generated from a 2013 structure from motion (SFM) study completed by researchers at University of Oregon (Dietrich, 2014).

Bottom width, bank angle z: Heat Source assumes a trapezoidal channel geometry and requires bottom width and bank angle as model inputs. Because bottom width could not be feasibly measured for the 3.234 km reach, a combination approach was undertaken to calibrate these parameters. Using measured flow and top widths, Heat Source’s hydraulic modeling component was run to generate bottom widths and flow depths. Bank angles and bottom widths were then iterated until modeled flow depths matched surveyed flow depths.

Bathymetry Calibration:

Channel angle and bottom widths were calibrated using depth measurements and top widths derived from 2013 structure from motion imagery. For this procedure, bank angles (width/depth ratios) were initially set to zero to represent a rectangular section and then increased until model-generated depths and angles matched measured data. Corresponding bottom widths were changed to match bank angles during this procedure. For overestimates of depth, Manning’s n was decreased in increments of 0.05. Modeled and measured depths converged to a fit of 0.75 coefficient of determination.

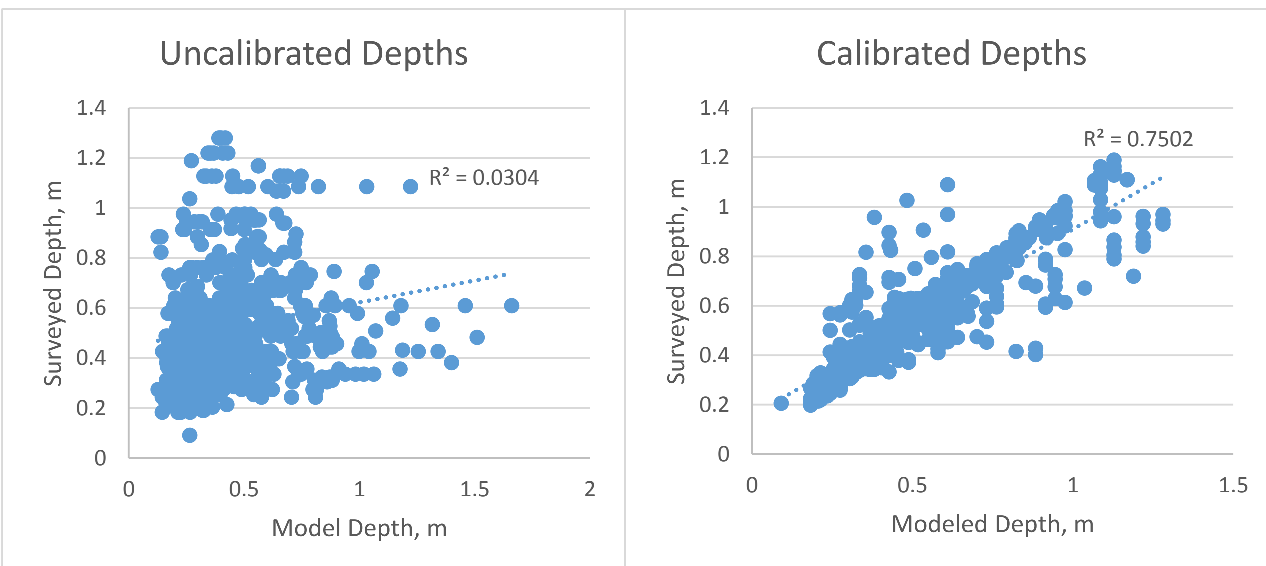

Appendix Figure 1: Calibrated model depths, fit to surveyed channel depths. Accurately modeling depths was important for modeling the amount of solar radiation entering the water column.

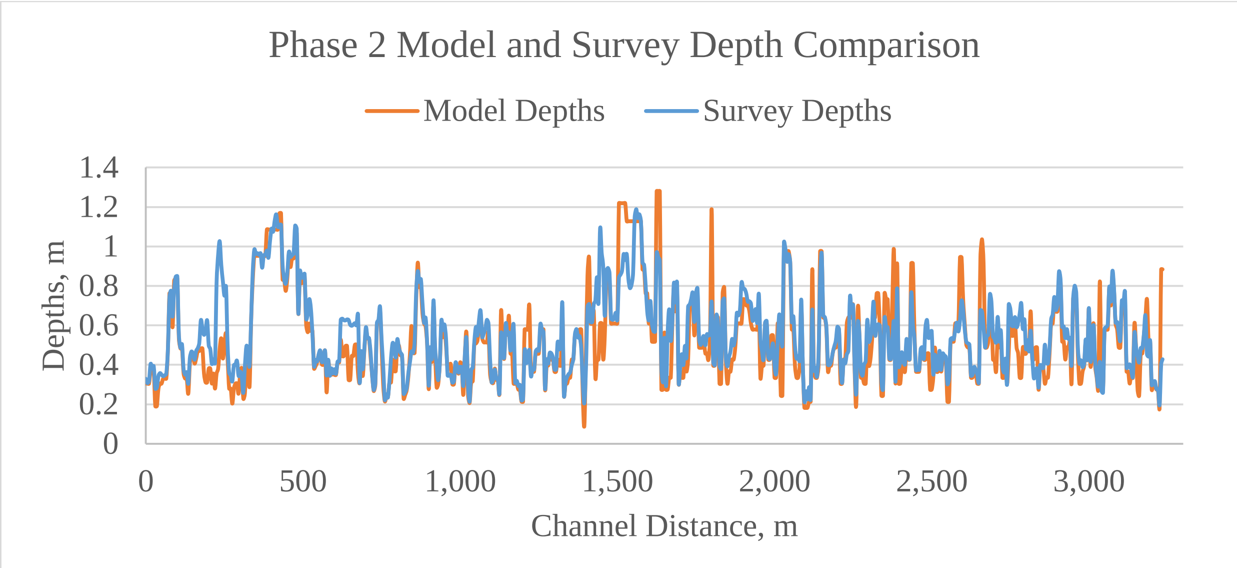

Appendix Figure 2:Spatial comparison of model and surveyed depths, post-calibration.

Manning's n: Manning's n was initially set to 0.070 to prevent model instability due to dewatering of the channel. Through model calibration, this value was varied within a range of 0.045 to 0.07   While this value is higher than typical literature values (Te Chow 1959), other studies indicate a large Manning's n for comparable mountain streams is appropriate (Marcus et al. 1992; Dietrich 2014) .

Streambed Composition:

Streambed composition determines streambed conduction flux in the stream. Properties of the streambed were referenced from rock type and by the measured particle size distribution data and embeddedness estimates provided by Unviersity of Oregon for 2008-2011.

Adopting the methodology of Bedient and Huber 1992 as sited by Boyd and Kasper , porosity was estimated using:

$$\eta = 0.3683 * [(d_{50} * (1 - E)) + (d_{50} * E)]^{0.0641}$$

Results yielded from these calculations reveals that the porosity varied little across sampling sites with average values of 0.29. This value is consistent with literature values for Columbia River basalt, typically found in Middle Fork of the John Day River basin (Crown and Butcher, 2010; Diabat, 2014). Constant values for thermal conductivity and thermal diffusivity were set to 2.0 W/m/°C and 0.006 cm^2/sec respectively, reflecting common values for basalt rock (Eppelbaum, Kutasov, and Pilchin 2014).

Appendix Figure 3: Exposed streambed on the Middle Fork on the Oxbow Conservation Property. The size and composition suggests higher roughness and a streambed heating contributions

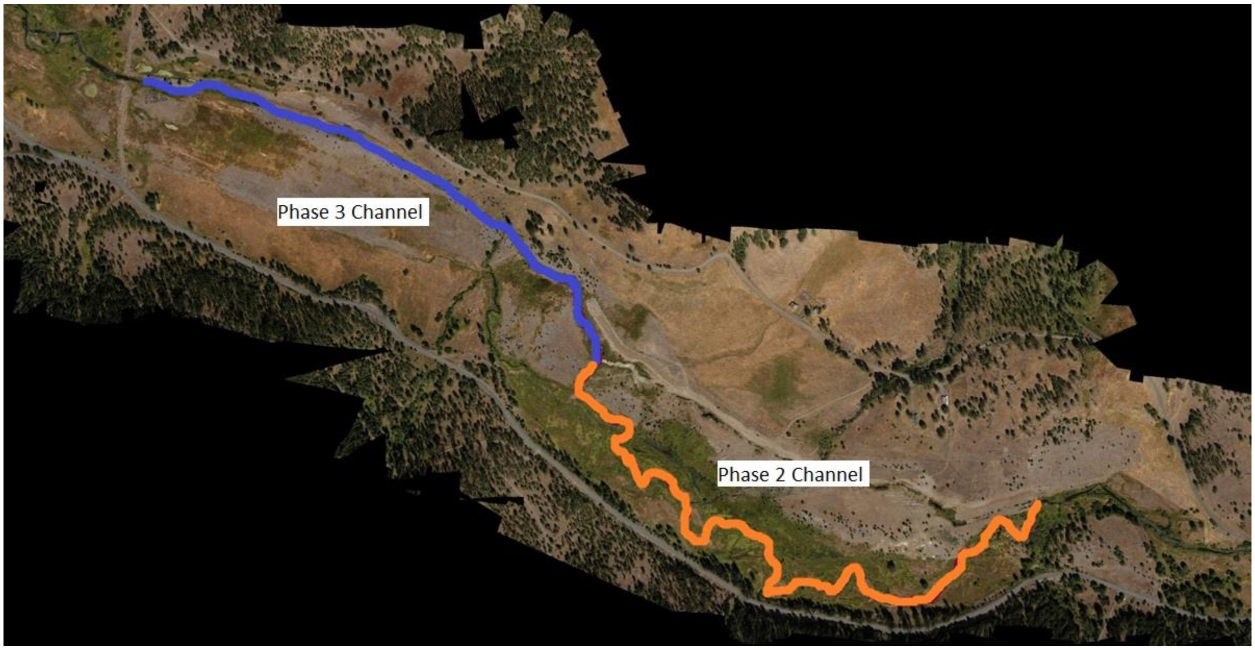

Appendix Figure 4: Location of the existing channels that surveyed in 2013 and 2014.

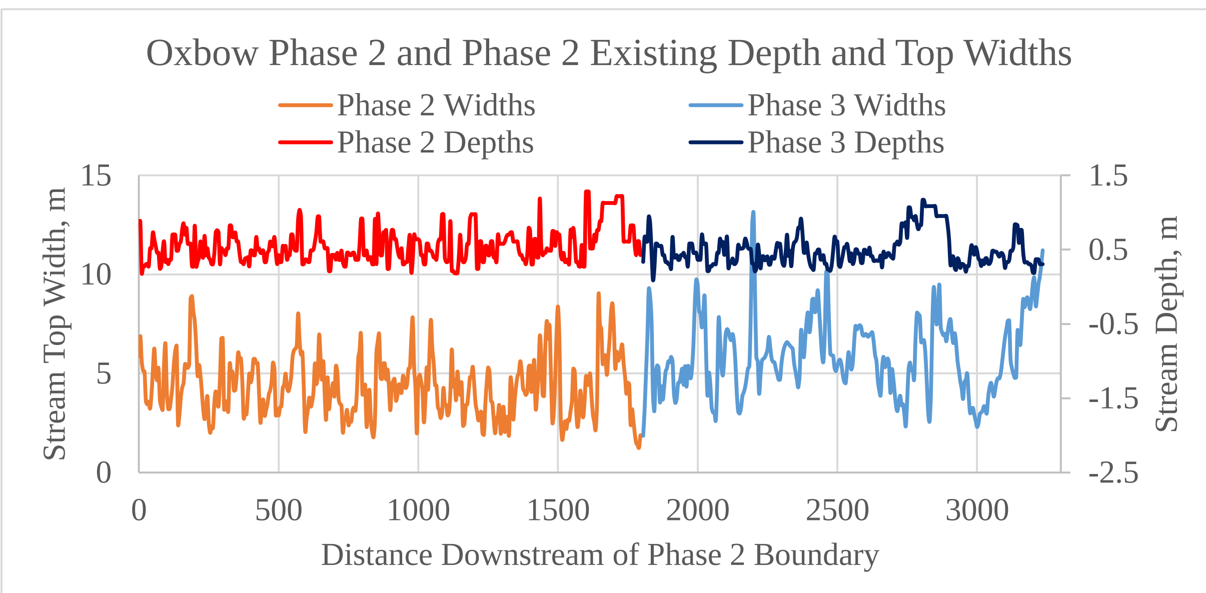

Appendix Figure 5: Longitudinal stream profile of depths and stream widths for the Phase 2 and Phase 3 projects on the Oxbow Conservation Property.

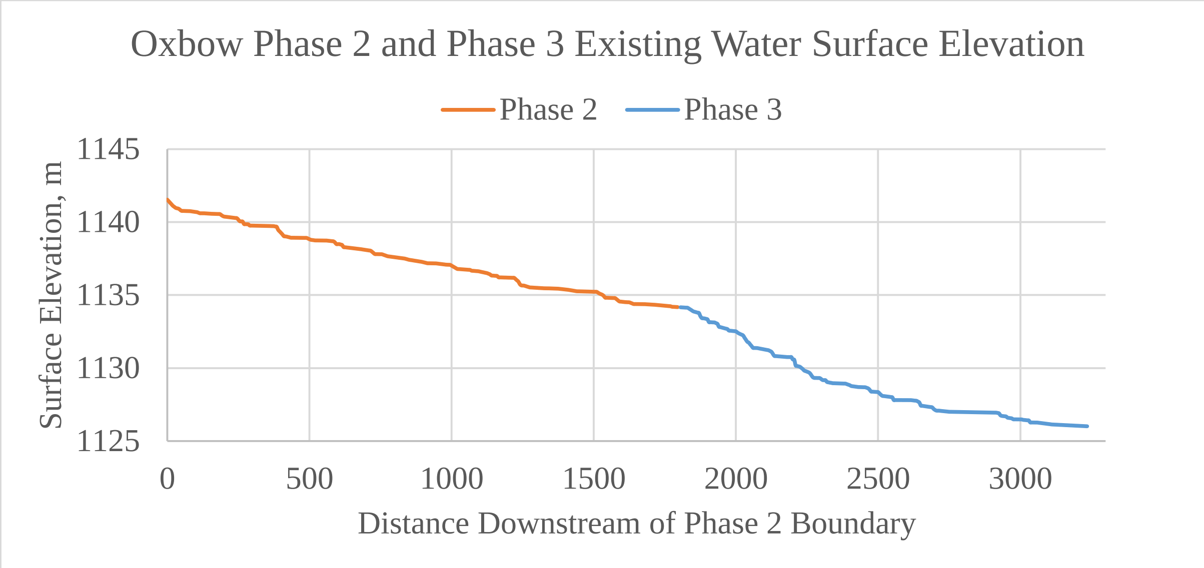

Appendix Figure 6: Longitudinal stream profile of stream surface elevations for the Phase 2 and Phase 3 projects on the Oxbow Conservation Property.

Continuous Data Inputs

Boundary Temperatures: Hourly boundary temperatures at the upstream model node were set to measured temperatures collected using distributed temperature sensing.

Streamflows: Streamflow was assumed constant for the modeling period and assigned according to synoptic discharge measurements made during the 2014 monitoring period. Typical hourly streamflow measurements recorded at the Ritter USGS gaging station showed little flow variation from year to year during the late summer, validating this assumption. Streamflows for smaller tributaries along the reach were sourced from North Fork John Day Watershed Council (NFJDWC) measurements. Flow was negligible as minor tributaries ran dry in late summer while Granite Boulder Creek measured to provide ~0.18 m^3/s of flow in the south channel.

In the historic model, the same upstream flow was assumed as measured in 2014 with flow distributed 75% and 25% to the north and south channels, respectively. This distribution was based on flow measurements conducted prior to restoration in 2011 (O'Donnell 2012).

Streamflow Survey

Appendix Table 1: Synoptic flow survey conducted on Oxbow Conservation Property in 2014

Latitude	Longitude	Location	Date	Flow (cms)
44.6439333	-118.6352056	Oxbow – Up Stream	8/9/2014 14:19	0.40
44.6426611	-118.6613222	Oxbow – GBC Up Stream	8/8/2014 16:30	0.46
44.6432194	-118.6617167	Oxbow – GBC Down Stream	8/8/2014 16:45	0.65
44.6452972	-118.6642389	Oxbow – Old Channel Upstream	8/8/2014 16:00	0.59
44.6475944	-118.6651639	Oxbow – Down Stream	8/8/2014 15:30	0.55

Appendix Figure 7: Synoptic discharge locations on the Oxbow Conservation Area used to source flows for the Heat Source Phase 2 and Phase 3 models.

Tributary Temperatures: Temperatures were recorded in Granite Boulder Creek using temperature loggers deployed by the NFJDWC. Temperatures did not however, accurately reflect the temperatures at the confluence of Granite Boulder Creek and the Middle Fork, so an energy-mass balance approach was taken similar to Selker et al. 2006 where:

$$(m_3 * T_3 * c_3) = (m_1 * T_1 * c_1) + (m_2 * T_2 * c_2) \tag{A-1}$$

Or, in terms of flow and desired tributary temperature as:

$$T_2 = \frac{Q_3 * T_3 - Q_1 * T_1}{Q_2} \tag{A-2}$$

$m_{1,2,3}$=mass of fluid

$Q_{1,2,3}$=flow of fluid

$c_{1,2,3}$=heat capacity of the material

$T_{1,2,3}$=temperature, °C, of the inflows

Groundwater Inflows: Synoptic discharge measurements revealed an accretion of approximately 0.06 m^3/s of flow between the upstream model boundary and Granite Boulder Creek. Temperature data from nearby shallow groundwater wells on the Oxbow Conservation floodplain were used in conjunction with initial model/DTS temperature differences to add this flow as an evenly distributed accumulation for this segment.

Hyporheic Flows: Previous literature has found no conclusive evidence of hyporheic flow at reach and subreach scales (Huff 2009; Kristopher K. Wright 2005). While flow patterns may have changed as the result of restoration efforts, hyporheic exchange was not found to influence stream temperatures in the DTS data. Hyporheic flow was therefore ignored for all model scenarios.

Weather Data: Continuous weather data were sourced from one of three Oregon State maintained weather stations on the Middle Fork of the John Day River. Data from the Dunstan Nature Conservancy property located 9.2 km downstream (northwest) was used to define wind speed, shortwave solar radiation (represented as cloudiness), relative humidity, and air temperature within the model. Because model inputs are defined hourly, 10-minute data outputs reported by the station were linearly averaged for half hour intervals surrounding the hour to improve model accuracy.

Weather data were collected at three independent weather stations on the Middle Fork providing data which defined physical heat transfer processes in the Heat Source temperature model. All three stations were operational during the DTS collection period, providing key validation data and cross station comparison. Data recorded by the weather stations included shortwave radiation, net longwave radiation (Forrest), barometric pressure, air temperature, wind speed, relative humidity, and precipitation. Dunstan conservation property data was ultimately utilized for final model calibration.

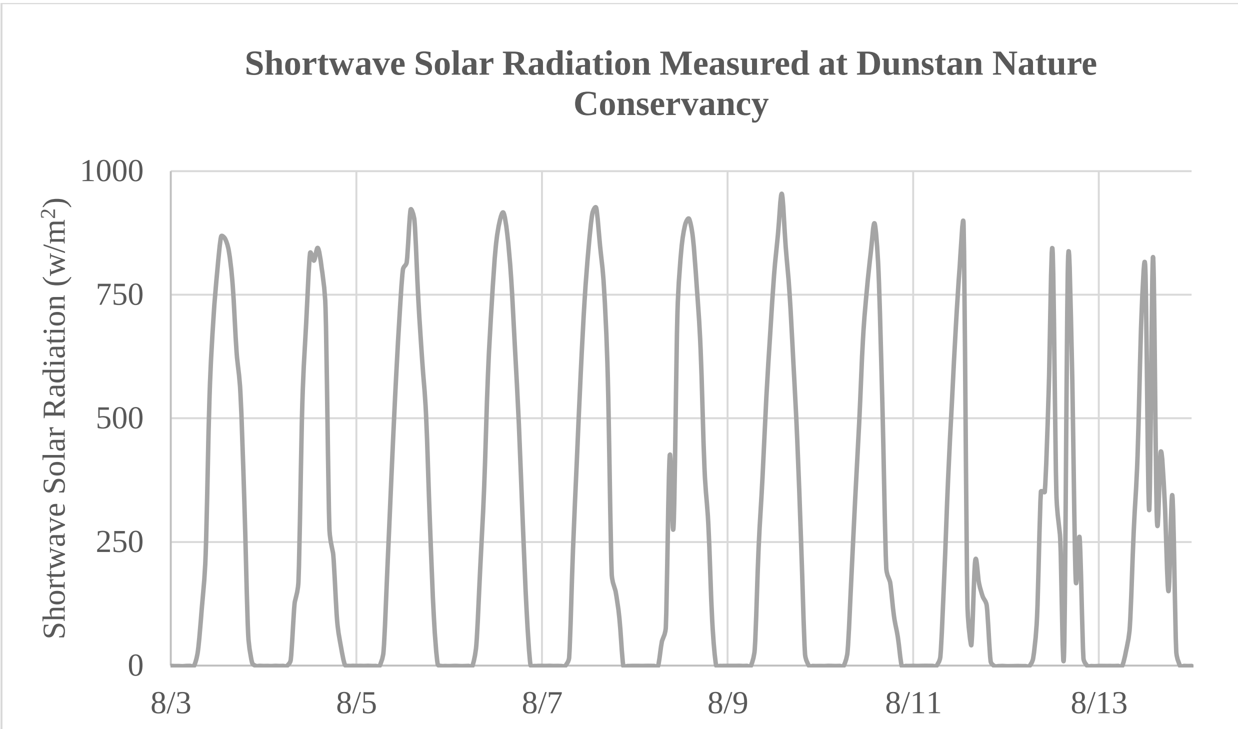

Appendix Figure 8: Measured shortwave solar radiation data indicating clear and cloudy modeling days in 2014

Appendix Table 2: Local meteorological stations on the Middle Fork of the John Day River

Weather Station	Latitude	Longitude	Distance to OCA
Forrest	44°36'4.54"N	118°32'7.41"W	10.8 km
Dunstan	**44°40'43.35"N**	**118°45'43.77"W**	**9.2 km**
RPB	44°44'44.81"N	118°51'17.07"W	19.3 km

Physical Parameters

Evaporation: Penmen Monteith evaporation was selected among the available computation methods in Heat Source. The wind function $f(w) = a + bw$ was defined using Heat Source default coefficients as $f(w) = \mathbf{1.51} * \mathbf{10^{-9}} + \mathbf{1.60 * 10^{-9}}$w and with coefficients derived from David Benner's evaporation study conducted in 2000 $f(w) = \mathbf{4.00} * \mathbf{10^{-9}} + \mathbf{2.36 * 10^{-9}}$w. Because evaporation was not feasibly quantifiable given the varied microclimates on the study reach, these values seek to provide a range of model temperatures.

Appendix B: Phase 2 Supporting Figures

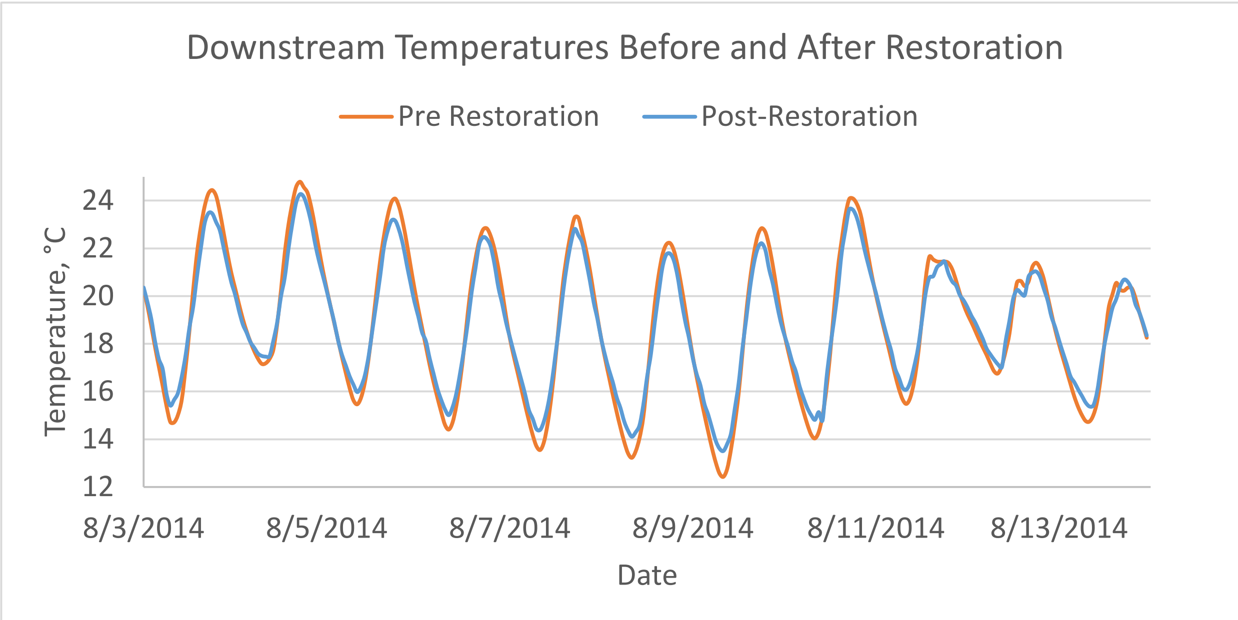

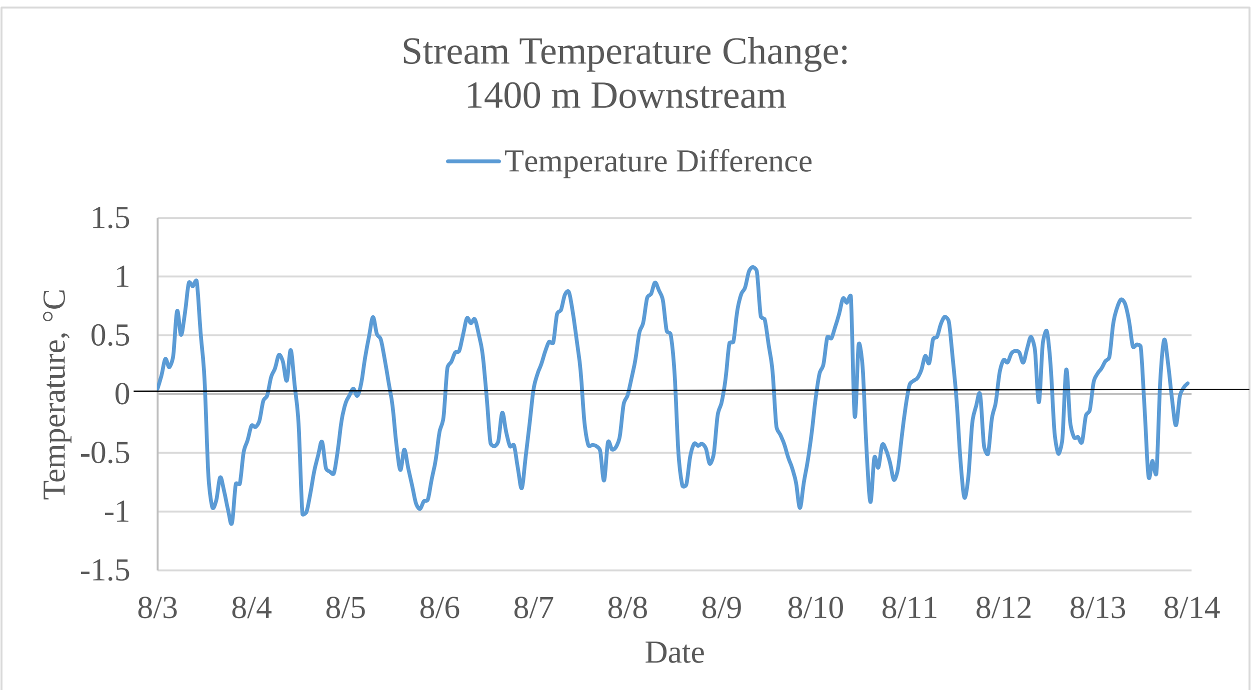

Appendix Figure 9 & 10: Modeled temperatures and temperature differences for Phase 2 restored channel, projected downstream. Results are lower in magnitude than differences measured immediately downstream

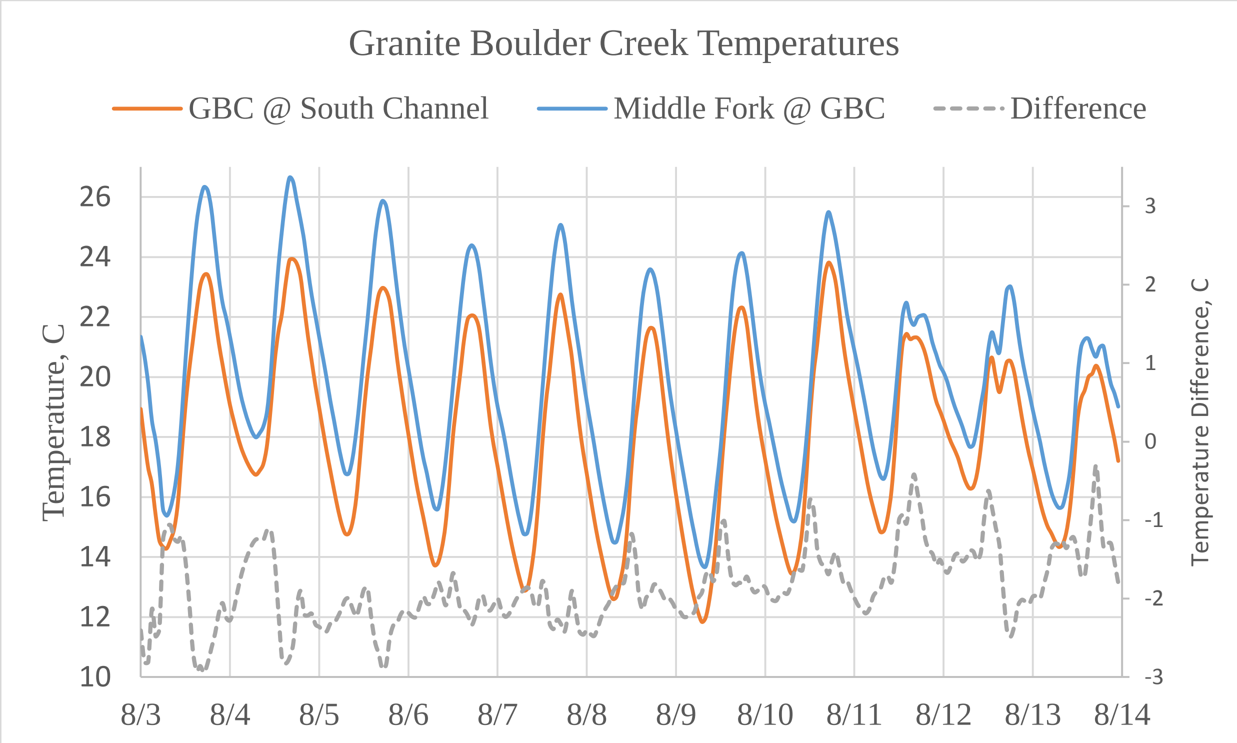

Appendix Figure 11: Temperatures of Granite Boulder Creek, the Middle Fork, and differences. Greatest differences between Granite Boulder Creek and the Middle fork are present during the day, while the lowest differences are at night. Granite Boulder Creek is responsible for the overall cooling of the Middle Fork in the stream reach which distinguishes its behavior from the Phase 3 channel.

Appendix C: Phase 3 Supporting Figures

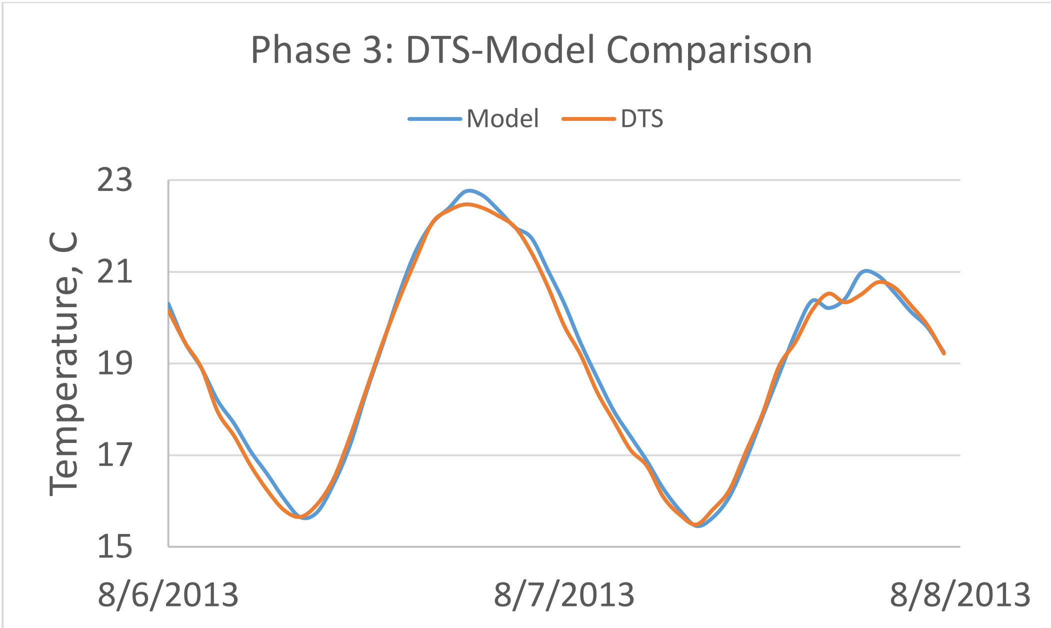

Appendix Figure 12: Phase 3 Calibration Model and 2013 DTS temperature comparison. Comparison data is limited due to channel construction in the summer of 2014.

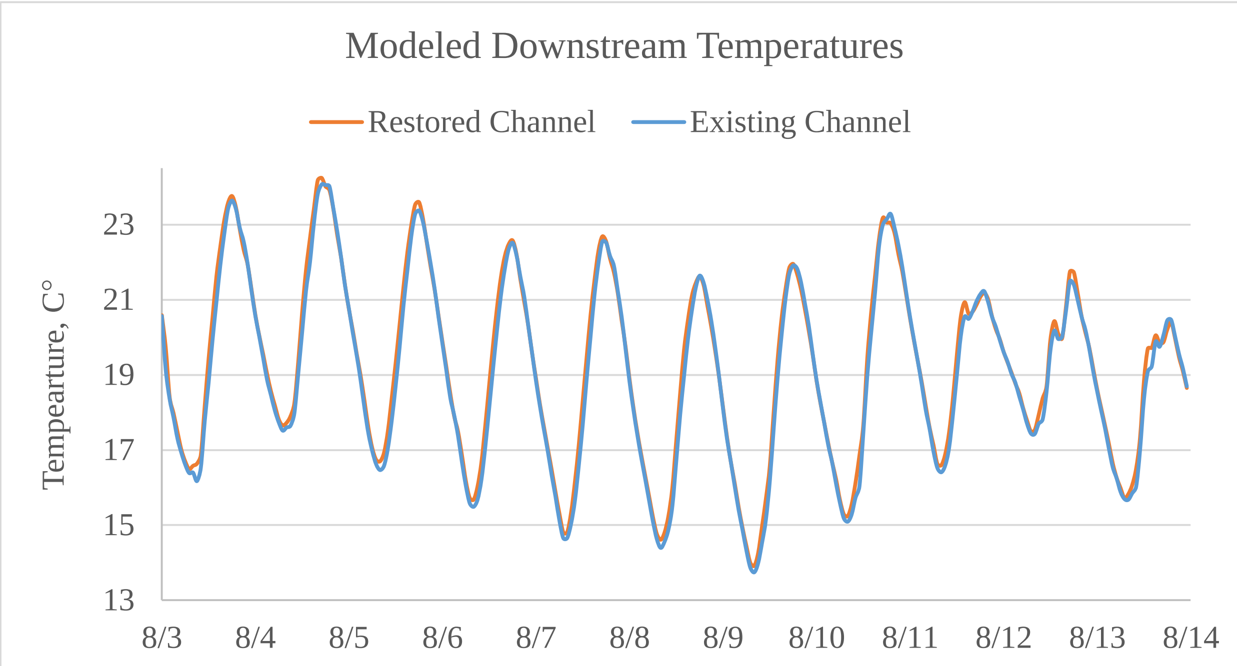

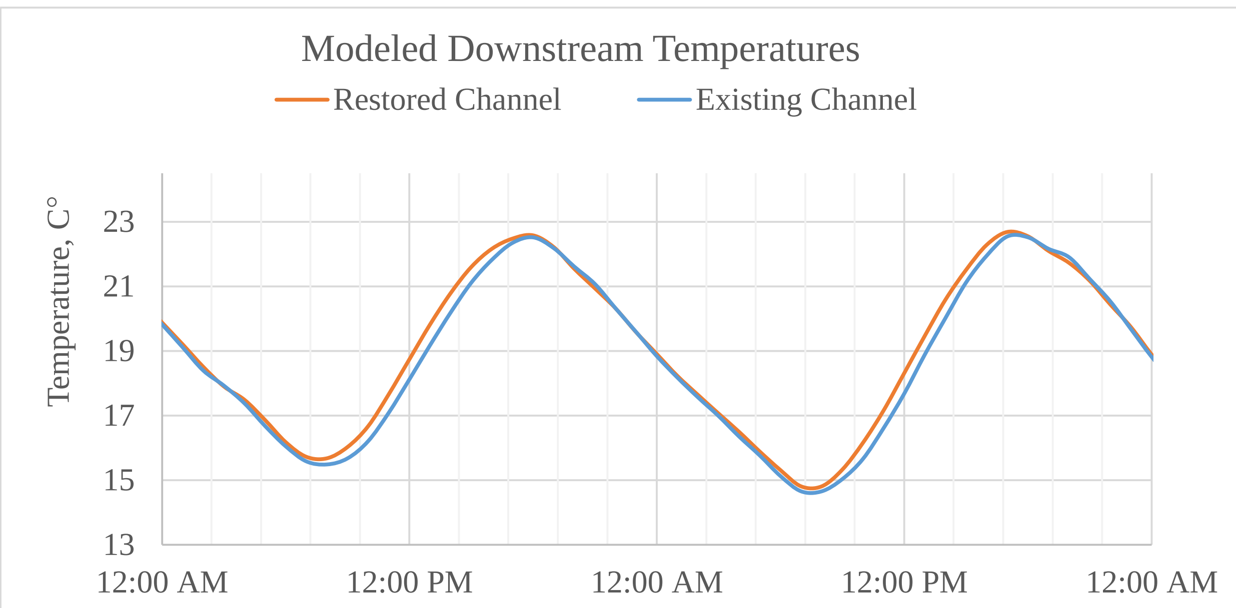

Appendix Figure 13: Modeled temperatures for the non-vegetated existing and projected Phase 3 restored channel at the downstream boundary. Daytime temperatures are shown to increase while maximum daytime and nightly temperatures do not change.

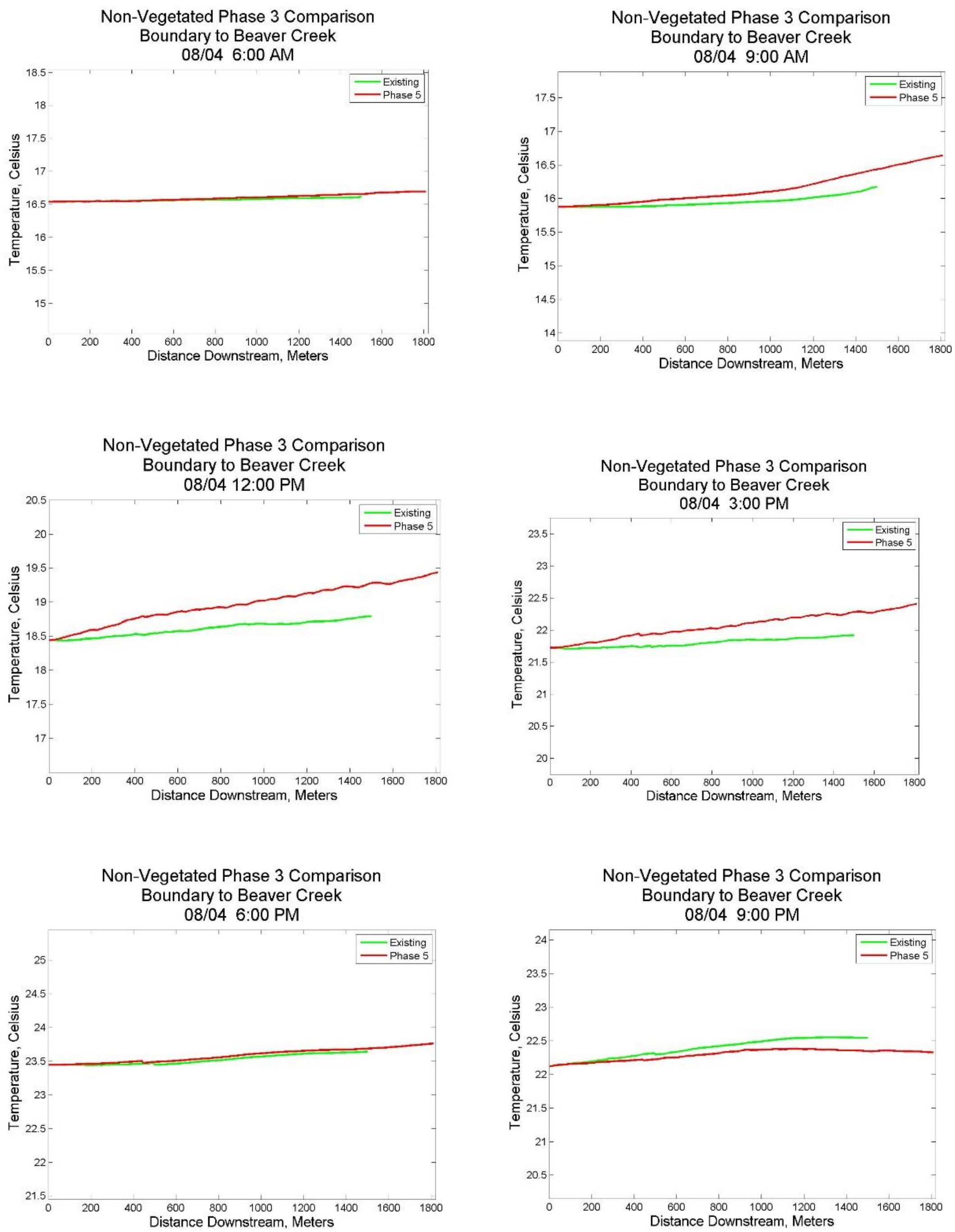

Appendix Figure 14: Spatial comparison of the existing and projected Phase 3 restored channel sections 6:00 AM to 9:00 PM showing how modeled temperatures change throughout the stream.

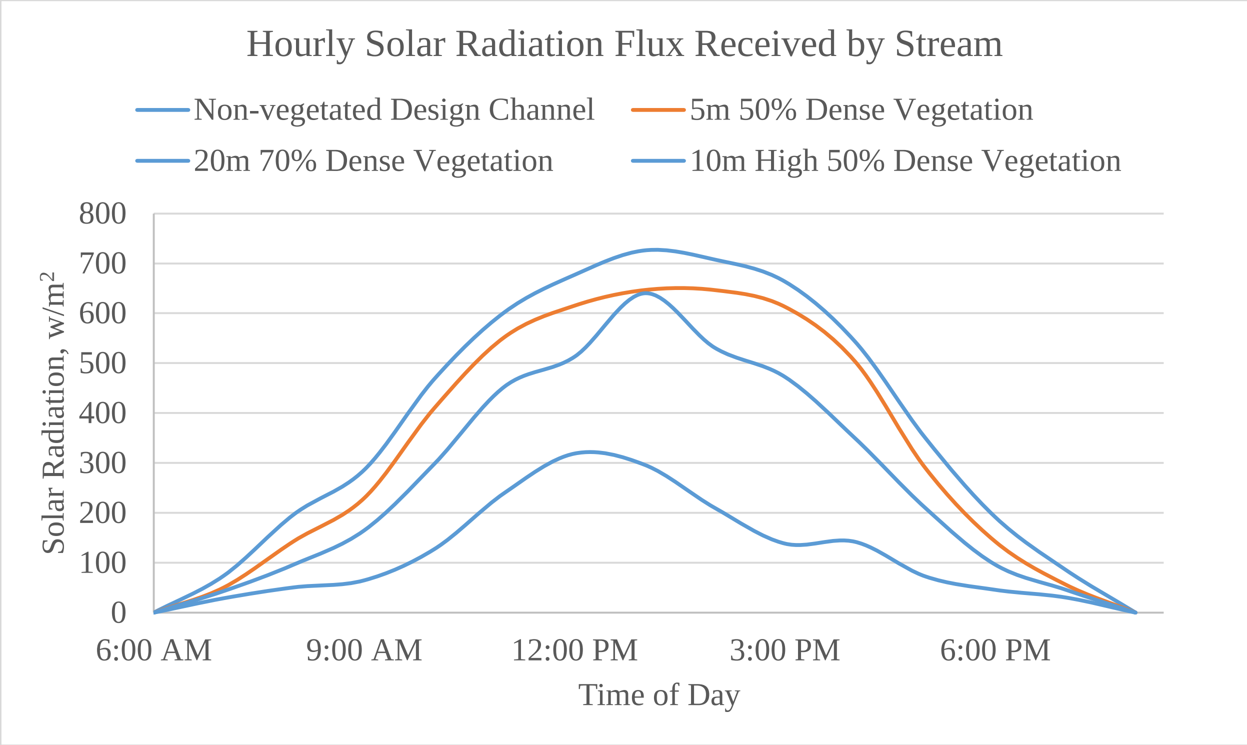

Appendix Figure 15: Hourly solar radiation flux received by the vegetated Phase 3 restored channel models. Increasing vegetation provides more effective shade, resulting in less solar radiation received by the stream.

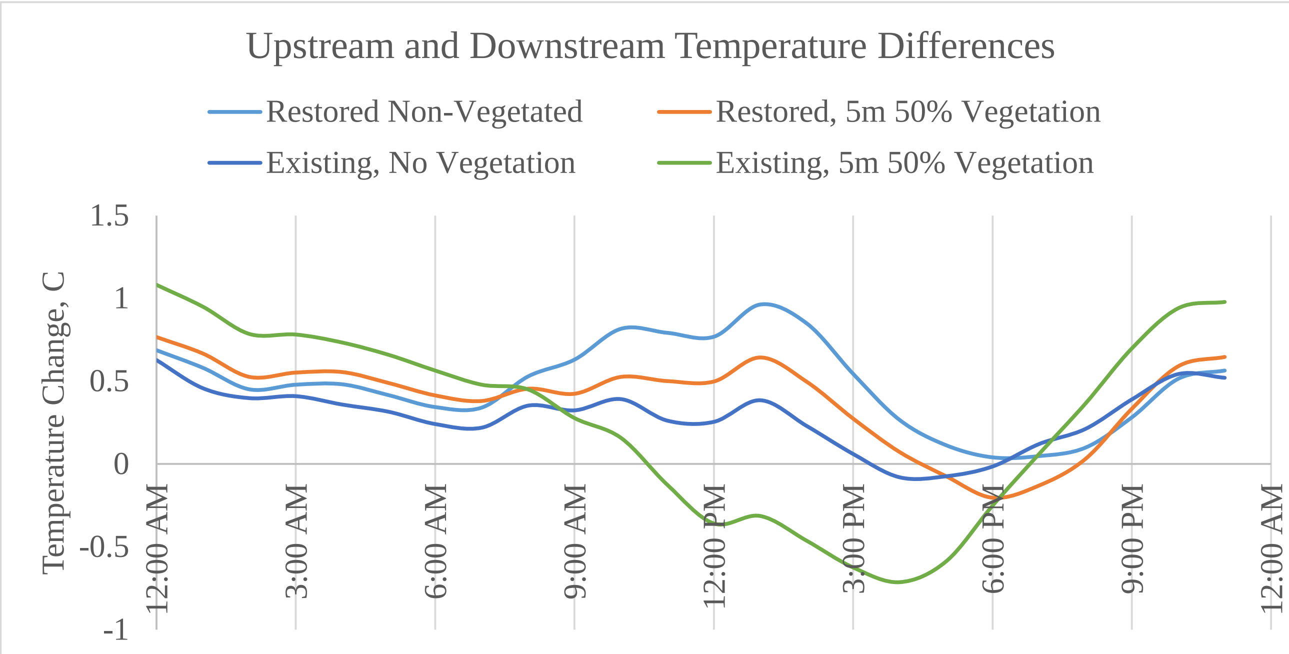

Appendix Figure 16: Average hourly temperature change across channel for existing and planned Phase 3 restored channels, with the addition of 5m, 50% vegetation. The existing channel is shown to provide more effective temperature change for the same vegetation case, a result of the stream's orientation to the sun.

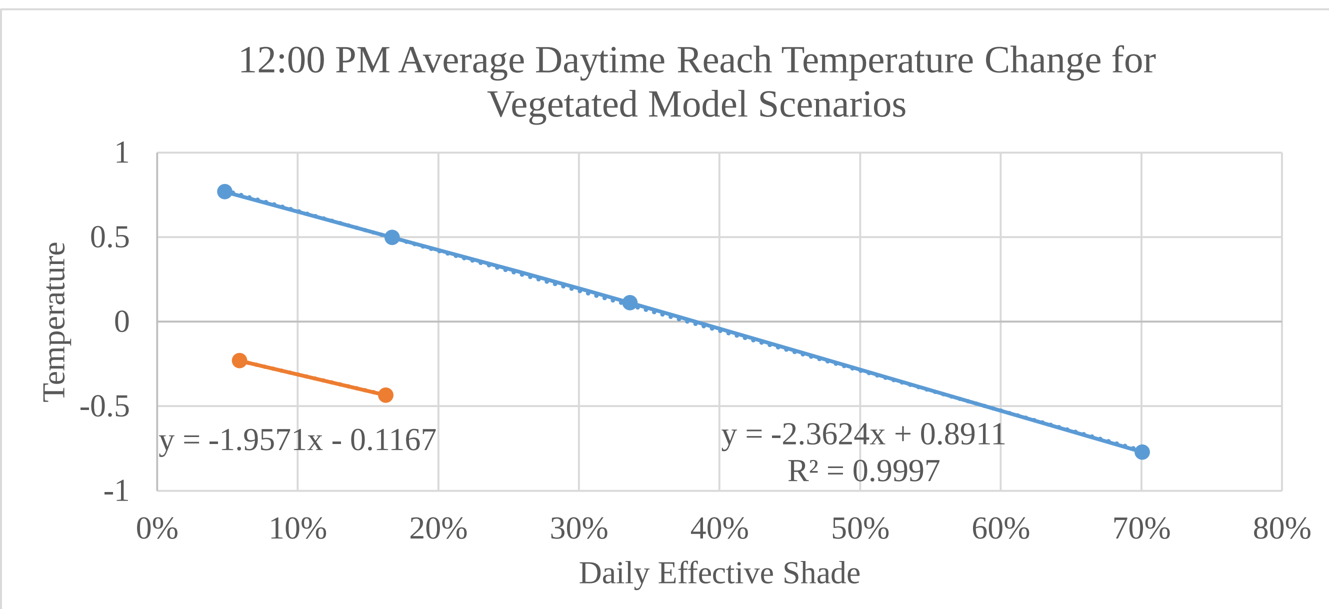

Appendix Figure 17: Average 12:00 PM channel temperature differences and correlations for restored and existing vegetated channels. Relationship is strongly as indicated on the restored channel.

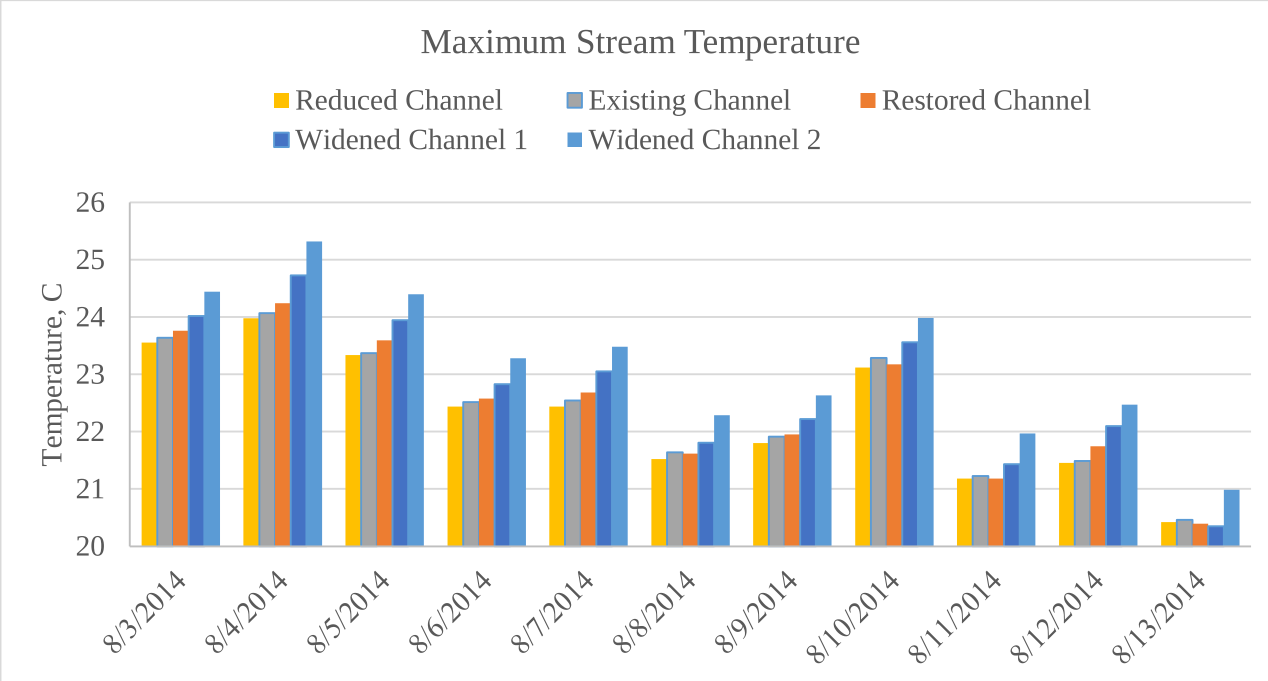

Appendix Figure 18: Comparison of maximum daily temperatures for the varied area stream scenarios

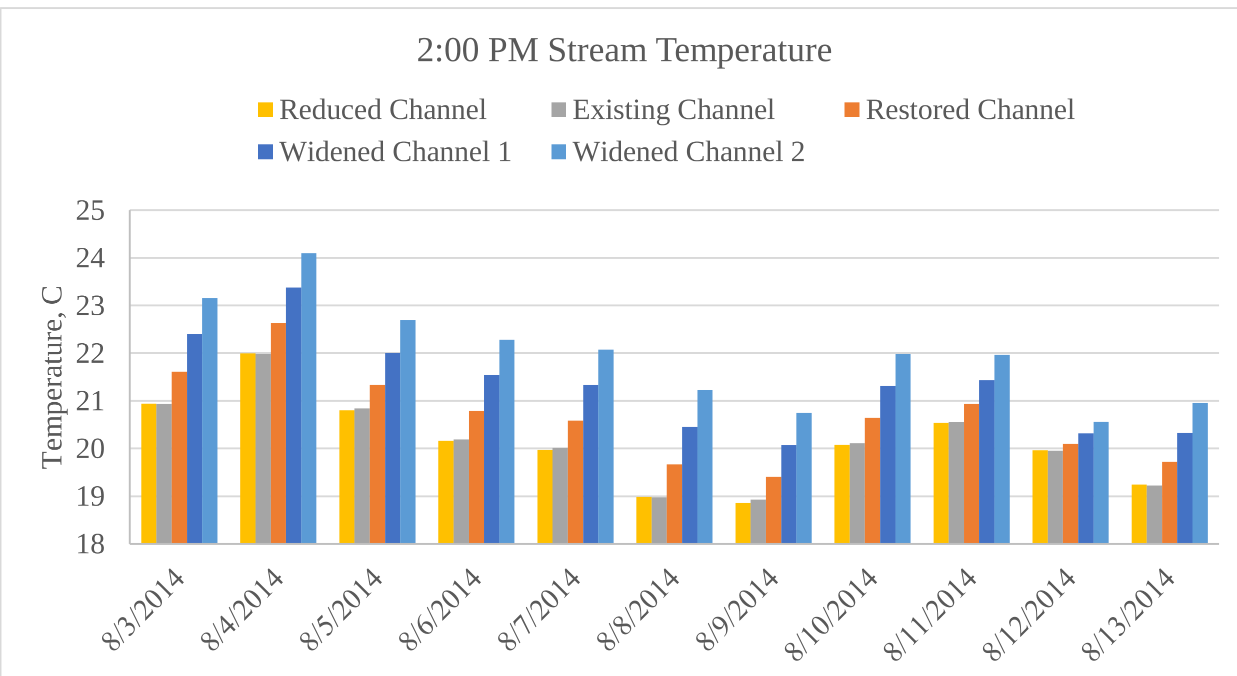

Appendix Figure 19: Comparison of 2:00 PM temperatures for the varied area stream scenarios

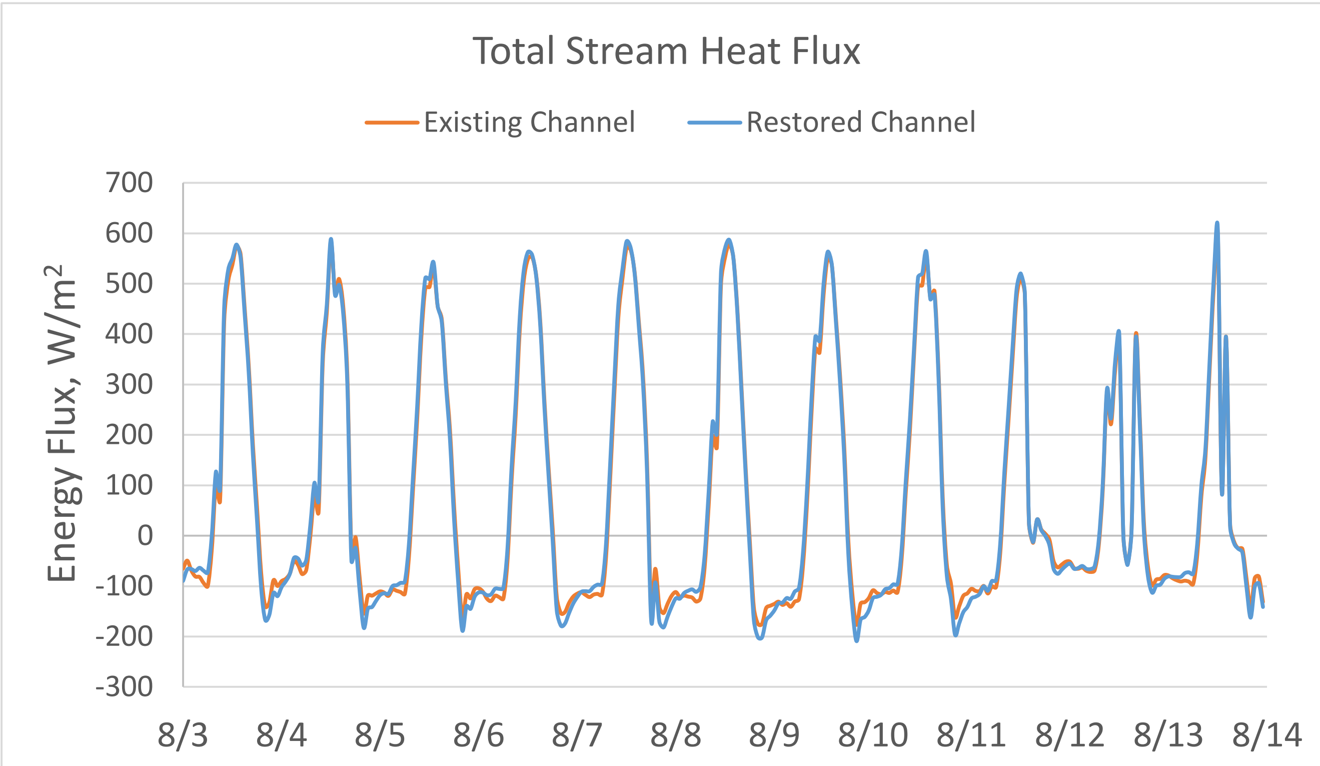

Appendix Figure 20: Comparison of total heat flux between the existing and non-vegetated restored channel. The totals for both streams are similar, indicating that temperature differences between the channels are the result of stream area, stream depth, and residence time changes

Appendix D: DTS Error, Field Setup, and Calibration

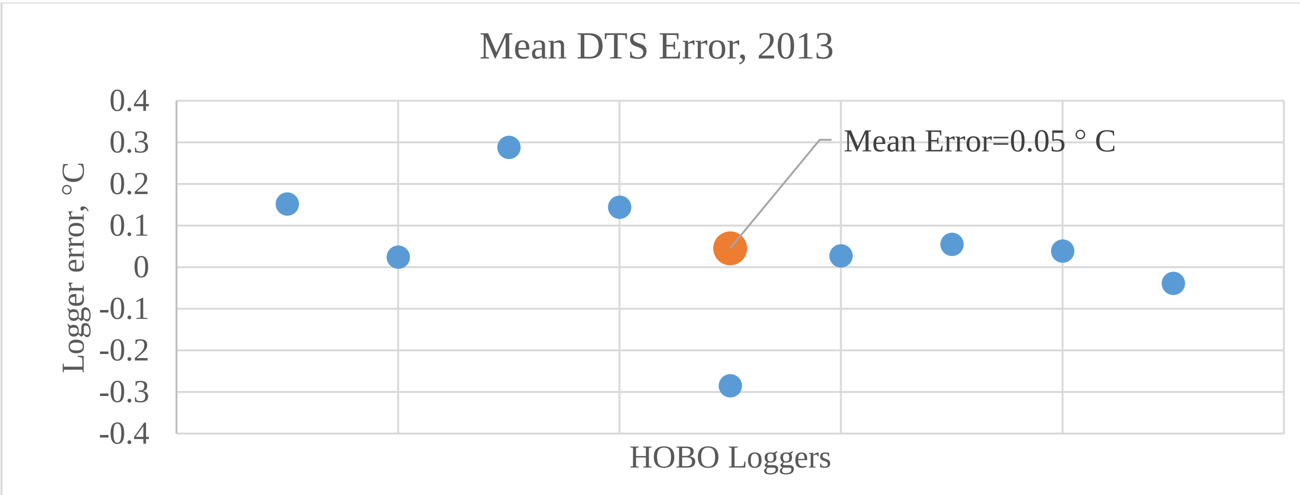

Appendix Figure 21: 2013 DTS error relative to independent temperature loggers on the reach. Average error is shown to be 0.05 relative to independent temperature loggers. These loggers are limited to ±0.2° C, and govern the accuracy of the installation.

Appendix Table 3: Mean and absolute error for 2013 DTS installation

Mean Error	0.05 °C
Absolute Mean Error	0.32 °C

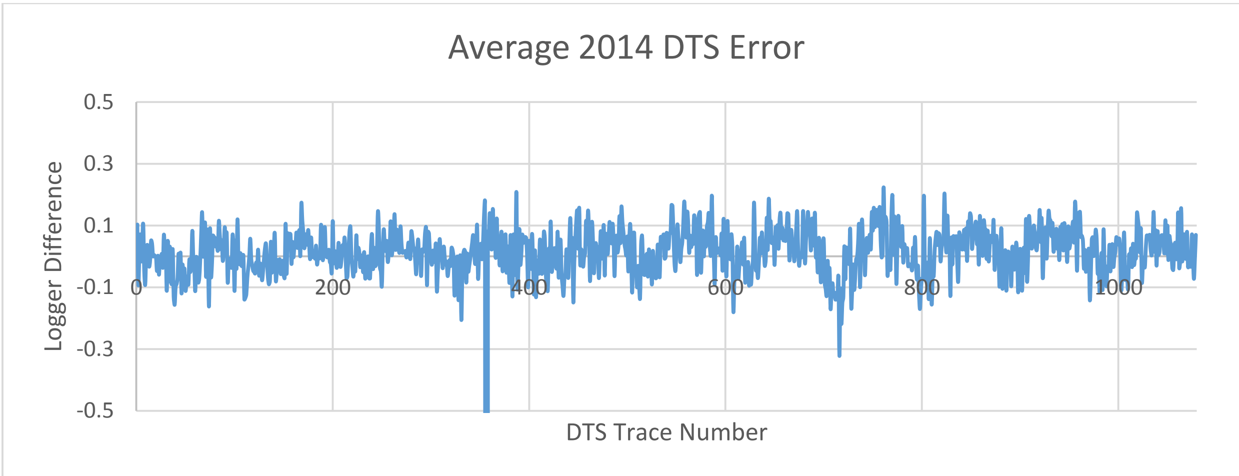

Appendix Figure 22: Average 2014 DTS error relative to Onset HOBO loggers, (accuracy +/- 0.2 C). Anomalies near trace 375 and 725 are associated with ice bath over freezing.

Appendix Table 2: Mean and absolute error for 2014 DTS installation

Mean Error	-0.13 °C
Absolute Mean Error	0.20 °C

2014 Field Setup:

Three controlled, independently measured baths were maintained during the experiment to provide reference temperatures for post-experiment data processing. One ambient temperature bath and a solar-powered chest freezer were located at the site of the DTS, while an ice chest was placed at the downstream project terminus. High precision RBRsolo T (accuracy +/-0.002°C) temperature loggers were embedded within cable sections housed in the baths. Aquarium bubblers circulated temperatures within these baths to prevent temperature stratification. 5 additional HOBO TidbiT v2 and HOBO U22 loggers (accuracies +/-0. 2°C) were secured to the cable in the stream to provide external references for improved calibration and validation. Power was provided to the chest freezer, DTS, and bubblers by a field designed solar trailer which carried 9 120-watt polycrystalline solar panels. These panels provided power to the installation during the day while charging 6 12V deep cycle marine batteries which provided power to the installation at night. An independent 12V 7 AH battery was configured with a 15-watt solar panel to provide power for the bubbler at the isolated reference bath at the end of the installation.

Fiber Optic Cable Installation

To deploy loaded spools of fiber optic cable (134 kg) a pontoon system was adapted to float the cable over the stream. The origin of deployment was selected to provide a clear view to the sky for the solar power generation, accessibility to the stream, and adequate coverage of the target stream reaches. To capture the most representative stream temperature, the fiber optic cable was installed in the thalweg and secured to the streambed every 5-10m using alluvial rocks. As the cable was placed, a high precision RTK TOPCON GR-3 survey grade GPS (10mm horizontal, 15mm vertical accuracy) was used to map its location and associated stream depths. At the terminating end of the fiber optic cable, the inner fibers were spliced together to provide double measurements of temperature along the stream. This spliced section was secured next to a final reference ice bath downstream.

Following cable deployment, the installation was monitored for any problems and the ice baths were restocked daily to maintain a constant temperature of 0° C in the bath. The stream was successfully monitored for 11 days, capturing a variety of climate conditions.

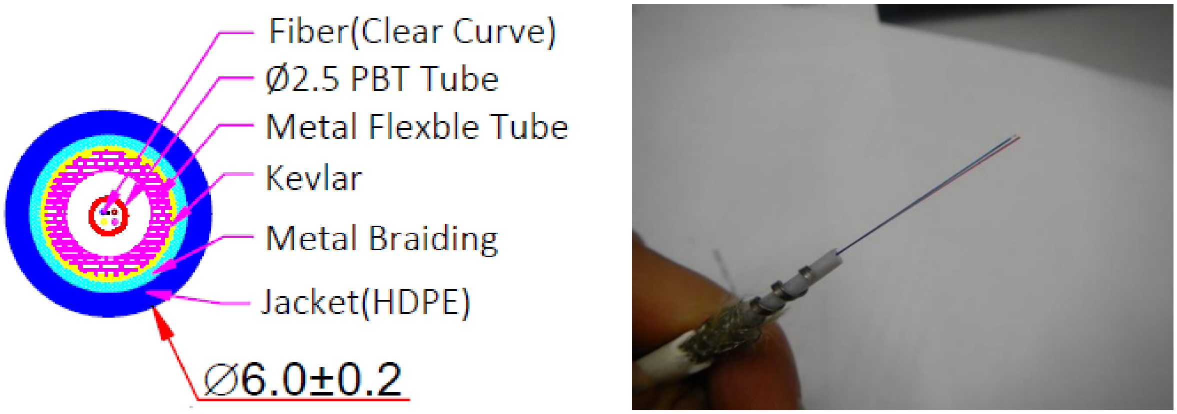

Appendix Figure 23: White Kaiphone style fiber optic cable utilized in the 2013 and 2014 monitoring studies. Cable was resilient during the installation, though deteriorated after it was uninstalled.

Appendix Figure 24 & 25: 2014 solar trailer housing the DTS along with calibration bath setup. ~25 meters of cable is dedicated to each bath. The installation is powered by 9 120 W solar panels.

DTS Calibration

Calibration of raw DTS signal data is based on the relationship between the intensities of backscattered Stokes and anti-Stokes light signals where the temperature at any position along the cable can be calculated using $T(z) = \frac{\gamma}{ln\frac{P_S(z)}{P_{aS}(z)}+C-\Delta\alpha}$ (Hausner, 2011). $C, \Delta\alpha,$ and γ represent physical calibration parameters which can be determined using three known temperatures sections and their locations along the cable. While these parameters are often calculated only once for an installation and assumed constant, DTS hardware inconsistencies showed that this was not an acceptable approach in the Middle Fork of the John Day River. MatLab code was developed to process this raw signal data, calculating calibration coefficients for every data trace collected. For more information on the fundamentals of distributed temperature sensing technology, the reader is referred to current literature (Selker 2007; Tyler 2008; Suarez 2011; others).

Processing the calibrated temperature data required additional care and extensive documentation of cable location as it was pulled out of the water to navigate the engineering log structures that were placed across the stream in the Phase 1 Tailings construction phase. Sporadic fluctuations in DTS performance were manually removed to improve data quality.

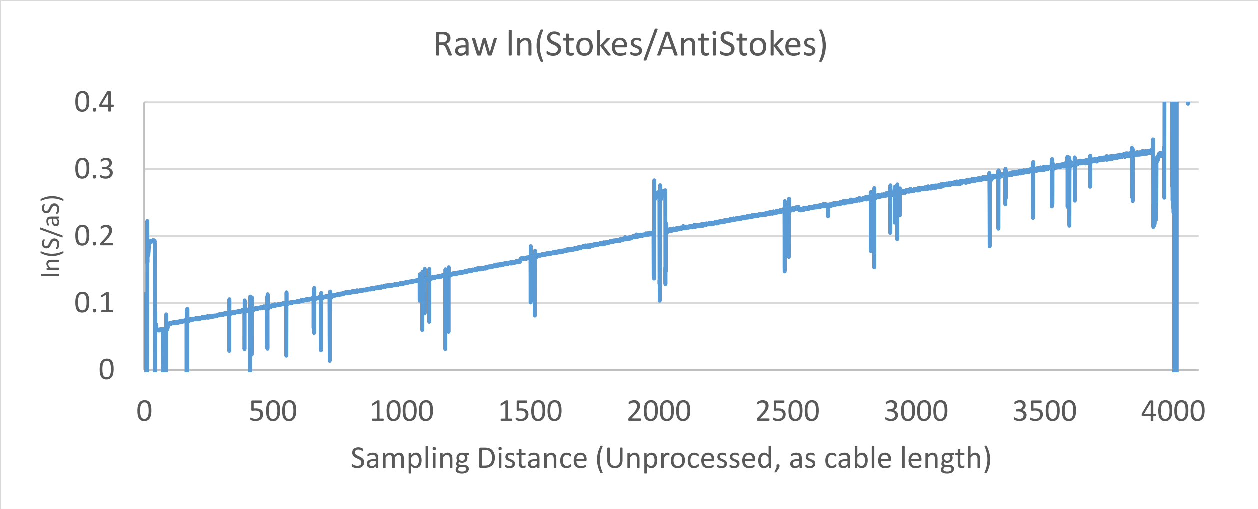

Appendix Figure 26: Ratio of stokes and antiStokes signals, prior to final calibration. Spikes are associated with log jams which were present across the Phase 2 channel.

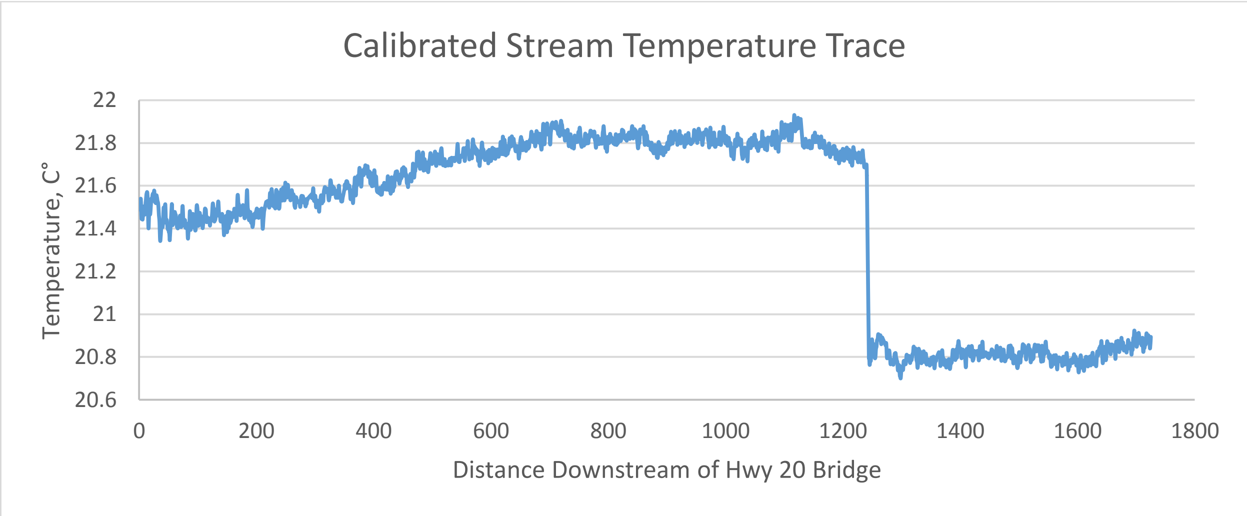

Appendix Figure 27: Calibrated temperature trace, averaged and processed using reference data and spatial information of log structures

Example DTS Calibration Code

```
%%%This is an example calibration code that was used to calibrate raw DTS
%%%data from stokes/anti-stokes into temperature. This code uses matrix
%%%inversion and assumes three reference sections are included for the
%%%installation.

%Forrest Calibration

%S=stokes ln ratio data computed in the precalibration code. Be sure to set
%S= to the ln matrix produced by that code
dist=size(S,1);  %distance
time=size(S,2);  %time

Toffcor = zeros(dist,time);
ForrestUS2013_CAL = zeros(dist,time);

%%Sets matrix for Ax=B where x can be solved for with matrix inversion '\'
operator. The three calibration constants are the resulting output (See
Selker
%%DTS Calibration publication for more information on this)
A=zeros(3,3);
X=zeros(3,1);
B=zeros(3,1);


%Loops through process for each trace in time series
for t = 1:time

   %Section 1
   avgibath1=mean(S((33:206),t));  %Determines the average signal within the
ice bath. Note that the array index is not the same as the meter mark.
                                   %Sensortran records temperatures every
                                   %0.253 meters. Graph the data first to see
                                   %where these sections are
   zibath1=(8+52)/2;               %The distance to the center of the ice
bath
   T1=HOBO2(t)+273.15;             %The absolute temperature of the ice bath
from an independent point logger (HOBO here)

   avgamb=mean(S((253:403),t)); %Same as above, for the ambient bath
   zamb=(64+102)/2;
   T2=HOBO1(t)+273.15;

   avgibath2=mean(S((7897:8004),t));%Same as above, for the second ice bath
at the end of the reach
   zibath2=(1998+2025)/2;
   T3=HOBO24(t)+273.15;

   A=[1 -T1 T1*zibath1; 1 -T2 T2*zamb; 1 -T3 T3*zibath2]; %Sets up first
matrix (See Selker/Tyler pub on DTS calibration on CTemps)
```

```
   B=[T1*avgibath1;T2*avgamb;T3*avgibath2]; %Fills in values for the second
matrix

   X=A\B;   %Solves for calibration coefficients

   gamma=X(1,1);
   C=X(2,1);
   dAlpha=X(3,1);

   %This loop applies the calibration coefficients to the signal data
   for d=1:8012
       ForrestUS2013_CAL(d,t)=gamma/(S(d,t)+C-dAlpha*(d*.253))-273.15;
   end


%Section 2 (2027=halfway meter) Because there are two fibers in the cable,
%this section calibrates the same section of river from the farthest stream
%section, moving back towards the DTS

   avgibath1=mean(S((8032:8154),t));
   zibath1=(2032+2063)/2-2027;
   T1=HOBO24(t)+273.15;

   avgamb=mean(S((15668:15806),t));
   zamb=(3964+3999)/2-2027;
   T2=HOBO1(t)+273.15;

   avgibath2=mean(S((15850:15972),t));
   zibath2=(4010+4041)/2-2027;
   T3=HOBO2(t)+273.15;

   A=[1 -T1 T1*zibath1; 1 -T2 T2*zamb; 1 -T3 T3*zibath2];


   B=[T1*avgibath1;T2*avgamb;T3*avgibath2];

   X=A\B;

   gamma=X(1,1);
   C=X(2,1);
   dAlpha=X(3,1);

   for d=8012:dist
       ForrestUS2013_CAL(d,t)=gamma/(S(d,t)+C-dAlpha*(d*.253-2027))-273.15;
   end
```